

The Standard Model

Part I

Contents

1	Introduction: Matter and Forces	2
1.1	Matter content of the universe	2
1.1.1	Leptons	2
1.1.2	Quarks	3
1.1.3	Bosons	3
1.2	Forces	4
1.2.1	Gravity	4
1.2.2	Electromagnetism	6
1.2.3	The weak force	6
1.2.4	The strong force	7
1.3	Local gauge invariance	7
1.4	Spontaneous symmetry breaking	8
1.5	Grand unified theories	8
2	Experimental Concepts	9
2.1	Experimental possibilities	9
2.2	Cross section	9
2.2.1	Beam incident on a target	9
2.2.2	Beam-beam collision	10
2.3	Luminosity	10
2.4	Natural units and conversion factors	11

3	Experiments of the Last 60 Years	12
4	Non-Relativistic Quantum Mechanics	13
4.1	Schrödinger's equation and probability current density	13
4.2	Heisenberg and interaction pictures	14
4.2.1	Heisenberg picture	14
4.2.2	The interaction picture	15
4.3	Quantum harmonic oscillator	15
4.3.1	Energy spectrum	16
4.3.2	Zero-point energy	17
4.3.3	Action of the ladder operators	17
4.4	The anharmonic oscillator (perturbation theory)	18
4.5	Lagrangian mechanics	19
4.5.1	Relation to the Hamiltonian	20
4.5.2	Application to the QHO	20
4.6	Dirac δ function	20
4.7	Heaviside step function	22
5	Special relativity	24
5.1	4-vectors	24
5.2	Lorentz transformation	25
5.3	The light cone	25
5.4	Relativistic kinematics	25
5.4.1	Fixed target particle production	26
5.4.2	Beam-beam collisions	26
5.5	Mandelstam variables	27
6	Relativistic spin-0 particles	30
6.1	The Klein-Gordon equation	30
6.1.1	4-current density	30

6.1.2	Application to a plane wave	31
6.2	Negative energy particles and the Fenyman-Stueckelberg interpretation	31
7	Calculating Amplitudes	33
7.1	Single scattering potential	33
7.2	Two scattering potentials	34
7.3	Free particle propagator	35
8	Spinless $e^- + \mu^-$ scattering	36
8.1	Electrodynamics of scalars	36
8.2	Scattering amplitude	37
8.3	Scattering rate	38
8.4	Density of states	39
8.5	Incoming flux	39
8.6	Cross-section	40
8.7	Application: high-energy scattering	41
8.8	$1 \rightarrow 2$ scattering (decay)	42
9	Relativistic Spin-$\frac{1}{2}$ particles	43
9.1	Spin in non-relativistic QM	43
9.2	The Dirac equation	44
9.2.1	Constraints on α_i, β	44
9.2.2	Covariant form	45
9.2.3	Properties of the γ matrices	45
9.3	Adjoint Dirac equation	46
9.3.1	Conserved current	46
9.4	Free particle solutions	47
9.4.1	Particles at rest	47
9.4.2	Moving particle solutions	47
9.4.3	Antiparticles	48

9.5	Orthogonality and normalisation	48
9.6	Helicity	49
9.6.1	Helicity	50
9.7	The γ^5 matrix	50
9.8	Completeness relations	51
9.9	Forms of interaction in Dirac theory	52
9.10	Trace theorems	52
10	$e^- \mu^-$ scattering	55
10.1	Electron in an EM field	55
10.2	Current-potential formulation	55
10.3	Scattering amplitude	56
10.3.1	Sum over spins	57
10.4	Differential cross section	58
11	$e^- e^+$ annihilation	59
11.1	Total cross section	59
11.2	R at $e^- e^+$ colliders	60
11.3	Helicity conservation at high energies	62
12	Massless Spin-1 Particles	63
12.1	Maxwell's equation and the classical potential	63
12.2	Gauge transformations and the Lorenz condition	64
12.2.1	Polarisation states of a free photon	64
12.3	Virtual photons and the photon propagator	65
12.3.1	Momentum-space propagators	66
12.4	Longitudinal and timelike virtual photons	67
12.4.1	Coulomb's law	67
12.4.2	Completeness relation	67

13 Compton Scattering	69
13.1 s-channel	69
13.2 u-channel	70
13.3 Interference term	71
13.4 Cross-section	71
13.4.1 $e^-e^+ \rightarrow \gamma\gamma$ cross-section	72
13.4.2 Total cross-section when $m \rightarrow 0, s \rightarrow \infty$	72
14 Massive Spin-1 Particles	74
14.1 Polarisations	74
14.1.1 Transformation of the polarisation vector	75
14.2 Completeness relation	75
14.3 Virtual vector bosons	76
14.3.1 Polarisations	76
14.3.2 Propagator	76
A Experiments of the Last 60 Years	78
B Special Relativity	99
C Fermi <i>beta</i>-Decay	114
D 2-Flavor Neutrino Model	118
E Electroweak Unification	121
F Lorentz Invariant Phase Space	125

Chapter 1

Introduction: Matter and Forces

The definition of the Standard Model (SM) is not fully agreed upon in the scientific community. The minimal acceptable definition is that of the unified electroweak (EW) interaction according to Glashow, Salam, and Weinberg (GSW). Quantum chromodynamics (QCD) explains the strong force, but there is currently no theory of unified EW and QCD interactions. The most commonly used Standard Model is that of EW plus QCD interactions. In this model, neutrinos are massless. However, in principle, the SM could include the phenomena of neutrino oscillations by adding a kinetic term to the Standard Model Lagrangian, \mathcal{L}_{SM} . If neutrinos were found to be Majorana fermions (their own antiparticles), this would explain the small neutrino mass. The widest definition of the Standard Model includes general relativity and cosmology. This extreme version is not generally used, since its large- and small-scale behaviours cannot presently be unified. In what follows, we work with $SM = EW + QCD$.

1.1 Matter content of the universe

The Standard Model splits the fundamental particles into fermions (spin- $\frac{1}{2}$) and bosons (integer spin). Fermions are the building-blocks of matter due to the Pauli exclusion principle. The fundamental bosons are the results of gauge invariances and serve to mediate the forces of the Standard Model.

Fermions are further divided into leptons and quarks.

1.1.1 Leptons

I	II	III
$\begin{pmatrix} \nu_e \\ e \end{pmatrix}$	$\begin{pmatrix} \nu_\mu \\ \mu \end{pmatrix}$	$\begin{pmatrix} \nu_\tau \\ \tau \end{pmatrix}$

Table 1.1: The leptons of the Standard Model arranged into three generations. The top row has charge $Q = 0$ and the bottom row $Q = -1$.

Leptons do not experience the strong force (they are color neutral) and do not mix. Due to its mass, the τ lepton can decay hadronically, whereas muon decay is purely leptonic. The most common muon decay is

ℓ	Mass
e	511 keV/c ²
μ	106 MeV/c ²
τ	1.78 GeV/c ²

Table 1.2: The masses of the charged leptons.

$$\mu^- \rightarrow e^- \nu_\mu \bar{\nu}_e.$$

1.1.2 Quarks

Similarly, the three generations of quarks are organised into isospin doublets.

I	II	II
$\begin{pmatrix} u \\ d \end{pmatrix}$	$\begin{pmatrix} c \\ s \end{pmatrix}$	$\begin{pmatrix} t \\ b \end{pmatrix}$

Table 1.3: The quarks arranged into three isospin doublets. The top row has its third component of isospin $I_3 = +\frac{1}{2}$ and the bottom $I_3 = -\frac{1}{2}$. Equivalently, they have charges $Q = +\frac{2}{3}$ and $Q = -\frac{1}{3}$, respectively.

It is difficult to assign masses to the individual quarks since they are always bound. Most of the proton's mass is created dynamically by the strong interaction between the light valence quarks. For heavy quarks, assigning a mass from the difference between hadron masses becomes easier, and approximate masses are given in Table 1.4.

q	Mass
u	2.2 MeV/c ²
d	5 MeV/c ²
c	1.25 GeV/c ²
s	95 MeV/c ²
t	174.2 GeV/c ²
b	4.2 GeV/c ²

Table 1.4: Approximate quark masses. It is difficult to assign masses to the lighter quarks due to quark confinement and their strong interactions (see main body).

1.1.3 Bosons

The fundamental Standard Model bosons and their properties are listed in Table 1.5.

Quarks may combine to form hadrons that are non-fundamental bosons, e.g. $J^P(\pi^+) = 0^-$.

	Spin	Charge	Mass	Force
γ	1	0	0	EM
W^\pm	1	± 1	$80.4 \text{ GeV}/c^2$	Weak
Z	1	0	$91.2 \text{ GeV}/c^2$	Weak
g	1	0	0	Strong
H	0	0	$125 \text{ GeV}/c^2$	-

Table 1.5: The fundamental bosons of the Standard Model. The Higgs boson, H, does not mediate a force but rather is required for the W and Z bosons to have mass under electroweak symmetry breaking.

1.2 Forces

At our energy scale there are four fundamental forces of nature: electromagnetism (EM), weak, strong, and gravity.

Gravity does not currently have a quantum formulation. Quantum gravity (QG) is in its theoretical infancy and, as shown below, experiments cannot reach the energy scales required for gravity to manifest itself at subatomic scales.

1.2.1 Gravity

Our best understanding of gravity – that of general relativity (GR) – describes the force as a result of the geometrical properties of spacetime. As such, GR predicts the existence of gravitational waves; ripples in spacetime emerging from extreme astrophysical situations causing large masses to oscillate. Gravitational waves have not yet been directly observed, but observations from Hulse and Taylor over a 17 year period observed a change in the period of a binary neutron star system. This change can only be accounted for by gravitational radiation, thus the experiment is an indirect detection of gravitational waves. This work won the Nobel Prize in 1993.

Gravity is known to be by far the weakest of the four fundamental forces. It is thought to be mediated by a spin-2 boson, the graviton. The strength of a force is proportional to the exchange momentum of the mediating boson, so very large energies will be required to observe gravity in a collider.

For a theory of everything (TOE), there is some energy scale at which gravity will unify with the Standard Model describing EW and QCD interactions. This is called the Planck mass and is derived here from the uncertainty principle.

The Planck mass

According to the uncertainty principle, a particle with mass m can exist for time

$$\delta t \sim \frac{\hbar}{mc^2} \quad (1.1)$$

with a characteristic range

$$\delta r = \delta t \times c = \frac{\hbar}{mc}. \quad (1.2)$$

At this separation from the point mass, the gravitational potential energy between two particles with mass m is

$$V = \frac{Gm^2}{\delta r} = \frac{Gm^3 c}{\hbar}. \quad (1.3)$$

When this potential energy is similar to a particle's mass energy, then gravitational effects become important and a theory of quantum gravity is needed. This occurs when $V \sim mc^2$, i.e.

$$\frac{Gm^3 c}{\hbar} \sim mc^2 \quad (1.4)$$

which is rearranged to define the Planck mass

$$m_{\text{Planck}} \equiv \sqrt{\frac{\hbar c}{G}} \quad (1.5)$$

whose value is of the order $10^{19} \text{ GeV}/c^2$. Similarly, we may define the Planck length $\lambda_{\text{Planck}} \sim 10^{-35} \text{ m}$, and the Planck time $t_{\text{Planck}} \sim 10^{-43} \text{ s}$.

When calculating integrals in the Standard Model (such as when evaluating loops in Feynman diagrams), the upper limit of integration should be the Planck scale, since this is where our understanding of nature breaks down.

Dark matter

Dark matter is believed to constitute about 25% of the matter-energy content of the universe. This comes from observations of the rotational velocity curve of galaxies.

A simple model of a galaxy has a uniformly distributed spherical core with mass density ρ at radii below R and zero above. At gravitational equilibrium inside the galaxy, the centripetal force on some test star with mass m is equal to the gravitational pull from the core inside the shell at distance r from the centre,

$$\frac{mv^2}{r} = \frac{GmM(r)}{r^2} \quad (1.6)$$

$$\Rightarrow v^2 = \frac{GM(r)}{r} \quad (1.7)$$

$$= \frac{GM_{\text{galaxy}}}{r} \left(\frac{r}{R}\right)^3 \quad (1.8)$$

$$\Rightarrow v = \sqrt{\frac{GM_{\text{galaxy}}}{R^3} r}. \quad (1.9)$$

Outside the galaxy core we expect

$$v = \sqrt{\frac{GM_{\text{galaxy}}}{r}}. \quad (1.10)$$

The observed discrepancy is known as the galaxy rotation problem, where the mass distribution of the galaxy is calculated from its luminous regions. The solution to the problem predicts a halo of dark matter around the edge of the galaxy.

Candidates for dark matter include:

- Massive cool hadronic objects (MaCHOs). Brown dwarves are small, dark stars that have been observed via gravitational lensing. A large abundance of MaCHOs is unlikely due to the known baryonic makeup of the early universe. There is not a sufficient number of MaCHOs to account for the dark matter problem.
- Neutrinos. Since the mass of the neutrino is almost zero, neutrinos form hot dark matter. They carry thermal energy away from hot areas of the universe and do not cluster as halos around galaxies.
- Supersymmetric particles as cold dark matter. Cold dark matter (CDM) must be made up of heavy particles for little thermal movement. Supersymmetric particles are the favourite CDM candidates in light of observations such as the anisotropy of the early universe. Supersymmetry (SUSY) solves some problems of the Standard Model and provides a natural CDM candidate, a particle with mass $\sim 100 \text{ GeV}/c^2$. These heavy particles are known as WIMPs (weakly interacting massive particles).
- Light supersymmetric particles (LSPs) or hidden sector. Not yet explored area of particle physics could yield CDM candidates. There could be less massive particles that interact very weakly with ordinary matter; this is called the hidden sector. Additional theories of supersymmetry could predict light weakly interacting particles.

1.2.2 Electromagnetism

The electromagnetic (EM) force is described in the Standard Model by quantum electrodynamics (QED). All EM interactions involve the exchange of a virtual photon. The strength of the electromagnetic interaction is given by

$$\frac{e^2}{q^2} \quad (1.11)$$

where q is the virtual photon's 4-momentum. e is the electromagnetic coupling constant and is related to the fine structure constant by

$$e = \sqrt{4\pi\alpha}. \quad (1.12)$$

The fine structure constant is itself defined as the ratio of the energy to overcome electrostatic repulsion between two electrons a distance r apart and the energy of a photon of wavelength $\lambda = 2\pi r$,

$$\alpha = \frac{e^2}{4\pi\epsilon_0 r} \bigg/ \frac{hc}{\lambda} = \frac{e^2}{4\pi\epsilon_0 r} \bigg/ \frac{\hbar c}{r} = \frac{e^2}{4\pi\epsilon_0 \hbar c}. \quad (1.13)$$

In natural units, where $\hbar = c = \epsilon_0 = 1$, this becomes

$$\boxed{\alpha = \frac{e^2}{4\pi}}. \quad (1.14)$$

1.2.3 The weak force

The Fermi theory of weak interactions treats the nuclear beta decay as a single four-point vertex with strength g_F . The reaction is

$$n \rightarrow p + e^- + \bar{\nu}_e. \quad (1.15)$$

A more sophisticated treatment recognises the role of the virtual W boson being exchanges as quarks change flavor,

$$d \rightarrow u + W^- \rightarrow u + e^- + \bar{\nu}_e. \quad (1.16)$$

In contrast to the EM interaction above, the strength of an interaction involving the exchange of the massive W boson is

$$\frac{g_W^2}{q^2 + m_W^2} \quad (1.17)$$

where g_W is similar to the electromagnetic e . This means, at energies much less than the W mass, $q^2 \ll m_W^2$, the weak force is much weaker than the electromagnetic force. However, for energies near to and above the W mass, $q^2 \geq m_W^2$, the forces are comparable and unify at energies around 100 GeV or greater.

To first order, individual lepton numbers (i.e. electron, muon, tau number) are conserved in weak interactions. This is equivalent to saying there is no mixing in the lepton sector, since leptons do not experience the strong force. Some example weak processes follow.

$$\nu_e + n \rightarrow p + e^- \quad (1.18)$$

$$\bar{\nu}_e + p \rightarrow n + e^+ \quad (1.19)$$

$$\mu^- \rightarrow e^- + \nu_\mu + \bar{\nu}_e \quad (1.20)$$

1.2.4 The strong force

Protons and neutrons are confined to the nucleus, so there must be a force which overcomes the electrostatic repulsion of the positive EM charges and also acts on neutrons. In scattering experiments,

$$\pi^+ + p \xrightarrow{\Delta^{++}(1238)} \pi^+ + p \quad (1.21)$$

a resonance peak was seen at 1238 MeV/c², corresponding to the Δ^{++} resonance with valence quark contents uuu. Since all three quarks in the baryon have the same spatial wavefunction, flavor, and at least two must have the same spin projection, this violates the exclusion principle without further quantum numbers. Introducing a color quantum number, with three color charges, solves this problem and provides a mechanism responsible for nuclear structure and quark confinement. The extra quantum number also means that for every hadronic decay there are three possible final states, giving a three-times color degeneracy to those decay modes.

The $SU(3)$ gauge model of the strong force results in an octet of gluons, which can self-interact via three- and four-point vertices. These extra vertices mean there are many more QCD diagrams for a given process, and calculating amplitudes in QCD is, in general, quite difficult. Furthermore, the QCD coupling constant is large – owing to its high strength versus the electromagnetic interaction – so, in general, one cannot stop with the first-order diagram. However, the running of the strong coupling constant means it decreases at high energies, so at LHC energies it is possible to use perturbation theory with QCD processes.

1.3 Local gauge invariance

The Lagrangian of a gauge theory is invariant under local transformations belonging to a particular symmetry group. This gauge invariance gives rise to the forces in the Standard Model – EW and QCD. Why nature insists on gauge invariance is unknown.

As an example, consider a scalar theory of electromagnetism. Local gauge invariance under transformations belonging to the group $U(1)$ requires the Lagrangian is invariant to a rotation in phase space,

$$\psi(x, t) \rightarrow e^{i\alpha(x)}\psi(x, t). \quad (1.22)$$

The transformation is said to be *local* because the phase $\alpha(x)$ is a general function of space. Now requiring $\delta\mathcal{L} = 0$ leads to the introduction of a massless gauge field, A^μ ; this is the photon field.

Similarly, local gauge invariance under transformations belonging to the groups $SU(2)$ and $SU(3)$ gives rise to the weak and strong forces, respectively. In this approach, however, the gauge bosons are all required to be massless, contrary to observations.

1.4 Spontaneous symmetry breaking

The EM and weak interactions have been successfully unified. That is, they have been shown to be two manifestations of the same $[SU(2) \times U(1)]$ electroweak (EW) force, which they become at a higher energy (around 100 GeV ¹). As the universe cooled below this electroweak unification energy, the distinct EM and weak forces we see at normal energies froze out of the more general EW force. The spontaneous symmetry breaking leading to the EM and weak forces was described by Glashow, Salam, and Weinberg (GSW). The mechanism that allows the W and Z bosons to have mass after the EW symmetry breaking is the Higgs mechanism, of which the Higgs boson is a result. The strong force is described by quantum electrodynamics (QCD) and has not yet been unified with the EW interaction.

1.5 Grand unified theories

A grand unified theory (GUT) would bring the EW and QCD interactions together under a grand unified group, G or $SU(5)$. Such theories would have to restore the broken symmetry we observe between colorless leptons and colored quarks, allowing quarks to turn into antileptons and vice versa. These interactions would violate conservation of baryon number, B , but $B - L$ (where L is lepton number) would be conserved. The exchange boson is called the X boson, which would have a mass of order $10^6\text{ GeV}/c^2$ and hence a range 10^{-4} times the weak force's.

This GUT force hence predicts the decay of the proton, which has not yet been observed although current experiments are attempting to measure the lifetime of the proton, if it is indeed unstable. An example decay is $p \rightarrow e^+ + \pi^0$.

¹In fact, the phase transition occurs at the Higgs vacuum expectation value (VEV), about 246 GeV . The strength of the EM and weak forces merge at around 100 GeV , so they appear as similar forces.

Chapter 2

Experimental Concepts

This chapter serves as a reminder of commonly used ideas in high-energy physics (HEP) experiments.

2.1 Experimental possibilities

In reality there are rather few experimental possibilities for HEP experiments:

- Scatter one particle off another and observe the reaction;
- Generate a particle in a reaction and observe its decay;
- Detect neutrinos and observe neutrino oscillations;
- Measure a particular particle's properties such as mass, charge, spin, parity, lifetime.

2.2 Cross section

The cross section, σ , for a particular reaction is proportional to the probability for the interaction to take place. In HEP experiments, it is expressed in the unit barns, where $1 \text{ b} = 1 \times 10^{-28} \text{ m}^2$.

2.2.1 Beam incident on a target

Assume the beam is comprised of bunches with N_B particles per bunch. The beam is incident on a target with area A , length l inside the luminous region, and mass density ρ . Then the number of target particles seen by the beam is

$$N_T = \frac{A l \rho N_A}{m} \quad (2.1)$$

where N_A is Avagadro's number and m is the molecular mass, such that N_A/m is the mass of each target particle.

Now we can define the cross section as

$$P(\text{interaction}) = (\text{Number of target particles per unit area}) \times \sigma \quad (2.2)$$

$$\begin{aligned} &= \frac{Al\rho N_A}{m} \times \frac{\sigma}{A} \\ &= \frac{l\rho N_A \sigma}{m}. \end{aligned} \quad (2.3)$$

Therefore the total number of interactions per bunch is given by

$$N_I = \frac{l\rho N_A N_B \sigma}{m}. \quad (2.4)$$

Now take the target and bunch to contain number densities n_B and n_T of particles, respectively. They have relative speed $u \simeq c$. Then the number of target particles in the luminous region is $n_T V$, so the probability of interaction may now be written

$$P(\text{interaction}) = \frac{n_T V \sigma}{A}. \quad (2.5)$$

There are $n_B u A$ beam particles passing through the luminous region per second, so the rate of interactions is

$$\frac{dN_I}{dt} = n_B n_T V u \sigma. \quad (2.6)$$

2.2.2 Beam-beam collision

For a circular collider, assume a rotation frequency f for both counter-circulating beams consisting of n bunches, each with N_B particles and area A . Then the rate of interactions is

$$\frac{dN_I}{dt} = P(\text{collision}) \times (\text{particles per second in one beam}) \quad (2.7)$$

$$\begin{aligned} &= \frac{N_B \sigma}{A} \times n f N_B \\ &= \frac{n f N_B^2 \sigma}{A}. \end{aligned} \quad (2.8)$$

2.3 Luminosity

Using the result from (2.8), we define the instantaneous luminosity

$$L \equiv \frac{1}{\sigma} \frac{dN_I}{dt} \quad (2.9)$$

hence for beam-beam collisions

$$L = \frac{n f N_B^2}{A}. \quad (2.10)$$

In an effort to increase the luminosity, focussing magnets near to the collision regions are used to decrease the bunch area. Also, the number of particles per bunch should be made as large as possible while also maintaining a stable bunch.

Spontaneous luminosity tends to decrease with run time due to collision remnants decreasing the vacuum in the beam pipe and consequently deforming the bunches. An LHC beam has a typical lifetime of around 10–15 hours (the lifetime is the time for L to decay by a factor e). At this point the beam is dumped and a new beam is accelerated and injected into the storage ring ready for collisions.

The units of L are typically $\text{pb}^{-1} \text{s}^{-1}$. To get a measure of the total number of interactions observed, and hence the amount of data collected, L may be integrated to give the integrated luminosity,

$$\boxed{L_{\text{int}} = \int L \, dt} \quad (2.11)$$

which often has the units of inverse femtobarns, fb^{-1} .

2.4 Natural units and conversion factors

In natural units, we have $\hbar = c = 1$. c is the conversion factor between space and time or mass and energy, and \hbar is the conversion between energy and time. Consider the units of their product:

$$\begin{aligned} [\hbar c] &= [ET][LT^{-1}] \\ &= [E][L]. \end{aligned} \quad (2.12)$$

Now we have $c = 3 \times 10^8 \text{ m s}^{-1}$ and $\hbar = 1.05 \times 10^{-34} \text{ J s} = 6.56 \times 10^{-22} \text{ MeV s}$, so

$$\boxed{\hbar c = 197 \text{ MeV fm} \equiv 1}. \quad (2.13)$$

Therefore, we have

$$1 \text{ GeV} = \frac{1000}{197 \text{ fm}} = 5.08 \times 10^{15} \text{ m}^{-1} = 1.52 \times 10^{24} \text{ s}^{-1} \quad (2.14)$$

$$\Rightarrow \frac{1}{\text{GeV}^2} = 3.88 \times 10^{-32} \text{ m}^2 = 0.388 \text{ mb}. \quad (2.15)$$

Chapter 3

Experiments of the Last 60 Years

Chapter 4

Non-Relativistic Quantum Mechanics

Here an overview of some basic results from Schrödinger and Heisenberg's quantum mechanics are given. The quantum harmonic oscillator (QHO) is solved exactly, and extended to the anharmonic case with first-order perturbation theory. Lagrangian mechanics is briefly covered, before some consideration of the important Dirac δ and Heaviside θ step functions.

A time-varying quantum state may be expressed by a vector $|\psi(t)\rangle$. In the position representation, this yields the wavefunction, $\psi(x, t) \equiv \langle x | \psi(t) \rangle$.

4.1 Schrödinger's equation and probability current density

We start from the classical energy-momentum relation for a non-relativistic particle with mass m ,

$$E = \frac{p^2}{2m}. \quad (4.1)$$

Replace the energy with the operator $E \rightarrow \hat{E} = i\frac{\partial}{\partial t}$ and momentum with $p \rightarrow \hat{p} = -i\nabla$. Then (4.1) becomes the time-dependent Schrödinger equation (TDSE),

$$i\frac{\partial\psi}{\partial t} = -\frac{1}{2m}\nabla^2\psi. \quad (4.2)$$

Multiplying this by the complex conjugate of the wavefunction, ψ^* ,

$$i\psi^*\frac{\partial\psi}{\partial t} = -\frac{1}{2m}\psi^*\nabla^2\psi. \quad (4.3)$$

Take the complex conjugate of (4.2) and multiply by ψ ,

$$-i\frac{\partial\psi^*}{\partial t}\psi = -\frac{1}{2m}(\nabla^2\psi^*)\psi. \quad (4.4)$$

Subtracting (4.4) from (4.3),

$$i\left(\psi^*\frac{\partial\psi}{\partial t} + \frac{\partial\psi^*}{\partial t}\psi\right) = -\frac{1}{2m}\left[\psi^*(\nabla^2\psi) - \psi(\nabla^2\psi^*)\right] \quad (4.5)$$

and rearranging using the product rule,

$$\frac{\partial}{\partial t}(\psi^* \psi) + \frac{i}{2m} \nabla \cdot [\psi(\nabla \psi^*) - (\nabla \psi)\psi^*] = 0. \quad (4.6)$$

This is nothing but a continuity equation for the probability density $\rho = \psi^* \psi = |\psi|^2$ and the probability current density $\mathbf{j} = \frac{i}{2m} [\psi(\nabla \psi^*) - (\nabla \psi)\psi^*]$.

Application to a plane wave

Consider a free plane wave whose wavefunction is given by $\psi(x, t) = \mathcal{N}e^{i(\mathbf{p} \cdot \mathbf{x} - Et)}$, where \mathcal{N} is a normalisation constant. Then, applying the definitions for ρ and \mathbf{j} above,

$$\rho = |\psi|^2 = |\mathcal{N}|^2 \quad (4.7)$$

$$\mathbf{j} = \frac{i}{2m} [\psi(\nabla \psi^*) - (\nabla \psi)\psi^*] = \frac{|\mathcal{N}|^2}{m} \mathbf{p} \quad (4.8)$$

4.2 Heisenberg and interaction pictures

4.2.1 Heisenberg picture

In the above, we have used the Schrödinger picture where operators remain constant in time, and the states can vary. In contrast, the Heisenberg picture treats the states as constants, and the operators evolve in time. To show that these are equivalent, solve the time-independent Schrödinger equation for an energy eigenstate $|\psi(t)\rangle$.

$$i \frac{d}{dt} |\psi(t)\rangle = \hat{H} |\psi(t)\rangle \quad (4.9)$$

$$\Rightarrow \int_0^t \frac{d}{dt'} |\psi(t')\rangle = -i \int_0^t \hat{H} dt' \quad (4.10)$$

$$\Rightarrow |\psi(t)\rangle = e^{-i\hat{H}t} |\psi(0)\rangle \quad \text{for time-independent } \hat{H}. \quad (4.11)$$

In quantum mechanics, observables connect the theory with measurements. Observable quantities are expectation values of operators. Consider some general operator, \hat{A} , whose expectation value is given by

$$\langle A \rangle = \langle \psi(t) | \hat{A} | \psi(t) \rangle \quad (4.12)$$

$$= \langle \psi(0) | e^{i\hat{H}t} \hat{A} e^{-i\hat{H}t} | \psi(0) \rangle. \quad (4.13)$$

Therefore, it is equivalent to define time-independent states and time-dependent operators in the Heisenberg picture:

$$|\psi_H\rangle \equiv |\psi(0)\rangle \quad (4.14)$$

$$\hat{A}_H \equiv e^{i\hat{H}t} \hat{A} e^{-i\hat{H}t}. \quad (4.15)$$

Then the expectation value is simply

$$\langle A \rangle = \langle \psi_H | \hat{A}_H | \psi_H \rangle \quad (4.16)$$

and

$$\begin{aligned} \frac{d\hat{A}_H}{dt} &= i\hat{H}e^{i\hat{H}t}\hat{A}e^{-i\hat{H}t} - ie^{i\hat{H}t}\hat{A}\hat{H}e^{-i\hat{H}t} \\ &= i(\hat{H}\hat{A} - \hat{A}\hat{H}) \\ &= i[\hat{H}, \hat{A}] \end{aligned} \quad (4.17)$$

4.2.2 The interaction picture

In the interaction picture, both states and operators have some time dependence. In the interaction picture, we split the Hamiltonian into a free part \hat{H}_0 and interaction part \hat{H}' ,

$$\hat{H} = \hat{H}_0 + \hat{H}'. \quad (4.18)$$

The free part is generally time-independent and easily solved. We then say that operators \hat{A}_I evolve according to the free part of the Hamiltonian,

$$\hat{A}_I(t) = e^{i\hat{H}_0 t} \hat{A} e^{-i\hat{H}_0 t}. \quad (4.19)$$

Then the operator in the interaction picture evolves according to

$$\frac{d\hat{A}_I}{dt} = i[\hat{H}_0, \hat{A}_I(t)]. \quad (4.20)$$

Now consider the expectation value of the operator, $\langle A \rangle = \langle \psi_I(t) | e^{i\hat{H}_0 t} \hat{A} e^{-i\hat{H}_0 t} | \psi_I(t) \rangle$. We see that for this to be equivalent to the Schrödinger picture expectation value, the states must evolve according to the interaction part of the Hamiltonian \hat{H}' ,

$$|\psi_I(t)\rangle = e^{-i\hat{H}' t} |\psi(0)\rangle \quad (4.21)$$

or equivalently

$$|\psi_I(t)\rangle = e^{i\hat{H}_0 t} |\psi(t)\rangle. \quad (4.22)$$

The interaction picture is used in the perturbative expansion of the S -matrix in quantum field theory (QFT). This leads to the concept of using Feynman diagrams to calculate amplitudes.

Note that the three different pictures of quantum mechanics coincide at $t = 0$.

4.3 Quantum harmonic oscillator

The quantum harmonic oscillator is an exactly solvable problem that neatly introduces ladder operators.

Consider a Hamiltonian of the form

$$H = \frac{p^2}{2m} + \frac{1}{2}m\omega^2 x^2 \quad (4.23)$$

where it should be clear from the context which quantities are operators, so we drop the hat notation, $\hat{O} \rightarrow O$.

Introduce the ladder operator

$$a = \frac{m\omega x + ip}{\sqrt{2m\omega}} \quad (4.24)$$

and bearing in mind that x and p are hermitian,

$$a^\dagger = \frac{m\omega x - ip}{\sqrt{2m\omega}}. \quad (4.25)$$

The product $a^\dagger a$ is

$$\begin{aligned} a^\dagger a &= \frac{(m\omega x - ip)(m\omega x + ip)}{2m\omega} \\ &= \frac{1}{2m\omega} \left\{ (m\omega x)^2 + im\omega[x, p] + p^2 \right\} \\ &= \frac{H}{\omega} - \frac{1}{2}. \end{aligned} \quad (4.26)$$

Rearranging, the Hamiltonian can be written

$$H = \left(a^\dagger a + \frac{1}{2} \right) \omega. \quad (4.27)$$

Similarly,

$$aa^\dagger = \frac{H}{\omega} + \frac{1}{2}. \quad (4.28)$$

We also have that

$$[a, a^\dagger] = 1 \quad (4.29)$$

and

$$[a, H] = \omega a \quad (4.30)$$

$$[a^\dagger, H] = -\omega a^\dagger. \quad (4.31)$$

4.3.1 Energy spectrum

Now consider the action of the operator a^\dagger on a stationary state $|n\rangle$ with some energy E_n . What is the energy of the state $a^\dagger |n\rangle$?

$$\begin{aligned} H a^\dagger |n\rangle &= \left(a^\dagger H - [a^\dagger, H] \right) |n\rangle \\ &= \left(a^\dagger H + \omega a^\dagger \right) |n\rangle \\ &= (E_n + \omega) a^\dagger |n\rangle. \end{aligned} \quad (4.32)$$

So $a^\dagger |n\rangle$ is also an energy eigenstate with energy $(E_n + \omega)$. Since a^\dagger has raised the energy of the state $|n\rangle$ by one quantum of energy, we call it the raising operator.

Similarly, the application of a to $|n\rangle$ lowers the energy by ω ,

$$H a |n\rangle = (E_n - \omega) a |n\rangle. \quad (4.33)$$

a is called the lowering operator and together a and a^\dagger are ladder operators that span the energy spectrum of the QHO. In QFT, these operators correspond to the creation and annihilation of particles since particles are wave excitations of the vacuum.

4.3.2 Zero-point energy

There must be some state $|0\rangle$ for which $a|0\rangle$ vanishes. Equating to zero the square length of this state vector,

$$0 = |a|0\rangle|^2 = \langle 0|a^\dagger a|0\rangle \quad (4.34)$$

$$\begin{aligned} &= \langle 0|\frac{H}{\omega} - \frac{1}{2}|0\rangle \\ &= \frac{E_0}{\omega} - \frac{1}{2}. \end{aligned} \quad (4.35)$$

Rearranging gives the energy of the vacuum state, $|0\rangle$,

$$E_0 = \frac{\omega}{2}. \quad (4.36)$$

4.3.3 Action of the ladder operators

Now we can build up the ladder of energy states by continuous action of the raising operator,

$$\begin{aligned} a^\dagger |0\rangle &= \alpha_0 |1\rangle \\ a^\dagger |1\rangle &= \alpha_1 |2\rangle \\ &\dots \\ a^\dagger |n\rangle &= \alpha_n |n+1\rangle \end{aligned}$$

where the normalisation constant can be found via

$$\begin{aligned} \alpha_n^2 &= |a^\dagger |n\rangle|^2 = \langle n|aa^\dagger|n\rangle \\ &= \langle n|\frac{H}{\omega} + \frac{1}{2}|n\rangle \\ &= n+1 \end{aligned} \quad (4.37)$$

so $\alpha_n = \sqrt{n+1}$. Therefore the general action of the raising operator is

$$\boxed{a^\dagger |n\rangle = \sqrt{n+1} |n+1\rangle}. \quad (4.38)$$

Similarly,

$$\boxed{a |n\rangle = \sqrt{n} |n-1\rangle}. \quad (4.39)$$

A general state $|n\rangle$ can be made from repeated application of a^\dagger from the ground state:

$$|n\rangle = \frac{1}{\sqrt{n!}} (a^\dagger)^n |0\rangle. \quad (4.40)$$

Notice that $a^\dagger a |n\rangle = n |n\rangle$, so $a^\dagger a$ is called the number operator.

4.4 The anharmonic oscillator (perturbation theory)

We now generalise the above QHO to include an anharmonic term,

$$H = \frac{p^2}{2m} + \frac{1}{2}m\omega^2 x^2 + \lambda x^3 \quad (4.41)$$

$$= H_0 + \lambda H' \quad (4.42)$$

where the second line expresses the Hamiltonian as in the interaction picture. In this case, the interaction hamiltonian is $H' = x^3$. In what follows, we assume that λ is small such that H' is a perturbation to the QHO solution and we stop expansions after first order in λ .

The eigenvectors of the full Hamiltonian may be expanded as

$$|n\rangle = |n\rangle^0 + \lambda |n\rangle^1 + \dots \quad (4.43)$$

where all the $|n\rangle^i$ are assumed to be orthogonal. The state has corresponding energy

$$E_n = E_n^0 + E_n^1 + \dots \quad (4.44)$$

such that it is the solution of the TISE,

$$H |n\rangle = E_n |n\rangle \quad (4.45)$$

$$(H_0 + \lambda H' + \dots) (|n\rangle^0 + \lambda |n\rangle^1 + \dots) = (E_n^0 + \lambda E_n^1 + \dots) (|n\rangle^0 + \lambda |n\rangle^1 + \dots) \quad (4.46)$$

Equating the coefficients of λ^0 gives the trivial harmonic part of the solution,

$$H_0 |n\rangle^0 = E_n^0 |n\rangle^0. \quad (4.47)$$

Equating the coefficients of λ^1 gives

$$H_0 |n\rangle^1 + H' |n\rangle^0 = E_n^0 |n\rangle^1 + E_n^1 |n\rangle^0. \quad (4.48)$$

Rearranging and multiplying by ${}^0\langle n|$,

$${}^0\langle n| H_0 - E_n^0 |n\rangle^1 + {}^0\langle n| H' - E_n^1 |n\rangle^0 = 0. \quad (4.49)$$

Now use that ${}^0\langle n| H_0 = {}^0\langle n| E_n^0$ to see that the first term is equal to zero. This gives the solution for the change in energy (up to first order in λ) of the n th excited state,

$$\boxed{E_n^1 = {}^0\langle n| H' |n\rangle^0}. \quad (4.50)$$

Now we wish to find the first-order correction to the state, $|n\rangle^1$. First, use the representation of $|n\rangle^1$ in the basis of harmonic solutions, $|m\rangle^0$,

$$|n\rangle^1 = \sum_m |m\rangle^0 {}^0\langle m|n\rangle^1. \quad (4.51)$$

The eigenstates of the harmonic problem $|m\rangle^0$ may serve as a basis since they are all orthonormal, i.e. ${}^0\langle m|n\rangle^0 = \delta_{nm}$.

Now to get the coefficients ${}^0\langle m|n\rangle^1$, multiply (4.48) by ${}^0\langle m|$,

$$\underbrace{{}^0\langle m|H_0|n\rangle^1}_{E_m^0 {}^0\langle m|n\rangle^1} + {}^0\langle m|H'|n\rangle^0 = {}^0\langle m|E_n^0|n\rangle^1 + \underbrace{{}^0\langle m|E_n^1|n\rangle^0}_0. \quad (4.52)$$

Rearranging,

$${}^0\langle m|n\rangle^0 = \frac{{}^0\langle m|H'|n\rangle^0}{E_n^0 - E_m^0}. \quad (4.53)$$

Notice that this approach only works if the energy levels are non-degenerate, i.e. $E_n^0 \neq E_m^0$ for all $n \neq m$. For the QHO this is the case, but in more general cases one must diagonalise the Hamiltonian first.

Now, substituting (4.53) into (4.51) gives the value of the first-order correction to the energy eigenstates,

$$|n\rangle^1 = \sum_m \frac{{}^0\langle m|H'|n\rangle^0}{E_n^0 - E_m^0} |m\rangle^0. \quad (4.54)$$

In the particular case where $H' = x^3$ it is helpful to express the perturbation in terms of the ladder operators,

$$x^3 = \frac{(a + a^\dagger)^3}{(2m\omega)^{\frac{3}{2}}}. \quad (4.55)$$

Then the determination of E_n^1 and $|n\rangle^1$ is achievable via the application of the ladder operators to the QHO eigenstates.

4.5 Lagrangian mechanics

In general, a Lagrangian is a function of coordinates q and their derivatives, $L = L(q, \dot{q})$. The action is the integral of L ,

$$S = \int L(q, \dot{q}) dt. \quad (4.56)$$

Classical paths are those paths with stationary action, where $\delta S = 0$. This requires,

$$\delta S = \int dt \left\{ \frac{\partial L}{\partial q} \delta q + \frac{\partial L}{\partial \dot{q}} \delta \dot{q} \right\} \quad (4.57)$$

$$= \int dt \left\{ \left[\frac{\partial L}{\partial q} - \frac{d}{dt} \left(\frac{\partial L}{\partial \dot{q}} \right) \right] \delta q \right\} + \left[\frac{\partial L}{\partial \dot{q}} \delta q \right]_{t_1}^{t_2} = 0. \quad (4.58)$$

The last term is a total derivative and vanishes for any δq that decays at spatial infinity and obeys $\delta q(t_1) = \delta q(t_2)$. For all such paths, we obtain the Euler-Lagrange equations of motion,

$$\boxed{\frac{\partial L}{\partial q} - \frac{d}{dt} \left(\frac{\partial L}{\partial \dot{q}} \right) = 0}. \quad (4.59)$$

4.5.1 Relation to the Hamiltonian

Each coordinate q has a conjugate momentum,

$$p = \frac{\partial L}{\partial \dot{q}}. \quad (4.60)$$

Then the Hamiltonian is related to the Lagrangian by

$$\boxed{H = p\dot{q} - L} \quad (4.61)$$

For a quantum treatment, we replace the coordinates with operators. The operators and their conjugate momenta have the commutation relations

$$[\hat{q}, \hat{p}] = i \quad (4.62)$$

in natural units.

4.5.2 Application to the QHO

The QHO Lagrangian is

$$L = \frac{1}{2}m\dot{x}^2 - \frac{1}{2}m\omega^2 x^2. \quad (4.63)$$

Therefore the momentum, $p = \frac{\partial L}{\partial \dot{x}} = m\dot{x}$. So the Hamiltonian is

$$H = p\dot{x} - L \quad (4.64)$$

$$= \frac{p^2}{m} - \left(\frac{1}{2}m\dot{x}^2 - \frac{1}{2}m\omega^2 x^2 \right) \quad (4.65)$$

$$= \frac{1}{2}m\dot{x}^2 + \frac{1}{2}m\omega^2 x^2 \quad (4.66)$$

which is the same as we used for the QHO above.

The Lagrangian and Hamiltonian treatments are equivalent, but often a problem is more soluble in one over the other. QFT makes use of the Lagrangian density, and this is used to express the particles and interactions of the Standard Model.

4.6 Dirac δ function

The δ function may be thought of as a peaked function of width Δx and height $1/\Delta x$ around a value $x = x_0$ in the limit $\Delta x \rightarrow 0$. It has the properties

$$\int_{-\infty}^{+\infty} \delta(x - x_0) dx = 1 \quad (4.67)$$

and

$$\int_{-\infty}^{+\infty} f(x) \delta(x - x_0) dx = f(x_0). \quad (4.68)$$

As a result, $\delta(x) - \delta(-x)$ is an even function and $\delta(ax) = \delta x/|a|$. The proof is as follows:

$$\int_{-\infty}^{+\infty} \delta(ax) dx = \int_{-\infty}^{+\infty} \delta(y) \frac{dy}{a} \quad \text{for } y = ax, \quad (4.69)$$

$$= \frac{1}{|a|}. \quad (4.70)$$

Now consider a function $f(x)$ with roots a_i such that $f(a_i) = 0$. Then $\delta(f(x))$ function is non-zero only in the vicinity $x \sim a_i$. Expanding $f(x)$ about a particular root,

$$f(x) = \underbrace{f(a_i)}_0 + (x - a_i) \left[\frac{\partial f}{\partial x} \right]_{x=a_i} + \dots \quad (4.71)$$

so, using the preceding result, we have

$$\delta(f(x)) = \sum_i \delta \left((x - a_i) \left[\frac{\partial f}{\partial x} \right]_{x=a_i} \right) \quad (4.72)$$

$$= \sum_i \frac{\delta(x - a_i)}{\left| \frac{\partial f}{\partial x} \right|_{x=a_i}}. \quad (4.73)$$

The δ function is normally constructed by taking the limit of some test function. Here, various test functions are discussed.

Discrete δ function

Consider some function $f(x)$ as a set of values x_i in bins of width Δx . Then the integral becomes a discrete sum,

$$\int_{-\infty}^{+\infty} f(x) \delta_t(x - x_0) dx \rightarrow \sum_{i=-\infty}^{+\infty} f(x_i) \delta(x_i - x_0) \Delta x \quad (4.74)$$

where $\delta_t(x - x_0) = 0$ for $i \neq 0$ and $\delta_t(0) = 1/\Delta x$. In the limit $\Delta x \rightarrow 0$, δ_t becomes the Dirac δ function. However, it is not particularly useful to have a discrete, non-differentiable definition.

Breit-Wigner lineshape

Consider a test function of a Breit-Wigner resonance peak,

$$\delta_t(x) = \frac{1}{\pi} \frac{\epsilon}{x^2 + \epsilon^2}. \quad (4.75)$$

Its integral is

$$\int_{-\infty}^{+\infty} \frac{1}{\pi} \frac{\epsilon}{x^2 + \epsilon^2} dx = \int_{-\pi/2}^{+\pi/2} \frac{1}{\pi} \frac{\sec^2 \theta}{1 + \tan^2 \theta} d\theta = 1 \quad (4.76)$$

where the substitution $x = \epsilon \tan \theta$ has been used. At $x = 0$, $\delta_t(0) = 1/\pi\epsilon$ and the full width at half-maximum is 2ϵ . The Breit-Wigner lineshape approaches the Dirac δ function in the limit $\epsilon \rightarrow 0$.

Fourier analysis

The Fourier integral theorem states that

$$f(x) = \frac{1}{2\pi} \int_{-\infty}^{+\infty} e^{ipx} \left(\int_{-\infty}^{+\infty} e^{-p\alpha} f(\alpha) d\alpha \right) dp. \quad (4.77)$$

That is, the reverse transform of the Fourier transform of a function returns the original function. Rearranging¹,

$$f(x) = \frac{1}{2\pi} \int_{-\infty}^{+\infty} \left(\int_{-\infty}^{+\infty} e^{pix} e^{-ip\alpha} dp \right) f(\alpha) d\alpha = \int_{-\infty}^{+\infty} \delta(x - \alpha) f(\alpha) d\alpha \quad (4.78)$$

where we see the δ function can now be defined

$$\delta(x) = \frac{1}{2\pi} \int_{-\infty}^{+\infty} e^{ipx} dp. \quad (4.79)$$

4.7 Heaviside step function

The Heaviside step function is defined in discrete form

$$\theta(x) = \begin{cases} 1 & x > 0 \\ 0 & x < 0 \end{cases} \quad (4.80)$$

An integral representation for θ can be reached through recognising that its derivative is the Dirac δ function,

$$\frac{d\theta}{dx} = \delta(x) = \frac{1}{2\pi} \int_{-\infty}^{+\infty} e^{ipx} dp. \quad (4.81)$$

Integrating with respect to x ,

$$\theta(x) = \frac{1}{2\pi} \int_{-\infty}^{+\infty} \int e^{ipx} dp dx \quad (4.82)$$

$$= \frac{1}{2\pi i} \int_{-\infty}^{+\infty} \frac{e^{ipx}}{p} dp \quad (4.83)$$

where the constant of integration is zero. Adding a small offset to the denominator, we get the final integral form of the θ step function

$$\theta(x) = \lim_{\epsilon \rightarrow 0^+} \frac{1}{2\pi i} \oint_C \frac{e^{ipx}}{p + i\epsilon} dp. \quad (4.84)$$

where C is a contour along the real axis closed in the upper-half plane.

¹Cauchy showed that the order of integration matters, but this rearrangement is justified under the *theory of distributions*.

The residue theorem states that

$$\oint_C \frac{f(z)}{z-a} dz = 2\pi i f(a) \quad (4.85)$$

for a contour C containing a . Applying this to the integral representation for θ above,

$$\theta(x) = \lim_{\epsilon \rightarrow 0^+} \frac{2\pi i}{2\pi i} e^{ip(-i\epsilon)} = \lim_{\epsilon \rightarrow 0^+} e^{p\epsilon} = 1 \quad (4.86)$$

for $x > 0$. For $x < 0$, the contour must be closed in the lower-half plane and the integral evaluates to 0.

Chapter 5

Special relativity

The study of high energy physics involves particles travelling at speeds close to c and often with energies much greater than their mass. Therefore, much of the notation and calculations used stem from a proper treatment of special relativity (SR).

5.1 4-vectors

SR places space and time on an equal footing and they adopt the same units in the system of natural units. We combine the information in time and space as components in a 4-vector, for example,

$$x^\mu = \begin{pmatrix} t \\ \mathbf{r} \end{pmatrix}, \quad p^\mu = \begin{pmatrix} E \\ \mathbf{p} \end{pmatrix}.$$

Note that in contravariant form (with the index up), 4-vectors are written as column vectors.

The metric tensor is a symmetric matrix that tells us how to link space and time. In the case of special relativity, it is simply a diagonal matrix¹,

$$g_{\mu\nu} = \begin{pmatrix} 1 & & & \\ & -1 & & \\ & & -1 & \\ & & & -1 \end{pmatrix} = g^{\mu\nu}. \quad (5.1)$$

The metric tensor may be used to perform index gymnastics to raise or lower an index. For example, we can find the covariant forms of the above 4-vectors,

$$x_\mu = g_{\mu\nu}x^\nu = (t, -\mathbf{r}), \quad p_\mu = g_{\mu\nu}p^\nu = (E, -\mathbf{p}).$$

The scalar product of two 4-vectors is given by

$$a_\mu b^\mu = g_{\mu\nu}a^\nu b^\mu = b_\mu a^\mu. \quad (5.2)$$

¹The $(+, -, -, -)$ signature is most often used in high energy physics since most 4-vector quantities we deal with will be timelike. By contrast, general relativity usually uses the $(-, +, +, +)$ signature. Using either signature is valid, but it is important to not confuse them.

Note the scalar product is invariant to which vector is covariant. Often, when only dealing with scalar products, we use the notation of a capital letter with no index for a 4-vector: X , P , A , etc. Then a scalar product may be written, for instance, as $XX = X^2$.

Finally, introduce the 4-vector derivative in covariant form,

$$\partial_\mu = \left(\frac{\partial}{\partial t}, \nabla \right). \quad (5.3)$$

then its square length is

$$\partial^2 = \partial_\mu \partial^\mu = \left(\frac{\partial}{\partial t} \right)^2 - \nabla^2. \quad (5.4)$$

5.2 Lorentz transformation

The Lorentz transformation is given by $x^\mu \rightarrow (x')^\mu$ where

$$\begin{pmatrix} t' \\ x' \\ y' \\ z' \end{pmatrix} = \begin{pmatrix} \gamma & -\beta\gamma & & \\ -\beta\gamma & \gamma & & \\ & & 1 & \\ & & & 1 \end{pmatrix} \begin{pmatrix} t \\ x \\ y \\ z \end{pmatrix} \quad (5.5)$$

for a 4-vector boosted by speed β along the x -axis. For completeness, we define γ here,

$$\gamma = \frac{1}{\sqrt{1 - \beta^2}}. \quad (5.6)$$

The scalar product $a_\mu b^\mu$, and in fact any fully-contracted quantity, is invariant under Lorentz transformations, since they do not depend on the coordinates.

5.3 The light cone

Consider two events with 4-coordinates X and Y . The square of their spacetime separation is given by

$$s^2 = (X - Y)^2 = (t_x - t_y)^2 - (\mathbf{x} - \mathbf{y})^2. \quad (5.7)$$

Along the surface of the light cone, $s = 0$. This condition gives

$$t_x - t_y = |\mathbf{x} - \mathbf{y}| \quad (5.8)$$

i.e. if a flash of light is emitted at X , it reaches \mathbf{y} at t_y . If $s^2 > 0$, then $t_x - t_y > |\mathbf{x} - \mathbf{y}|$ and a light pulse emitted at X reaches \mathbf{y} before t_y . Therefore, the events are causally connected and their separation is said to be timelike. For $s^2 < 0$, the events have spacelike separation and are causally disjoint.

5.4 Relativistic kinematics

In particle physics, there are two processes we could consider. Firstly, the decay of one particle into daughter particles,

$$A \rightarrow B + C + \dots \quad (5.9)$$

where the simplest case is that of two-body decay, $A \rightarrow B + C$. Here the centre of mass (CM) energy is simply the mass of the parent particle, m_A . Secondly, a scattering process,

$$A + B \rightarrow C + D + \dots \quad (5.10)$$

where the CM energy is given by $E_{CM}^2 = (P_A + P_B)^2 = (P_C + P_D + \dots)^2$ (recall that P_i is a 4-momentum).

5.4.1 Fixed target particle production

Consider the process

$$A + B \rightarrow C \quad (5.11)$$

where the target B is at rest in the laboratory frame. Therefore, $P_B = (m_B, \mathbf{0})$.

The centre of mass energy is given by

$$E_{CM}^2 = (P_A + P_B)^2 \quad (5.12)$$

$$= E_A^2 + 2E_A m_B + m_B^2 - |\mathbf{p}_A|^2 \quad (5.13)$$

Use that $E_A^2 - |\mathbf{p}_A|^2 = m_A^2$,

$$E_{CM}^2 = m_A^2 + m_B^2 + 2E_A m_B \quad (5.14)$$

A typical beam has energy much greater than either of the masses involved, so we may write

$$\boxed{E_{CM} \approx \sqrt{2E_A m_B}} \quad (5.15)$$

At the production threshold, $E_{CM} = E_C$. This means that for a proton target ($m_B \sim 1 \text{ GeV}$), the incident particle energy required to produce a Higgs boson ($m_C \sim 100 \text{ GeV}$) is about 5 TeV. For a hadronic beam about one tenth of the beam energy goes into collisions so this would require a 50 TeV beam. In fact, fixed-target collisions rarely even produce b quarks. This means fixed-target experiemnts are not suitable for modern high-energy discoveries with present accelerator technology, and we must instead look towards beam-beam colliders.

5.4.2 Beam-beam collisions

In this type of collider, two beams are collided with opposite momenta:

$$P_A = \begin{pmatrix} E_A \\ \mathbf{p} \end{pmatrix}, \quad P_B = \begin{pmatrix} E_B \\ -\mathbf{p} \end{pmatrix}$$

so the CM frame is the laboratory frame:

$$P_{CM} = P_A + P_B = \begin{pmatrix} E_{CM} \\ \mathbf{0} \end{pmatrix} = \begin{pmatrix} E_A + E_B \\ \mathbf{0} \end{pmatrix}. \quad (5.16)$$

We want to find the required energy for one of the beams, E_A , as a function of E_{CM} . Start by considering the product

$$P_A P_{CM} = (E_A, \mathbf{p}) \begin{pmatrix} E_{CM} \\ \mathbf{0} \end{pmatrix} = E_A E_{CM} \quad (5.17)$$

$$\text{also, } P_A P_{CM} = P_A (P_A + P_B) = P_A^2 + P_A P_B \quad (5.18)$$

so, using $P_A^2 = m_A^2$, we have

$$E_A E_{CM} = m_A^2 + P_A P_B. \quad (5.19)$$

To determine $P_A P_B$ consider

$$E_{CM}^2 = P_{CM}^2 \quad (5.20)$$

$$= (P_A + P_B)^2 \quad (5.21)$$

$$= m_A^2 + m_B^2 + 2P_A P_B. \quad (5.22)$$

Substituting this into (5.19),

$$\begin{aligned} E_A E_{CM} &= m_A^2 + \frac{1}{2}(E_{CM}^2 - m_A^2 - m_B^2) \\ &= \frac{E_{CM}^2 + m_A^2 - m_B^2}{2} \end{aligned} \quad (5.23)$$

therefore,

$$E_A = \frac{E_{CM}^2 + m_A^2 - m_B^2}{2E_{CM}}. \quad (5.24)$$

In the case where $m_A = m_B$ this becomes $E_A = E_{CM}/2$.

5.5 Mandelstam variables

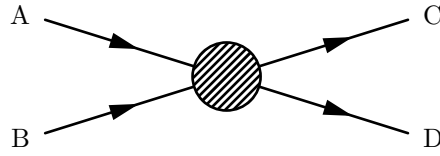

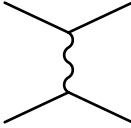
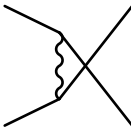


Figure 5.1: Some process $A + B \rightarrow C + D$.

Consider some process $A + B \rightarrow C + D$. The three Mandelstam variables, s , t , and u are combinations of the incoming and outgoing 4-momenta. For different diagrams, they are the momentum of the propagator:

Process	Propagator momentum	Mandelstam variable
	$P_A + P_B$	$s = (P_A + P_B)^2$
	$P_C + P_D$	$= (P_C + P_D)^2$
	$P_A - P_C$	$t = (P_A - P_C)^2$
	$P_B - P_D$	$= (P_B - P_D)^2$
	$P_A - P_D$	$u = (P_A - P_D)^2$
	$P_B - P_C$	$= (P_B - P_C)^2$

The sum of s , t , and u gives the sum of the squares of the mass of the four particles,

$$s + t + u = (P_A + P_B)^2 + (P_A - P_C)^2 + (P_A - P_D)^2 \quad (5.25)$$

$$= 3P_A^2 + P_B^2 + P_C^2 + P_D^2 + 2P_A(P_B - P_C - P_D) \quad (5.26)$$

By conservation of 4-momentum, we have $P_A + P_B = P_C + P_D$, therefore $P_B - P_C - P_D = -P_A$, so

$$s + t + u = 3P_A^2 + P_B^2 + P_D^2 + 2P_A(-P_A) \quad (5.27)$$

$$= P_A^2 + P_B^2 + P_C^2 + P_D^2 \quad (5.28)$$

$$= m_A^2 + m_B^2 + m_C^2 + m_D^2. \quad (5.29)$$

Chapter 6

Relativistic spin-0 particles

6.1 The Klein-Gordon equation

The Schrödinger equation is the quantum mechanical equivalent of the classical $E = p^2/2m$. Now we want a relativistic version. Start from the relationship between energy, momentum, and mass,

$$E^2 - p^2 = m^2. \quad (6.1)$$

Replacing the appropriate values with operators,

$$E \rightarrow i\frac{\partial}{\partial t}, \quad p \rightarrow -i\nabla$$

and applying them to some general wavefunction,

$$\left(-\frac{\partial^2}{\partial t^2} + \nabla^2\right)\psi = m^2\psi. \quad (6.2)$$

Rearranging and using equation (5.4) gives the Klein-Gordon equation

$$\boxed{\left(\partial^2 + m^2\right)\psi = 0}. \quad (6.3)$$

This is the fully relativistic equation of motion for spin-0 particles.

6.1.1 4-current density

We now wish to derive the probability 4-current from the Klein-Gordon equation. Taking the complex conjugate of (6.3) and multiplying by ψ gives

$$\psi \left(\partial^2 + m^2\right) \psi^* = 0. \quad (6.4)$$

Similarly, multiplying (6.3) by ψ^* gives

$$\psi^* \left(\partial^2 + m^2\right) \psi = 0. \quad (6.5)$$

Subtracting (6.4) from (6.5) and multiplying by i ,

$$i\psi^*\partial^2\psi - i\psi\partial^2\psi^* = 0 \quad (6.6)$$

$$\Rightarrow \frac{\partial}{\partial t} \left(i\psi^* \frac{\partial\psi}{\partial t} - i \frac{\partial\psi^*}{\partial t} \psi \right) - \nabla \cdot (i\psi^* \nabla\psi - i(\nabla\psi)\psi^*) = 0 \quad (6.7)$$

This result is a continuity equation,

$$\partial_\mu j^\mu = 0 \quad (6.8)$$

for the 4-current density

$$j^\mu = i\psi^* \partial^\mu \psi - i\psi \partial^\mu \psi^* \quad (6.9)$$

6.1.2 Application to a plane wave

Consider a particle with wavefunction $\phi = \mathcal{N}e^{-iPX}$. Applying the above definition of 4-current density gives the values

$$\rho = j^0 = 2|\mathcal{N}|^2 E \quad (6.10)$$

$$\mathbf{j} = 2|\mathcal{N}|^2 \mathbf{p}. \quad (6.11)$$

That ρ is proportional to E is to be expected. Under a Lorentz boost the volume element transforms as

$$d^3\mathbf{x} \rightarrow \frac{d^3\mathbf{x}}{\gamma}$$

so in order to preserve $\rho d^3\mathbf{x}$, ρ must transform as $\rho \rightarrow \gamma\rho$, in the same way energy does.

If the covariant normalization to $2E$ particles per unit volume is used, the result is that $\rho = 1$.

6.2 Negative energy particles and the Feynman-Stueckelberg interpretation

For the Klein-Gordon equation to be an accurate description of spin-0 particles, it should be able to describe antiparticles. Indeed, the Klein-Gordon equation does allow for particles with negative energy, i.e. the negative solution of

$$E_\pm = \pm \sqrt{p^2 + m^2}. \quad (6.12)$$

There are some problems associated with this. Firstly, the existence of negative energy states means that the energy of a particle can always be lowered. Secondly, the E_- solutions are associated with a negative probability density ρ , which doesn't make sense and is not allowed.

Pauli and Weisskopf showed that it is possible to have a negative energy solution of the Klein-Gordon equation if the scalar electron charge $-e$ is included in j^μ and it is interpreted as a charge-current density,

$$j^\mu = -ie (\psi^* \partial^\mu \psi - i\psi \partial^\mu \psi^*). \quad (6.13)$$

Now $\rho = j^0$ represents the charge density which is allowed to be negative.

Now that the theory has been fixed to allow the E_- particles, we need an interpretation for them. The Feynman-Stueckelberg interpretation states that the negative energy states correspond to antiparticles. Consider the 4-charge-current of a scalar electron with a plane wavefunction,

$$j^\mu(e^-) = -2e|\mathcal{N}|^2 \begin{pmatrix} E \\ \mathbf{p} \end{pmatrix}. \quad (6.14)$$

In the same way, a positron has the current

$$j^\mu(e^+) = 2e|\mathcal{N}|^2 \begin{pmatrix} E \\ \mathbf{p} \end{pmatrix} \quad (6.15)$$

$$= -2e|\mathcal{N}|^2 \begin{pmatrix} -E \\ -\mathbf{p} \end{pmatrix}. \quad (6.16)$$

This is the same as for an electron with $-E$, $-\mathbf{p}$. So far as a system is concerned, the emission of a positron with energy E is the same as the absorption of an electron with energy $-E$. In other words, positive-energy antiparticles travelling forwards in time are negative-energy particles travelling backwards in time. This gives the E_- solutions an interpretation.

Chapter 7

Calculating Amplitudes

There are a number of possible approaches to calculating an amplitude for a given interaction. These include relativistic generalisations of the Born approximation (Feynman-Stueckelberg) or perturbation theory (Halzen and Martin), and the mathematically heavy canonical field theory or the path integral approach. The idea of the propagator is common to some of these approaches and this is what we will consider in our treatment of amplitude calculations.

7.1 Single scattering potential

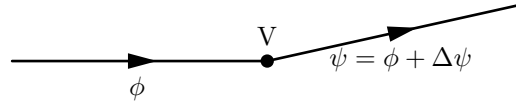


Figure 7.1: Scattering of a plane wave off a localised potential V .

Consider a particle $\psi(\mathbf{r}, t)$ that scatters off some potential $V(\mathbf{r}, t)$, where V acts only at a position \mathbf{r}_1 and for a short time Δt . In the interaction picture the Schrödinger equation is

$$(\hat{H}_0 + V) \psi(\mathbf{r}, t) = i \frac{\partial \psi}{\partial t} \quad (7.1)$$

where the interaction is large, $V \gg \hat{H}_0$. Ignoring the free \hat{H}_0 term and solving the separable differential equation,

$$i \int_{\phi}^{\phi + \Delta\psi} d\psi = \int_{-\infty}^{+\infty} V(\mathbf{r}, t) \psi(\mathbf{r}, t) dt \quad (7.2)$$

where ϕ is the original, unscattered plane wavefunction and $\psi = \phi + \Delta\psi$ is the scattered wavefunction. Since the potential V only acts at position \mathbf{r}_1 and has constant value V for time Δt , this evaluates to give

$$\Delta\psi(\mathbf{r}_1, t_1) = -iV(\mathbf{r}_1, t_1) \psi(\mathbf{r}_1, t_1) \Delta t \quad (7.3)$$

$$= -iV(x_1) [\phi(x_1) + \Delta\psi(x_1)] \Delta t \quad (7.4)$$

$$\approx -iV(x_1) \phi(x_1) \Delta t \quad (7.5)$$

where x_1 is the event at (\mathbf{r}_1, t_1) .

We wish to know the wavefunction after scattering at some event x' . Using the formalism of Green's functions,

$$\boxed{\Psi(x') = i \int G(x', x) \Psi(x) d^3\mathbf{r} \quad \text{for } t' > t} \quad (7.6)$$

where $G(x', x)$ is the Green's function of the Schrödinger equation, and is called the propagator from x to x' . Applying this to the change in wavefunction caused by the scattering potential, (7.5),

$$\Delta\psi(x') = i \int G(x', x_1) \Delta\psi(x_1) d^3\mathbf{r}_1 \quad (7.7)$$

$$= \int G(x', x_1) V(x_1) \phi(x_1) \Delta t d^3\mathbf{r}_1. \quad (7.8)$$

So overall, the particle's wavefunction at the event x' is, to first order,

$$\psi(x') = \phi(x') + \int G(x', x_1) V(x_1) \phi(x_1) \Delta t d^3\mathbf{r}_1. \quad (7.9)$$

In the limit of a continuous interaction, we can integrate over the time interval Δt ,

$$\boxed{\psi(x') = \phi(x') + \int G(x', x_1) V(x_1) \phi(x_1) d^4x_1}. \quad (7.10)$$

7.2 Two scattering potentials

The above result may be easily generalised to multiple scattering potentials. A long-range force can be modelled, to first order, by a particle scattering from two localised potentials.

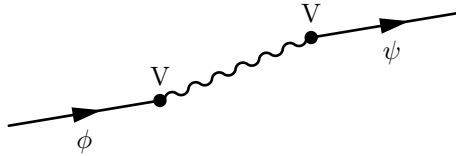


Figure 7.2: A particle undergoing double scattering in the propagator approach.

Consider two localised scattering potentials, each with strength V , at events x_1 and x_2 . Then extending the above result gives that the post-scattering wavefunction is

$$\begin{aligned} \psi(x') &= \phi(x') + \int G(x', x_1) V(x_1) \phi(x_1) d^4x_1 \\ &\quad + \int G(x', x_2) V(x_2) \phi(x_2) d^4x_2 \\ &\quad + \int \int G(x', x_2) V(x_2) G(x_2, x_1) V(x_1) \phi(x_1) d^4x_1 d^4x_2 \end{aligned} \quad (7.11)$$

7.3 Free particle propagator

Start from

$$\psi(x') = i \int d^3\mathbf{r} G(x'; x) \psi(x) \quad (7.12)$$

for $t' > t$. This condition can be encapsulated mathematically by the Heaviside function,

$$\theta(t' - t) \psi(x') = i \int d^3\mathbf{r} G(x', x) \psi(x). \quad (7.13)$$

Now multiply both sides by $\left[i \frac{\partial}{\partial t} - \hat{H}\right]$. The left-hand side becomes,

$$\begin{aligned} \left[i \frac{\partial}{\partial t} - \hat{H}\right] \theta(t' - t) \psi(x') &= i \frac{\partial \theta}{\partial t} \psi(x') + \theta(t' - t) \underbrace{\left(i \frac{\partial \psi}{\partial t} - \hat{H} \psi(x')\right)}_{0 \text{ by TDSE}} \\ &= i \delta(t' - t) \psi(x') \end{aligned} \quad (7.14)$$

$$= i \int d^3\mathbf{r} \delta(x' - x) \psi(x) \quad (7.15)$$

$$= i \int d^3\mathbf{r} \int \frac{d^4p}{(2\pi)^4} e^{i(x' - x)p} \psi(x) \quad (7.16)$$

Now consider the right-hand side of (7.13). Upon multiplication by $\left[i \frac{\partial}{\partial t} - \hat{H}\right]$ it becomes

$$i \int d^3\mathbf{r} \left[i \frac{\partial}{\partial t} - \hat{H}\right] G(x', x) \psi(x) = i \int d^3\mathbf{r} \left[E - \frac{p^2}{2m}\right] G(x', x) \psi(x) \quad (7.17)$$

where the operators have been applied to the free plane wavefunction. Taking the Fourier transform to 4-momentum space, the right hand side becomes

$$i \int d^3\mathbf{r} \int \frac{d^4p}{(2\pi)^4} \left[E - \frac{p^2}{2m}\right] \mathcal{G}(p', p) e^{i(x' - x)p} \psi(x). \quad (7.18)$$

where \mathcal{G} is the momentum-space propagator. Now we can compare the integrands of (7.16) and (7.18) to give an expression for the momentum-space free particle propagator:

$$\boxed{\mathcal{G}(p', p) = \frac{1}{E - \frac{p^2}{2m}}}. \quad (7.19)$$

This is used as the propagator for off-mass shell virtual particles. As the particle approaches its mass shell, this expression diverges. To allow for integration over momentum, a small complex factor may be added to the denominator,

$$\mathcal{G}(p', p) = \frac{1}{E - \frac{p^2}{2m} + i\epsilon} \quad (7.20)$$

and the result taken in the limit where $\epsilon \rightarrow 0$.

Chapter 8

Spinless $e^- + \mu^-$ scattering

For the following calculations we will consider the elastic electromagnetic scattering of scalar electrons and muons. That is, the particles considered are solutions of the Klein-Gordon equation.

The process has one diagram:

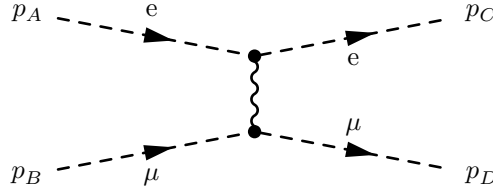


Figure 8.1: Diagram for the t-channel process $e^- + \mu^- \rightarrow e^- + \mu^-$ with scalar particles.

8.1 Electrodynamics of scalars

The equations of motion for a particle may be modified to include the electromagnetic interaction via a 4-potential A via the substitution

$$p^\mu \rightarrow p^\mu + eA^\mu. \quad (8.1)$$

Then the Klein-Gordon equation, (6.3), becomes

$$(i\partial_\mu + eA_\mu)(i\partial^\mu + eA^\mu)\psi = m^2\psi. \quad (8.2)$$

Expanding out the left-hand side and collecting the free-particle kinetic and mass terms, we can identify an expression for the electromagnetic potential, V ,

$$(\partial_\mu\partial^\mu + m^2)\psi = (ie\partial_\mu A^\mu + ieA_\mu\partial^\mu + e^2 A_\mu A^\mu)\psi \equiv -V(x)\psi. \quad (8.3)$$

Under the weak field approximation, we may ignore the second-order term $A_\mu A^\mu$, so that

$$V(x) \approx -ie(\partial_\mu A^\mu + A_\mu\partial^\mu) \quad (8.4)$$

8.2 Scattering amplitude

The amplitude for a particle with wavefunction ϕ_i to scatter from potential V and subsequently have the wavefunction ϕ_f is given by

$$T_{fi} = -i \int d^4x \phi_f^* V \phi_i \quad (8.5)$$

$$= -i \int d^4x \phi_f^* (-ie) (\partial_\mu A^\mu + A_\mu \partial^\mu) \phi_i \quad (8.6)$$

where the weak field form of the EM potential has been substituted for V . Integrating by parts, the first term in the integral evaluates to

$$\int d^4x \phi_f^* \partial_\mu A^\mu \phi_i = [\phi_f^* A^\mu \phi_i]_{-\infty}^{+\infty} - \int d^4x (\partial_\mu \phi_f^*) A^\mu \phi_i \quad (8.7)$$

and the boundary term in square brackets goes to zero for a vanishing (i.e. local) potential. Therefore, the scattering amplitude becomes

$$\begin{aligned} T_{fi} &= -i \int d^4x (-ie) (\phi_f^* A_\mu \partial^\mu \phi_i - (\partial_\mu \phi_f^*) A^\mu \phi_i) \\ &= -i \int d^4x A^\mu (-ie) (\phi_f^* \partial_\mu \phi_i - (\partial_\mu \phi_f^*) \phi_i) \\ &= -i \int d^4x A^\mu j_\mu^{fi} \end{aligned} \quad (8.8)$$

where we have identified the current density,

$$j_\mu^{fi} = -ie (\phi_f^* \partial_\mu \phi_i - (\partial_\mu \phi_f^*) \phi_i). \quad (8.9)$$

This is the current-potential formulation, where we identify the scattering process with a current j_μ^{fi} and potential A^μ .

At the vertex changing A to C, the scalar electron has plane wavefunctions,

$$\phi_A(x) = N_A e^{-iP_A x}, \quad \phi_C(x) = N_C e^{-iP_C x}, \quad (8.10)$$

giving the current,

$$j_\mu^{CA} = -e N_C^* N_A e^{i(P_C - P_A)x} (P_A + P_C)_\mu. \quad (8.11)$$

This will be the current in the current-potential formulation. Similarly, the current flowing through the other vertex is given by

$$j_\mu^{DB} = -e N_D^* N_B e^{i(P_D - P_B)x} (P_B + P_D)_\mu. \quad (8.12)$$

We wish to identify the potential A^μ associated with the current j_μ^{DB} . For the potential to describe fields that behave according to Maxwell's equations, it must itself obey the Poisson equation (see Section 12.1 below),

$$\partial^2 A^\mu = j^\mu. \quad (8.13)$$

It can be verified that the potential

$$A_{DB}^\mu = \frac{-g^{\mu\nu} j_\nu^{DB}}{q^2} \quad (8.14)$$

is a solution via substitution,

$$\begin{aligned}\partial^2 \left(\frac{-g^{\mu\nu} j_\nu^{DB}}{q^2} \right) &= -\frac{1}{q^2} [i(P_D - P_B)]^2 j_{DB}^\mu \\ &= j_{DB}^\mu\end{aligned}\tag{8.15}$$

where $q^2 = (P_D - P_B)^2 = t$ is the 4-momentum of the propagating photon.

Inserting the above forms for the current, (8.11), and potential, (8.14), into the expression for the scattering amplitude, (8.8),

$$T_{fi} = \frac{ie^2}{q^2} \int d^4x N_C^* N_A N_D^* N_B (P_A + P_C)_\mu (P_B + P_D)^\mu e^{i(P_C + P_D - P_A - P_B)x}\tag{8.16}$$

8.3 Scattering rate

To calculate the cross-section, we would like to know the rate W_{fi} of particles being scattered per unit time and volume,

$$W_{fi} = \frac{T_{fi}^* T_{fi}}{T \times V}\tag{8.17}$$

Assume the scattering takes place in a volume V . We use the covariant normalisation to $2E$ particles in the volume, giving

$$N_i = \frac{1}{\sqrt{V}} \quad \text{for } i = A, B, C, D.\tag{8.18}$$

Then the amplitude becomes

$$T_{fi} = \frac{ie^2}{q^2 V^2} \int d^4x (P_A + P_C)_\mu (P_B + P_D)^\mu e^{i(P_C + P_D - P_A - P_B)x}\tag{8.19}$$

giving a probability

$$T_{fi}^* T_{fi} = \frac{e^4}{q^4 V^4} \int_{TV} d^4x \int_{TV} d^4x' [(P_A + P_C)_\mu (P_B + P_D)^\mu]^2 e^{i(P_C + P_D - P_A - P_B)(x - x')}\tag{8.20}$$

$$\begin{aligned}&= \frac{e^4}{q^4 V^4} (\sqrt{2\pi})^4 \sqrt{TV} \int_{TV} d^4x [(P_A + P_C)_\mu (P_B + P_D)^\mu]^2 e^{i(P_C + P_D - P_A - P_B)x} \\ &= \frac{e^4}{q^4 V^4} (\sqrt{2\pi})^8 (\sqrt{TV})^2 \delta^{(4)}(P_C + P_D - P_A - P_B) [(P_A + P_C)_\mu (P_B + P_D)^\mu]^2 \\ &= \frac{e^4}{q^4 V^4} (2\pi)^4 [(P_A + P_C)_\mu (P_B + P_D)^\mu]^2 \delta^{(4)}(P_C + P_D - P_A - P_B) TV\end{aligned}\tag{8.21}$$

which gives the rate

$$W_{fi} = \frac{(2\pi)^4 e^4}{q^4 V^4} [(P_A + P_C)_\mu (P_B + P_D)^\mu]^2 \delta^{(4)}(P_C + P_D - P_A - P_B).\tag{8.22}$$

8.4 Density of states

The larger the number of final states per unit volume N_f available to a process, the more likely it is to happen and hence the cross-section is proportional to N_f .

In the scattering problem the number of final states is the number of possible momenta inside $[\mathbf{p}, \mathbf{p} + d^3\mathbf{p}]$ for the propagating photon with a given energy. This is given by

$$N_f = \frac{1}{2E} \frac{d^3\mathbf{p}}{\Delta p} \quad (8.23)$$

where Δp is the separation in momentum space between adjacent states and the $1/2E$ factor is due to the fact that there are $2E$ particles inside the volume and we want the number of states for one particle.

Since the scattering process is modelled as happening inside a volume V , the propagating photon has the wavefunction of a particle in an infinite potential well with the dimensions of V (Dirichlet boundary conditions, $\psi(0) = \psi(L) = 0$). This leads to the quantisation of its allowed momentum,

$$p_x = \frac{2\pi}{L_x} n_x, \quad p_y = \frac{2\pi}{L_y} n_y, \quad p_z = \frac{2\pi}{L_z} n_z. \quad (8.24)$$

Therefore, the separation between momentum states is $2\pi/L$ in each dimension. This leads to the density of states,

$$\begin{aligned} N_f &= \frac{1}{2E} \frac{L_x}{2\pi} \frac{L_y}{2\pi} \frac{L_z}{2\pi} d^3\mathbf{p} \\ &= \frac{1}{2E} \frac{V}{(2\pi)^3} d^3\mathbf{p}. \end{aligned} \quad (8.25)$$

Now the photon's energy is shared amongst particles C and D , so the density of final states becomes

$$N_f^{CD} = \frac{1}{2E_C} \frac{V}{(2\pi)^3} d^3\mathbf{p}_C \frac{1}{2E_D} \frac{V}{(2\pi)^3} d^3\mathbf{p}_D \quad (8.26)$$

$$= \frac{1}{4E_C E_D} \frac{V^2}{(2\pi)^6} d^3\mathbf{p}_C d^3\mathbf{p}_D \quad (8.27)$$

8.5 Incoming flux

The rate W_{fi} scales with the flux of incoming particles, so the in cross-section calculation, it should be divided by a flux factor, $\rho_A \rho_B u_{AB}$, where ρ_{AB} give the density of initial-state particles and $u_{AB} = u_A - u_B$ is their relative velocity.

$$\rho_A \rho_B u_{AB} = \frac{2E_A}{V} \frac{2E_B}{V} \left(\frac{p_A}{E_A} - \frac{p_B}{E_B} \right) \quad (8.28)$$

$$= \frac{4}{V^2} (p_A E_B - p_B E_A). \quad (8.29)$$

For a collider in the centre of momentum (CM) frame, we have $p_A = -p_B$,

$$\rho_A \rho_B u_{AB} = \frac{4p_A}{V^2} (E_B + E_A) = \frac{4p_A \sqrt{s}}{V^2} \quad (8.30)$$

where $\sqrt{s} = E_A + E_B$ is the CM energy.

8.6 Cross-section

Now we are ready to calculate the differential cross-section,

$$d\sigma = \frac{W_{fi}}{\rho_A \rho_B u_{AB}} N_f \quad (8.31)$$

$$\begin{aligned} &= \left\{ \frac{(2\pi)^4 e^4}{q^4 V^4} [(P_A + P_C)_\mu (P_B + P_D)^\mu]^2 \delta^{(4)}(P_C + P_D - P_A - P_B) \right\} \frac{V^2}{4p_A \sqrt{s}} \frac{1}{4E_C E_D} \frac{V^2}{(2\pi)^6} d^3 \mathbf{p}_C d^3 \mathbf{p}_D \\ &= \frac{e^4}{q^4 V^2} \frac{[(P_A + P_C)_\mu (P_B + P_D)^\mu]^2}{4p_A \sqrt{s}} dQ \end{aligned} \quad (8.32)$$

where dQ is the Lorentz-invariant phase space factor

$$dQ = \frac{V}{2E_C} \frac{d^3 \mathbf{p}_C}{(2\pi)^3} \frac{V}{2E_D} \frac{d^3 \mathbf{p}_D}{(2\pi)^3} (2\pi)^4 \delta^{(4)}(P_C + P_D - P_A - P_B) \quad (8.33)$$

In the CM frame, we have that $\mathbf{p}_A = -\mathbf{p}_B$, so

$$dQ = \frac{V^2}{(2\pi)^2} \delta(\sqrt{s} - E_C - E_D) \delta^{(3)}(\mathbf{p}_C + \mathbf{p}_D) \frac{d^3 \mathbf{p}_C}{2E_C} \frac{d^3 \mathbf{p}_D}{2E_D}. \quad (8.34)$$

We now integrate over all momenta for D , the unobserved particle. This gives,

$$dQ = \frac{V^2}{(2\pi)^2} \frac{1}{4E_C E_D} \delta(\sqrt{s} - E_C - E_D) d^3 \mathbf{p}_C \quad (8.35)$$

$$= \frac{V^2}{(2\pi)^2} \frac{1}{4E_C E_D} \delta(\sqrt{s} - E_C - E_D) p_C^2 dp_C d\Omega \quad (8.36)$$

Now from the relation $E^2 = p^2 + m^2$ we have that $E dE = p dp$, so

$$dQ = \frac{V^2}{(2\pi)^2} \frac{p_C}{4E_D} \delta(\sqrt{s} - E_C - E_D) dE_C d\Omega \quad (8.37)$$

We next want to integrate over E_C . To do so, write the expression in the δ function as

$$f(E_C) = \sqrt{s} - E_C - E_D \quad (8.38)$$

$$\begin{aligned} &= \sqrt{s} - E_C - \sqrt{p_D^2 + m_D^2} \\ &= \sqrt{s} - E_C - \sqrt{p_C^2 + m_D^2} \quad \text{since } \mathbf{p}_C = -\mathbf{p}_D \\ &= \sqrt{s} - E_C - \sqrt{E_C^2 - m_C^2 + m_D^2}. \end{aligned} \quad (8.39)$$

Therefore,

$$\begin{aligned} \left| \frac{df}{dE_C} \right| &= 1 + \frac{E_C}{\sqrt{E_C^2 - m_C^2 + m_D^2}} \\ &= \frac{\sqrt{s}}{E_D} \end{aligned} \quad (8.40)$$

so the δ -function becomes

$$\delta(\sqrt{s} - E_C - E_D) = \delta(E_C) \frac{E_D}{\sqrt{s}} \quad (8.41)$$

and the Lorentz-invariant phase space is

$$dQ = \frac{V^2}{(2\pi)^2} \frac{p_C}{4\sqrt{s}} \delta(E_C) dE_C d\Omega. \quad (8.42)$$

Integrating over the final-state particle's energy, E_C ,

$$dQ = \frac{V^2}{(2\pi)^2} \frac{p_C}{4\sqrt{s}} d\Omega. \quad (8.43)$$

Substituting this back into the expression for the differential cross section,

$$\boxed{\frac{d\sigma}{d\Omega} = \frac{1}{64\pi^2} \frac{e^4}{q^4} [(P_A + P_C)_\mu (P_B + P_D)^\mu]^2 \frac{1}{s} \frac{p_C}{p_A}}. \quad (8.44)$$

The fact that the cross-section is proportional to $1/s$, the inverse square of the SM energy means that we need increasingly higher luminosities to observe high energy scattering processes.

8.7 Application: high-energy scattering

Consider the ultra-relativistic case, where $E \gg m$ for all particles. In the CM frame, all particles now have the same energy $E = s/2$. Then we have that the Mandelstam t variable is

$$q^2 = t = (P_A - P_C)^2 \quad (8.45)$$

$$\begin{aligned} &= \begin{pmatrix} E_A - E_C \\ \mathbf{p}_A - \mathbf{p}_C \end{pmatrix}^2 \\ &= -2E^2(1 - \cos \theta) \end{aligned} \quad (8.46)$$

In this case, the differential cross-section becomes

$$\frac{d\sigma}{d\Omega} = \frac{e^4}{64\pi^2} \frac{[(P_A + P_C)_\mu (P_B + P_D)^\mu]^2}{4E^4(1 - \cos \theta)^2} \frac{1}{s}. \quad (8.47)$$

Now we have, in the CM frame,

$$P_A = \begin{pmatrix} E \\ \mathbf{p} \end{pmatrix} \quad P_B = \begin{pmatrix} E \\ -\mathbf{p} \end{pmatrix} \quad P_C = \begin{pmatrix} E \\ \mathbf{p}' \end{pmatrix} \quad P_D = \begin{pmatrix} E \\ -\mathbf{p}' \end{pmatrix},$$

and therefore,

$$\begin{aligned} (P_A + P_C)_\mu (P_B + P_D)^\mu &= \begin{pmatrix} 2E \\ \mathbf{p} + \mathbf{p}' \end{pmatrix} \begin{pmatrix} 2E \\ -\mathbf{p} - \mathbf{p}' \end{pmatrix} \quad \text{with } |\mathbf{p}| = |\mathbf{p}'| = E \\ &= (2E)^2 + (\mathbf{p} + \mathbf{p}')^2 \\ &= 6E^2 + 2E^2 \cos \theta \end{aligned} \quad (8.48)$$

$$\Rightarrow \quad \left[(P_A + P_C)_\mu (P_B + P_D)^\mu \right]^2 = 4E^4 (3 + \cos \theta)^2 \quad (8.49)$$

So the final answer is

$$\frac{d\sigma}{d\Omega} = \frac{e^4}{64\pi^2} \left(\frac{3 + \cos \theta}{1 - \cos \theta} \right)^2 \frac{1}{s}. \quad (8.50)$$

8.8 $1 \rightarrow 2$ scattering (decay)

For a single body of mass M decaying into two particles, we replace the flux factor with the normalised energy density,

$$\rho = \frac{2M}{V} \quad (8.51)$$

so the cross-section is given by

$$d\sigma = \frac{V}{2M} W_{fi} N_f. \quad (8.52)$$

where for a two-body final state, N_f is the same as for above. However, T_{fi} will obviously be different.

Chapter 9

Relativistic Spin- $\frac{1}{2}$ particles

9.1 Spin in non-relativistic QM

The quantum states corresponding to spin- $\frac{1}{2}$ particles are eigenstates of the spin operator,

$$\hat{S}_i = \frac{1}{2}\sigma_i \quad (9.1)$$

where σ_i are the Pauli matrices,

$$\sigma_x = \begin{pmatrix} 0 & 1 \\ 1 & 0 \end{pmatrix}, \quad \sigma_y = \begin{pmatrix} 0 & -i \\ i & 0 \end{pmatrix}, \quad \sigma_z = \begin{pmatrix} 1 & 0 \\ 0 & -1 \end{pmatrix}. \quad (9.2)$$

Application of \hat{S}_z on a state of definite spin projection on the z-axis gives

$$\hat{S}_z |s, m\rangle = m |s, m\rangle \quad (9.3)$$

and application of the operator $\hat{S}^2 = \sum_i \hat{S}_i^2$ – which corresponds to the total spin angular momentum of the state – gives

$$\hat{S}^2 |s, m\rangle = s(s+1) |s, m\rangle. \quad (9.4)$$

The commutator of any two spin operators is

$$[\hat{S}_i, \hat{S}_j] = i\epsilon_{ijk}\hat{S}_k \quad (9.5)$$

and they have the anticommutation relation

$$\{\hat{S}_i, \hat{S}_j\} = \delta_{ij}. \quad (9.6)$$

Therefore, we have that

$$\begin{aligned} \sigma_i \sigma_j &= \frac{[\sigma_i, \sigma_j] + \{\sigma_i, \sigma_j\}}{2} \\ &= \delta_{ij} + i\epsilon_{ijk}\sigma_k. \end{aligned} \quad (9.7)$$

So for any two vectors, \mathbf{a} and \mathbf{b} ,

$$\begin{aligned}
(\boldsymbol{\sigma} \cdot \mathbf{a})(\boldsymbol{\sigma} \cdot \mathbf{b}) &= \sigma_i a_i \sigma_j b_j \\
&= \sigma_i \sigma_j (a_i b_j) \\
&= (\delta_{ij} + i\epsilon_{ijk} \sigma_k)(a_i b_j) \\
&= a_i b_i + i \sigma_k \epsilon_{kij} a_i b_j \\
&= \mathbf{a} \cdot \mathbf{b} + i \boldsymbol{\sigma} \cdot (\mathbf{a} \times \mathbf{b}).
\end{aligned} \tag{9.8}$$

Applying this result to $\mathbf{a} = \mathbf{b} = \mathbf{p}$, the momentum operator,

$$\begin{aligned}
(\boldsymbol{\sigma} \cdot \mathbf{p})(\boldsymbol{\sigma} \cdot \mathbf{p}) &= \mathbf{p} \cdot \mathbf{p} + i \underbrace{\boldsymbol{\sigma} \cdot (\mathbf{p} \times \mathbf{p})}_0 \\
&= |\mathbf{p}|^2.
\end{aligned} \tag{9.9}$$

This allows us to express the energy as

$$E = \frac{(\boldsymbol{\sigma} \cdot \mathbf{p})(\boldsymbol{\sigma} \cdot \mathbf{p})}{2m} + V \tag{9.10}$$

which leads to the correct energy for a particle with a gyromagnetic ratio if the EM coupling is included.

9.2 The Dirac equation

To avoid the negative energy solutions seen in the treatment of the Klein-Gordon equation, Dirac proposed an equation of motion that is linear in $\frac{\partial}{\partial t}$. Also, there should be distinct solutions for particles with opposite spin.

$$\boxed{\hat{H}\psi = (\boldsymbol{\alpha} \cdot \mathbf{p} + \beta m)\psi} \tag{9.11}$$

is the Dirac equation. Here, α_i and β are 4×4 matrices and ψ therefore a 4-component Dirac spinor.

9.2.1 Constraints on α_i , β

For the Dirac equation to describe relativistic particles, it must agree with the relation

$$E^2 = p^2 + 2m. \tag{9.12}$$

Expanding out the operators in the Dirac equation above,

$$\begin{aligned}
\hat{H}^2 &= (\alpha_i p_i + \beta m)(\alpha_j p_j + \beta m) \\
&= \alpha_i \alpha_j p_i p_j + \{\alpha_i, \beta\} p_i + \beta^2 m^2.
\end{aligned} \tag{9.13}$$

So we see that the matrices α_i and β have the constraints:

- $\beta^2 = I_4$
- $\alpha_i \alpha_j = \delta_{ij} I_4$

- $\{\alpha_i, \beta\} = 0 \Rightarrow \alpha_i \beta = -\beta \alpha_i$

This final constraint further requires that α_i and β are all traceless:

$$\begin{aligned} \text{tr}(\alpha_i \beta) &= -\text{tr}(\beta \alpha_i) \\ \text{tr}(\alpha_i \beta^2) &= -\text{tr}(\beta \alpha_i \beta) \\ \text{tr}(\alpha_i) &= -\text{tr}(\beta^2 \alpha_i) \quad \text{by cyclicity of the trace} \\ &= -\text{tr}(\alpha_i) = 0. \end{aligned}$$

Moreover, we require that α_i and β are Hermitian.

These constraints still allow for many different representations of the Dirac equation. A commonly used choice is

$$\alpha_i = \begin{pmatrix} 0 & \sigma_i \\ \sigma_i & 0 \end{pmatrix}, \quad \beta = \begin{pmatrix} I_2 & 0 \\ 0 & -I_2 \end{pmatrix}. \quad (9.14)$$

9.2.2 Covariant form

Using the Schrödinger equation, express the Dirac equation in terms of differential operators

$$i \frac{\partial \psi}{\partial t} = -i \boldsymbol{\alpha} \cdot \boldsymbol{\nabla} \psi + \beta m \psi \quad (9.15)$$

and pre-multiply by β ,

$$i \beta \frac{\partial \psi}{\partial t} = -i \beta \boldsymbol{\alpha} \cdot \boldsymbol{\nabla} \psi + \beta^2 m \psi. \quad (9.16)$$

Now we recognise that $\beta^2 = I_4$ and define the Dirac gamma matrices $\gamma^0 = \beta$, $\gamma^k = \beta \alpha^k$. This gives

$$\boxed{(i \gamma^\mu \partial_\mu - m) \psi = 0}. \quad (9.17)$$

This is the covariant form of the Dirac equation. Explicitly, the Dirac matrices are

$$\gamma^0 = \begin{pmatrix} I_2 & 0 \\ 0 & -I_2 \end{pmatrix}, \quad \gamma^k = \begin{pmatrix} 0 & \sigma^k \\ -\sigma^k & 0 \end{pmatrix}.$$

9.2.3 Properties of the γ matrices

Clearly γ^0 is Hermitian,

$$(\gamma^0)^\dagger = \gamma^0 \quad (9.18)$$

but the γ^k are anti-Hermitian,

$$\begin{aligned} (\gamma^k)^\dagger &= (\beta \alpha^k)^\dagger \\ &= (\alpha^k)^\dagger \beta^\dagger \\ &= \alpha^k \beta \\ &= -\beta \alpha^k \\ &= -\gamma^k. \end{aligned} \quad (9.19)$$

Also we have that

$$(\gamma^0)^2 = I_4 \quad (9.20)$$

and

$$(\gamma^k)^2 = -I_4. \quad (9.21)$$

Finally, the anticommutator

$$\{\gamma^0, \gamma^k\} = 0. \quad (9.22)$$

These properties will prove useful in the following manipulations of the Dirac equation.

9.3 Adjoint Dirac equation

Taking the Hermitian conjugate of (9.17) and expanding out the space and time components,

$$-i\partial_0\psi^\dagger\gamma^0 + i\partial_k\psi^\dagger\gamma^k - m\psi^\dagger = 0. \quad (9.23)$$

Now multiply by $-\gamma^0$ from the right and use $\gamma^0\gamma^k = -\gamma^k\gamma^0$,

$$i\partial_0\psi^\dagger\gamma^0\gamma^0 + i\partial_k\psi^\dagger\gamma^0\gamma^k + m\psi^\dagger\gamma^0 = 0. \quad (9.24)$$

Here is it natural to identify the adjoint Dirac spinor,

$$\boxed{\bar{\psi} \equiv \psi^\dagger\gamma^0} \quad (9.25)$$

so the adjoint Dirac equation becomes

$$\boxed{i(\partial_\mu\bar{\psi})\gamma^\mu + m\bar{\psi} = 0} \quad (9.26)$$

9.3.1 Conserved current

Pre-multiply the standard Dirac equation, (9.17), by the adjoint spinor

$$i\bar{\psi}\gamma^\mu(\partial_\mu\psi) - m\bar{\psi}\psi = 0 \quad (9.27)$$

and post-multiply the adjoint Dirac equation, (9.26), by ψ ,

$$i(\partial_\mu\bar{\psi})\gamma^\mu\psi + m\bar{\psi}\psi = 0. \quad (9.28)$$

Adding these, we see that

$$\bar{\psi}\gamma^\mu(\partial_\mu\psi) + (\partial_\mu\bar{\psi})\gamma^\mu\psi = \partial_\mu(\bar{\psi}\gamma^\mu\psi) = 0 \quad (9.29)$$

where we can identify the 4-current density,

$$j^\mu = \bar{\psi}\gamma^\mu\psi. \quad (9.30)$$

Now the probability density is given by

$$\begin{aligned} j^0 &= \bar{\psi}\gamma^0\psi \\ &= \psi^\dagger\gamma^0\gamma^0\psi \\ &= |\psi|^2 \end{aligned}$$

which is always positive. Hence the Dirac equation avoids the negative probabilities we saw in the treatment of the Klein-Gordon equation.

As usual the electromagnetic charge-current density is given by $-e\bar{\psi}\gamma^\mu\psi$ for electrons.

9.4 Free particle solutions

Consider solutions of the form

$$\psi = u(p) e^{-ipx} \quad (9.31)$$

where $u(p)$ is a 4-component spinor and p and x are understood to be 4-vectors.

Substituting this into the covariant form of the Dirac equation, (9.17),

$$\begin{aligned} 0 &= (i\gamma^\mu \partial_\mu - m) u(p) e^{-ipx} \\ &= (\gamma^\mu p_\mu - m) u(p) e^{-ipx}. \end{aligned} \quad (9.32)$$

Now define the Feynman slash notation, $\not{p} \equiv \gamma^\mu p_\mu$. Solutions of the above equation are given by spinors $u(p)$ that satisfy

$$(\not{p} - m)u(p) = 0. \quad (9.33)$$

To find these solutions, it is helpful to return to the original α_i, β matrices. Do this by expanding out the \not{p} and pre-multiplying by γ^0 :

$$\begin{aligned} \gamma^0(\not{p} - m) &= \gamma^0 \gamma^0 E - \gamma^0 \gamma^k p_k - \gamma^0 m \\ &= E - \alpha^k p_k - \beta m \end{aligned} \quad (9.34)$$

so we look for solutions of

$$(E - \alpha^k p_k - \beta m) u(p) = 0. \quad (9.35)$$

9.4.1 Particles at rest

For a particle at rest $p_k = 0$ so we have to solve

$$(E - \beta m) u(p) = 0. \quad (9.36)$$

Solutions exist for

$$\begin{vmatrix} (E - m)I_2 & 0 \\ 0 & -(E + m)I_2 \end{vmatrix} = 0 \quad (9.37)$$

which has energy solutions $E = \pm m$. We have not escaped the negative energy solutions after all! In fact, this leads to four distinct solutions for the spinor

$$u_{1,2} = \begin{pmatrix} \chi_\pm \\ 0 \end{pmatrix}, \quad u_{3,4} = \begin{pmatrix} 0 \\ \chi_\pm \end{pmatrix} \quad \text{where} \quad \chi_+ = \begin{pmatrix} 1 \\ 0 \end{pmatrix}, \quad \chi_- = \begin{pmatrix} 0 \\ 1 \end{pmatrix}. \quad (9.38)$$

It is simple to see that $u_{1,2}$ are associated with positive energy states and $u_{3,4}$ with negative energy states. Furthermore, the spinors χ_\pm correspond to particles with spin projections $\pm \frac{1}{2}$.

9.4.2 Moving particle solutions

Now consider the case where $p_k \neq 0$. This gives the eigenvalue problem

$$\left[\begin{pmatrix} 0 & \boldsymbol{\sigma} \\ \boldsymbol{\sigma} & 0 \end{pmatrix} \cdot \mathbf{p} + \begin{pmatrix} I_2 & 0 \\ 0 & I_2 m \end{pmatrix} \right] \begin{pmatrix} u_A \\ u_B \end{pmatrix} = E \begin{pmatrix} u_A \\ u_B \end{pmatrix} \quad (9.39)$$

or the simultaneous equations

$$u_A = \frac{\boldsymbol{\sigma} \cdot \mathbf{p}}{E - m} u_B \quad (9.40)$$

$$u_B = \frac{\boldsymbol{\sigma} \cdot \mathbf{p}}{E + m} u_A. \quad (9.41)$$

There are still infinitely many solutions but u_B is determined from u_A or vice-versa. To agree with our choices for the spinor at rest, (9.38), we choose that for positive energy solutions

$$u_{1,2}(p) = \mathcal{N} \begin{pmatrix} \chi_{\pm} \\ \frac{\boldsymbol{\sigma} \cdot \mathbf{p}}{E + m} \chi_{\pm} \end{pmatrix} \quad (9.42)$$

and for negative energies, $E = -|E| < 0$,

$$u_{1,2}(p) = \mathcal{N} \begin{pmatrix} -\frac{\boldsymbol{\sigma} \cdot \mathbf{p}}{|E| + m} \chi_{\pm} \\ \chi_{\pm} \end{pmatrix} \quad (9.43)$$

9.4.3 Antiparticles

So far we have seen that there are four distinct solutions to the Dirac equation, accounting for each spin and positive and negative energy states. In keeping with the Feynman-Stueckelberg interpretation, we ought to demonstrate that the negative energy solutions of the Dirac equation correspond to the positron.

The full spinor states for the negative energy solutions are

$$\begin{aligned} \psi &= u_{3,4}(p) e^{-ipx} \\ &= u_{3,4}(p) \exp[-i(Et - \mathbf{p} \cdot \mathbf{x})] \\ &= u_{3,4}(p) \exp[i(|E|t + \mathbf{p} \cdot \mathbf{x})] \end{aligned} \quad (9.44)$$

so again the negative energy solution can be interpreted as a positive energy particle travelling backwards in time and space. Hence, we can write the spinor as

$$\phi = v_{1,2}(p) e^{-ipx} \quad (9.45)$$

where $v_{1,2}(p) = u_{4,3}(-p)$ and this describes a positive energy particle travelling forwards through time. Note that since what we have done is essentially a CT (or equivalently P) transformation, the spin states are reversed such that

$$v_1(p) = \mathcal{N} \begin{pmatrix} \frac{\boldsymbol{\sigma} \cdot \mathbf{p}}{E + m} \chi_- \\ \chi_- \end{pmatrix} \quad (9.46)$$

corresponds to a spin up positron, and

$$v_2(p) = \mathcal{N} \begin{pmatrix} \frac{\boldsymbol{\sigma} \cdot \mathbf{p}}{E + m} \chi_+ \\ \chi_+ \end{pmatrix} \quad (9.47)$$

corresponds to spin down.

9.5 Orthogonality and normalisation

Without loss of generality, consider electrons travelling along the z -axis. Then for a spin-up electron,

$$u_1(p) = \mathcal{N} \begin{pmatrix} 1 \\ 0 \\ \frac{p}{E + m} \\ 0 \end{pmatrix} \quad (9.48)$$

and for spin-down

$$u_2(p) = \mathcal{N} \begin{pmatrix} 0 \\ 1 \\ 0 \\ \frac{-p}{E+m} \end{pmatrix} \quad (9.49)$$

Consider two electron wavefunctions, ψ_1 , ψ_2 , with opposite spin. Their overlap is given by

$$\int \psi_1^\dagger \psi_2 \, d^3\mathbf{x}. \quad (9.50)$$

Now

$$\psi_1^\dagger \psi_2 = \mathcal{N}^* \mathcal{N} \left(1, 0, \frac{p}{E+m}, 0 \right) \begin{pmatrix} 0 \\ 1 \\ 0 \\ \frac{-p}{E+m} \end{pmatrix} = 0 \quad (9.51)$$

and therefore the overlap is zero. This shows that the solutions to the Dirac equation are orthogonal.

The normalisation condition is given by

$$2E = \int_V \psi_1^\dagger \psi_1 \, d^3\mathbf{x}. \quad (9.52)$$

For a spin-up electron travelling along the z -axis,

$$\begin{aligned} \psi_1^\dagger \psi_1 &= |\mathcal{N}|^2 \left(1, 0, \frac{p}{E+m}, 0 \right) \begin{pmatrix} 1 \\ 0 \\ \frac{p}{E+m} \\ 0 \end{pmatrix} \\ &= |\mathcal{N}|^2 \left(1 + \frac{p^2}{(E+m)^2} \right) \\ &= |\mathcal{N}|^2 \left(1 + \frac{E-m}{E+m} \right) \\ &= |\mathcal{N}|^2 \frac{2E}{E+m} \end{aligned} \quad (9.53)$$

Therefore the normalisation condition gives

$$2E = \mathcal{N}^2 \frac{2E}{E+m} V \quad (9.54)$$

$$\Rightarrow \mathcal{N} = \sqrt{\frac{E+m}{V}} \quad (9.55)$$

Often we will use $V = 1$ for convenience.

9.6 Helicity

We would like a way to describe the spin of a Dirac particle that is consistent in time. Such a good quantum number must commute with the Dirac Hamiltonian, \hat{H} , which the usual QM operator \hat{S} does not. To find

a suitable operator, it is instructive to expand out the Hamiltonian. According to the Dirac equation,

$$\begin{aligned}\hat{H}\begin{pmatrix} u_A \\ u_B \end{pmatrix} &= (\boldsymbol{\alpha} \cdot \mathbf{p} + \beta m) \begin{pmatrix} u_A \\ u_B \end{pmatrix} \\ &= \begin{pmatrix} m & \boldsymbol{\sigma} \cdot \mathbf{p} \\ \boldsymbol{\sigma} \cdot \mathbf{p} & -m \end{pmatrix} \begin{pmatrix} u_A \\ u_B \end{pmatrix}\end{aligned}\quad (9.56)$$

where it is to be understood that m stands for $\begin{pmatrix} m & 0 \\ 0 & m \end{pmatrix}$. We see from the matrix form of the Dirac Hamiltonian that $\boldsymbol{\sigma} \cdot \mathbf{p}$ commutes with \hat{H} and hence there exists a corresponding conserved quantity.

9.6.1 Helicity

Define the helicity operator

$$h \equiv \frac{1}{2} \boldsymbol{\sigma} \cdot \hat{\mathbf{p}} \quad (9.57)$$

where $\hat{\mathbf{p}} = \mathbf{p}/|\mathbf{p}|$. Notice that $\boldsymbol{\sigma}/2 = \mathbf{S}$ so that $h = \mathbf{S} \cdot \hat{\mathbf{p}}$ is nothing but the projection of the particle's spin along its direction of travel.

To find the spectrum of helicities, we solve the eigenvalue problem for the matrix $\frac{1}{2} \boldsymbol{\sigma} \cdot \hat{\mathbf{p}}$. This is most easily done by writing out the momentum in polar coordinates:

$$\hat{\mathbf{p}} = \begin{pmatrix} \sin \theta \cos \phi \\ \sin \theta \sin \phi \\ \cos \theta \end{pmatrix} \quad (9.58)$$

then

$$\boldsymbol{\sigma} \cdot \hat{\mathbf{p}} = \begin{pmatrix} \cos \theta & \sin \theta e^{-i\phi} \\ \sin \theta e^{i\phi} & -\cos \theta \end{pmatrix}. \quad (9.59)$$

This gives the eigenvalue problem,

$$\frac{1}{2} \begin{pmatrix} \cos \theta & \sin \theta e^{-i\phi} \\ \sin \theta e^{i\phi} & -\cos \theta \end{pmatrix} \begin{pmatrix} u_A \\ u_B \end{pmatrix} = \lambda \begin{pmatrix} u_A \\ u_B \end{pmatrix} \quad (9.60)$$

which has the characteristic equation

$$-(\cos \theta - 2\lambda)(\cos \theta + 2\lambda) - \sin^2 \theta = 0 \quad (9.61)$$

with solutions

$$\lambda_{\pm} = \pm \frac{1}{2}. \quad (9.62)$$

9.7 The γ^5 matrix

Define the useful γ^5 matrix

$$\gamma^5 = i\gamma^0\gamma^1\gamma^2\gamma^3. \quad (9.63)$$

In the Dirac-Pauli representation, it takes the form

$$\gamma^5 = \begin{pmatrix} 0 & I_2 \\ I_2 & 0 \end{pmatrix} \quad (9.64)$$

with the properties

$$(\gamma^5)^\dagger = \gamma^5 \quad (9.65)$$

$$(\gamma^5)^2 = I_4 \quad (9.66)$$

$$\gamma^5 \gamma^\mu = -\gamma^\mu \gamma^5. \quad (9.67)$$

Now consider the action of γ^5 on a solution of the Dirac equation,

$$\gamma^5 \begin{pmatrix} u_A \\ u_B \end{pmatrix} = \begin{pmatrix} 0 & I_2 \\ I_1 & 0 \end{pmatrix} \begin{pmatrix} \chi \\ \frac{\boldsymbol{\sigma} \cdot \mathbf{p}}{E+m} \chi \end{pmatrix} = \begin{pmatrix} \frac{\boldsymbol{\sigma} \cdot \mathbf{p}}{E+m} \chi \\ \chi \end{pmatrix}. \quad (9.68)$$

For ultra-relativistic particles $m \rightarrow 0$ and hence $\frac{\boldsymbol{\sigma} \cdot \mathbf{p}}{E+m} \rightarrow \boldsymbol{\sigma} \cdot \hat{\mathbf{p}}$. We also use the fact that $(\boldsymbol{\sigma} \cdot \hat{\mathbf{p}})(\boldsymbol{\sigma} \cdot \hat{\mathbf{p}}) = I_2$, as shown in (9.9).

$$\begin{aligned} \gamma^5 \begin{pmatrix} u_A \\ u_B \end{pmatrix} &= \begin{pmatrix} (\boldsymbol{\sigma} \cdot \hat{\mathbf{p}}) \chi \\ \chi \end{pmatrix} \\ &= \begin{pmatrix} (\boldsymbol{\sigma} \cdot \hat{\mathbf{p}}) \chi \\ (\boldsymbol{\sigma} \cdot \hat{\mathbf{p}})^2 \chi \end{pmatrix} \\ &= \boldsymbol{\sigma} \cdot \hat{\mathbf{p}} \begin{pmatrix} \chi \\ (\boldsymbol{\sigma} \cdot \hat{\mathbf{p}}) \chi \end{pmatrix} \\ &= \boldsymbol{\sigma} \cdot \hat{\mathbf{p}} \begin{pmatrix} u_A \\ u_B \end{pmatrix}. \end{aligned} \quad (9.69)$$

Therefore, in the limit where $m \rightarrow 0$, the helicity operator becomes $h \rightarrow \gamma^5/2$.

Define the chiral projection operators,

$$P_R = \frac{1}{2} (1 + \gamma^5), \quad P_L = \frac{1}{2} (1 - \gamma^5). \quad (9.70)$$

In the limit where $m \rightarrow 0$, a helicity eigenstate corresponds to a chiral state – i.e. $h = 1$ is a right-handed state. For small m , a helicity eigenstate will be mostly one chirality plus a small amount of the other.

9.8 Completeness relations

The completeness relations are used extensively in the evaluation of Feynman diagrams.

Sum over the spin states,

$$\begin{aligned} \sum_{s=\pm} u_s(p) \bar{u}_s(p) &= \sum_{s=\pm} (E+m) \begin{pmatrix} \chi_s \\ \frac{\boldsymbol{\sigma} \cdot \mathbf{p}}{E+m} \chi_s \end{pmatrix} \begin{pmatrix} \chi_s^\dagger & -\frac{(\boldsymbol{\sigma} \cdot \mathbf{p})^\dagger}{E+m} \chi_s^\dagger \end{pmatrix} \\ &= \sum_{i=\pm} (E+m) \begin{pmatrix} \chi_s \chi_s^\dagger & -\frac{(\boldsymbol{\sigma} \cdot \mathbf{p})^\dagger}{E+m} \chi_s \chi_s^\dagger \\ \frac{\boldsymbol{\sigma} \cdot \mathbf{p}}{E+m} \chi_s \chi_s^\dagger & -\frac{E-m}{E+m} \chi_s \chi_s^\dagger \end{pmatrix} \end{aligned} \quad (9.71)$$

where for the bottom-right element we have used $(\boldsymbol{\sigma} \cdot \mathbf{p})^2 = |\mathbf{p}|^2 = E^2 - m^2 = (E-m)(E+m)$.

The sum over spin states can be easily performed:

$$\sum_{i=\pm} \chi_s \chi_s^\dagger = \begin{pmatrix} 1 \\ 0 \end{pmatrix} (1, 0) + \begin{pmatrix} 0 \\ 1 \end{pmatrix} (0, 1) = \begin{pmatrix} 1 & 0 \\ 0 & 1 \end{pmatrix} = I_2 \quad (9.72)$$

So we have that

$$\begin{aligned}\sum_{i=\pm} u_s(p) \bar{u}_s(p) &= (E + m) \begin{pmatrix} I_2 & -\frac{\boldsymbol{\sigma} \cdot \mathbf{p}}{E+m} \\ \frac{\boldsymbol{\sigma} \cdot \mathbf{p}}{E+m} & \frac{m-E}{E+m} \end{pmatrix} \\ &= \begin{pmatrix} E + m & -\boldsymbol{\sigma} \cdot \mathbf{p} \\ \boldsymbol{\sigma} \cdot \mathbf{p} & m - E \end{pmatrix}\end{aligned}\quad (9.73)$$

Now consider the matrix given by

$$\not{p} + m = \gamma^\mu p_\mu + m \quad (9.74)$$

$$\begin{aligned}&= \begin{pmatrix} E & 0 \\ 0 & -E \end{pmatrix} - \begin{pmatrix} 0 & \boldsymbol{\sigma} \cdot \mathbf{p} \\ -\boldsymbol{\sigma} \cdot \mathbf{p} & 0 \end{pmatrix} + \begin{pmatrix} m & 0 \\ 0 & m \end{pmatrix} \\ &= \begin{pmatrix} E + m & -\boldsymbol{\sigma} \cdot \mathbf{p} \\ \boldsymbol{\sigma} \cdot \mathbf{p} & m - E \end{pmatrix}\end{aligned}\quad (9.75)$$

Comparing (9.73) and (9.75) gives the completeness relation

$$\boxed{\sum_{i=\pm} u_s(p) \bar{u}_s(p) = \not{p} + m.} \quad (9.76)$$

Similarly for antiparticles,

$$\sum_{i=\pm} v_s(p) \bar{v}_s(p) = \not{p} - m. \quad (9.77)$$

9.9 Forms of interaction in Dirac theory

Scalar (even parity): $\bar{\psi}\psi$

Pseudoscalar (odd parity): $\bar{\psi}\gamma^5\psi$

Polar vector (odd parity): $\bar{\psi}\gamma^\mu\psi$. Fermi β decay is described by a polar vector current.

Axial vector (even parity): $\bar{\psi}\gamma^5\gamma^\mu\psi$. The weak interaction is a mixture of polar and axial vector interactions.

Tensor: $\bar{\psi}\sigma^{\mu\nu}\psi$. This type of interaction has not been observed by experiment, although does provide a description of the mechanism behind the anomalous magnetic moment. Spin-2 gravitons would have interactions of this form.

9.10 Trace theorems

In scattering problems, we will often see calculations involving the traces of γ -matrices. What follows will simplify these calculations with some algebraic results.

We start with the facts that traces are associative:

$$\text{Tr}(A + B) \equiv \text{Tr}(A) + \text{Tr}(B) \quad (9.78)$$

and are unchanged by cyclic permutations of the argument:

$$\text{Tr}(AB \dots YZ) \equiv \text{Tr}(ZAB \dots Y). \quad (9.79)$$

Also the algebra of the γ -matrices is defined by their anticommutation relation,

$$\gamma^\mu \gamma^\nu + \gamma^\nu \gamma^\mu = 2g^{\mu\nu} I_4 \quad (9.80)$$

where the presence of the identity has been made explicit. Taking the trace,

$$\text{Tr}(\gamma^\mu \gamma^\nu) + \text{Tr}(\gamma^\nu \gamma^\mu) = 2g^{\mu\nu} \text{Tr}(I_4) \quad (9.81)$$

and using the cyclicity of the trace,

$$\boxed{\text{Tr}(\gamma^\mu \gamma^\nu) = 4g^{\mu\nu}}. \quad (9.82)$$

The trace of any odd number of γ -matrices can be shown to be zero by inserting $\gamma^5 \gamma^5 = I_4$ into the trace. For example,

$$\begin{aligned} \text{Tr}(\gamma^\mu \gamma^\nu \gamma^\rho) &= \text{Tr}(\gamma^5 \gamma^5 \gamma^\mu \gamma^\nu \gamma^\rho) \\ &= \text{Tr}(\gamma^5 \gamma^\mu \gamma^\nu \gamma^\rho \gamma^5) \\ &= -\text{Tr}(\gamma^5 \gamma^5 \gamma^\mu \gamma^\nu \gamma^\rho) \end{aligned} \quad (9.83)$$

where the last line is reached by commuting the last γ^5 through three γ -matrices, each time introducing a factor -1 . Hence we have that $\text{Tr}(\gamma^\mu \gamma^\nu \gamma^\rho) = -\text{Tr}(\gamma^\mu \gamma^\nu \gamma^\rho)$ which can only be true for

$$\boxed{\text{Tr}(\gamma^\mu \gamma^\nu \gamma^\rho) = 0}. \quad (9.84)$$

This is easily extended to the case for any odd number of γ -matrices.

The trace of four γ -matrices can be obtained using (9.80):

$$\begin{aligned} \gamma^\mu \gamma^\nu \gamma^\rho \gamma^\sigma &= (2g^{\mu\nu} - \gamma^\nu \gamma^\mu) \gamma^\rho \gamma^\sigma \\ &= 2g^{\mu\nu} \gamma^\rho \gamma^\sigma - 2g^{\mu\rho} \gamma^\nu \gamma^\sigma + \gamma^\nu \gamma^\rho \gamma^\mu \gamma^\sigma \\ &= 2g^{\mu\nu} \gamma^\rho \gamma^\sigma - 2g^{\mu\rho} \gamma^\nu \gamma^\sigma + 2g^{\mu\sigma} \gamma^\nu \gamma^\rho - \gamma^\nu \gamma^\rho \gamma^\sigma \gamma^\mu \end{aligned} \quad (9.85)$$

Hence,

$$\text{Tr}(\gamma^\mu \gamma^\nu \gamma^\rho \gamma^\sigma) = g^{\mu\nu} \text{Tr}(\gamma^\rho \gamma^\sigma) - g^{\mu\rho} \text{Tr}(\gamma^\nu \gamma^\sigma) + g^{\mu\sigma} \text{Tr}(\gamma^\nu \gamma^\rho) \quad (9.86)$$

Evaluating the traces with (9.82) gives the result

$$\boxed{\text{Tr}(\gamma^\mu \gamma^\nu \gamma^\rho \gamma^\sigma) = 4g^{\mu\nu} g^{\rho\sigma} - 4g^{\mu\rho} g^{\nu\sigma} + 4g^{\mu\sigma} g^{\nu\rho}} \quad (9.87)$$

The full set of trace theorems is:

- $\text{Tr}(I_4) = 4$;
- the trace of any odd number of γ -matrices is zero;
- $\text{Tr}(\gamma^\mu \gamma^\nu) = 4g^{\mu\nu}$;

- $\text{Tr}(\gamma^\mu \gamma^\nu \gamma^\rho \gamma^\sigma) = 4g^{\mu\nu} g^{\rho\sigma} - 4g^{\mu\rho} g^{\nu\sigma} + 4g^{\mu\sigma} g^{\nu\rho}$;
- the trace of γ^5 multiplied by an odd number of γ -matrices is zero;
- $\text{Tr}(\gamma^5) = 0$;
- $\text{Tr}(\gamma^5 \gamma^\mu \gamma^\nu) = 0$; and
- $\text{Tr}(\gamma^5 \gamma^\mu \gamma^\nu \gamma^\rho \gamma^\sigma) = 4i\varepsilon^{\mu\nu\rho\sigma}$, where $\varepsilon^{\mu\nu\rho\sigma}$ is the antisymmetric tensor under the exchange of any two indices.

Chapter 10

$e^- \mu^-$ scattering

This time the scattering between electrons and muons will be considered with spin taken into account. This calculation can be easily extended to similar scattering situations.

10.1 Electron in an EM field

As in Section 8.1 we replace $p^\mu \rightarrow p^\mu + eA^\mu$. Then the components transform as

$$E \rightarrow E + eV \quad (10.1)$$

$$\mathbf{p} \rightarrow \mathbf{p} + e\mathbf{A} \quad (10.2)$$

Starting from the free particle Dirac equation, $(\boldsymbol{\alpha} \cdot \mathbf{p} + \beta m)\psi = E\psi$, after the substitution we have

$$(\boldsymbol{\alpha} \cdot \mathbf{p} + \beta m + e[\boldsymbol{\alpha} \cdot \mathbf{A} - VI_4])\psi = E\psi \quad (10.3)$$

and we may identify V_D , the Dirac potential, to be $e(\boldsymbol{\alpha} \cdot \mathbf{A} - VI_4)$.

10.2 Current-potential formulation

Consider the scattering of a particle with wavefunction ψ_i off a potential V_D to wavefunction ψ_f . The amplitude is given by

$$T_{fi} = -i \int \psi_f^\dagger V_D \psi_i \, d^4x \quad (10.4)$$

$$\begin{aligned} &= -ie \int \psi_f^\dagger \gamma^0 \gamma^0 (-VI_4 + \alpha^k A_k) \psi_i \, d^4x \\ &= -ie \int \bar{\psi}_f (-\gamma^0 V + \gamma^k A_k) \psi_i \, d^4x \\ &= ie \int \bar{\psi}_f \gamma^\mu A_\mu \psi_i \, d^4x. \end{aligned} \quad (10.5)$$

Recall that in the current-potential formulation, the scattering amplitude is given by

$$T_{fi} = -i \int j_{fi}^\mu A_\mu d^4x \quad (10.6)$$

so we identify the current

$$j_{fi}^\mu = -e \bar{\psi}_f \gamma^\mu \psi_i = -e \bar{u}_f \gamma^\mu u_i e^{i(p_f - p_i)x} \quad (10.7)$$

where the second equality comes from the plane wavefunction.

10.3 Scattering amplitude

Now we can consider the full electron-muon scattering process.

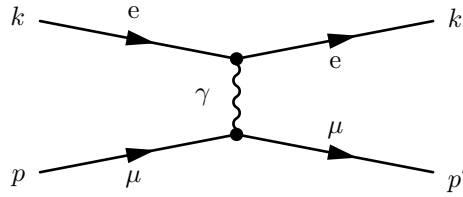


Figure 10.1: Elastic scattering of spin- $\frac{1}{2}$ electrons and muons. This is a t -channel process.

Using the currents j_1 , j_2 and propagator, the transition amplitude is

$$T_{fi} = -i \int j_1^\mu \frac{-1}{q^2} j_2^\mu d^4x \quad (10.8)$$

$$\begin{aligned} &= -i \int \left(-e \bar{u}(k') \gamma_\mu u(k) e^{i(k' - k)x} \right) \frac{-1}{q^2} \left(-e \bar{u}(p') \gamma^\mu u(p) e^{i(p' - p)x} \right) d^4x \\ &= \frac{ie^2}{q^2} \int [\bar{u}(k') \gamma_\mu u(k)] [\bar{u}(p') \gamma^\mu u(p)] e^{i(k' + p' - k - p)x} d^4x \end{aligned} \quad (10.9)$$

As before, in calculating $|T_{fi}|^2$, one exponential term becomes the phase space factor and the other becomes the 4-space volume. The result is

$$|T_{fi}|^2 = \frac{e^4}{q^4} [\bar{u}(k') \gamma_\mu u(k)]^\dagger [\bar{u}(p') \gamma^\mu u(p)]^\dagger [\bar{u}(k') \gamma_\nu u(k)] [\bar{u}(p') \gamma^\nu u(p)] \quad (10.10)$$

Evaluating the Hermitian conjugate (recall that $(\gamma^0)^\dagger = \gamma^0$, $(\gamma^k)^\dagger = -\gamma^k$, and $\gamma^0 \gamma^k = -\gamma^k \gamma^0$),

$$\begin{aligned} [\bar{u}(p') \gamma^0 u(p)]^\dagger &= [u^\dagger(p') \gamma^0 \gamma^0 u(p)]^\dagger \\ &= u^\dagger(p) \gamma^0 \gamma^0 u(p') \\ &= \bar{u}(p) \gamma^0 u(p') \end{aligned} \quad (10.11)$$

$$\begin{aligned}
\left[\bar{u}(p') \gamma^k u(p)\right]^\dagger &= \left[u^\dagger(p') \gamma^0 \gamma^k u(p)\right]^\dagger \\
&= -u^\dagger(p) \gamma^k \gamma^0 u(p') \\
&= u^\dagger(p) \gamma^0 \gamma^k u(p') \\
&= \bar{u}(p) \gamma^k u(p')
\end{aligned} \tag{10.12}$$

So $\left[\bar{u}(p') \gamma^\mu u(p)\right]^\dagger = \bar{u}(p) \gamma^\mu u(p')$ and similarly $\left[\bar{u}(k') \gamma_\mu u(k)\right]^\dagger = \bar{u}(k) \gamma_\mu u(k')$. Now the transition amplitude is

$$\begin{aligned}
|T_{fi}|^2 &= \frac{e^4}{q^4} \left[\bar{u}(k) \gamma_\mu u(k')\right] \left[\bar{u}(p) \gamma^\mu u(p')\right] \left[\bar{u}(k') \gamma_\nu u(k)\right] \left[\bar{u}(p') \gamma^\nu u(p)\right] \\
&= \frac{e^4}{q^4} {}^e L_{\mu\nu} {}^\mu L^{\mu\nu}
\end{aligned} \tag{10.13}$$

where

$${}^e L_{\mu\nu} = \left[\bar{u}(k) \gamma_\mu u(k')\right] \left[\bar{u}(k') \gamma_\nu u(k)\right] \tag{10.14}$$

is the electron tensor, and

$${}^\mu L_{\mu\nu} = \left[\bar{u}(p) \gamma_\mu u(p')\right] \left[\bar{u}(p') \gamma_\nu u(p)\right] \tag{10.15}$$

is the muon tensor.

10.3.1 Sum over spins

For the whole process we must sum over initial and final spins then average over the initial spins. Then the electron tensor becomes

$${}^e L_{\mu\nu} = \frac{1}{2} \sum_S \sum_{S'} \left[\bar{u}(k) \gamma_\mu u(k')\right] \left[\bar{u}(k') \gamma_\nu u(k)\right]. \tag{10.16}$$

Writing out the matrix indices,

$$\begin{aligned}
{}^e L_{\mu\nu} &= \frac{1}{2} \sum_S \sum_{S'} \bar{u}(k)_\alpha \gamma_\mu^{\alpha\beta} u(k')_\beta \bar{u}(k')_\epsilon \gamma_\nu^{\epsilon\sigma} u(k)_\sigma \\
&= \frac{1}{2} \sum_S \sum_{S'} u(k')_\beta \bar{u}(k')_\epsilon \gamma_\nu^{\epsilon\sigma} u(k)_\sigma \bar{u}(k)_\alpha \gamma_\mu^{\alpha\beta} \\
&= (k' + m)_{\beta\epsilon} \gamma_\nu^{\epsilon\sigma} (k + m)_{\sigma\alpha} \gamma_\mu^{\alpha\beta}
\end{aligned} \tag{10.17}$$

where we have used the completeness relation, (9.76), in the last step. This may be written as a trace, such that

$${}^e L_{\mu\nu} = \frac{1}{2} \text{Tr}[(k' + m) \gamma_\nu (k + m) \gamma_\mu] \tag{10.18}$$

$${}^\mu L_{\mu\nu} = \frac{1}{2} \text{Tr}[(p' + M) \gamma_\nu (p + M) \gamma_\mu]. \tag{10.19}$$

where the last equation follows from an identical calculation with the muon tensor, and m and M are the electron and muon masses, respectively.

Now the scattering probability is given by

$$|T_{fi}|^2 = \frac{e^4}{q^4} \frac{1}{2} \text{Tr}[(k' + m) \gamma_\nu (k + m) \gamma_\mu] \frac{1}{2} \text{Tr}[(p' + M) \gamma_\nu (p + M) \gamma_\mu]. \tag{10.20}$$

Using the trace theorems from Section 9.10, the only non-zero term are those with two or four γ -matrices:

$$\begin{aligned}
|T_{fi}|^2 &= \frac{e^4}{4q^4} \text{Tr}[\gamma_\alpha \gamma_\nu \gamma_\beta \gamma_\mu k'^\alpha k^\beta + \gamma_\nu \gamma_\mu m^2] \text{Tr}[\gamma^\alpha \gamma^\nu \gamma^\beta \gamma^\mu p'_\alpha p_\beta + \gamma^\nu \gamma^\mu M^2] \\
&= \frac{4e^4}{q^4} \left[(g_{\alpha\nu} g_{\beta\mu} - g_{\alpha\beta} g_{\nu\mu} + g_{\alpha\mu} g_{\nu\beta}) k'^\alpha k^\beta + g_{\nu\mu} m^2 \right] \left[(g^{\alpha\nu} g^{\beta\mu} - g^{\alpha\beta} g^{\nu\mu} + g^{\alpha\mu} g^{\nu\beta}) p'_\alpha p_\beta + g^{\nu\mu} M^2 \right] \\
&= \frac{8e^4}{q^4} \left[(k' \cdot p')(k \cdot p) + (k' \cdot p)(k \cdot p') - m^2(p' \cdot p) - M^2(k' \cdot k) + m^2 M^2 \right]
\end{aligned} \tag{10.21}$$

10.4 Differential cross section

In the ultrarelativistic limit the masses become negligible and the scattering probability simplifies to

$$|T_{fi}|^2 = \frac{8e^4}{q^4} [(k' \cdot p')(k \cdot p) + (k' \cdot p)(k \cdot p')] \tag{10.22}$$

Now we wish to express this in terms of the Mandelstam variables. The process is t -channel, so we have that

$$t = q^2 \tag{10.23}$$

$$\begin{aligned}
&= (k - k')^2 = (p - p')^2 \\
&\approx -2k \cdot k' \approx -2p \cdot p'
\end{aligned}$$

$$\tag{10.24}$$

The centre of momentum energy is

$$\begin{aligned}
s &= (k + p)^2 = (k' + p')^2 \\
&\approx 2k \cdot p \approx 2k' \cdot p'
\end{aligned} \tag{10.25}$$

and finally

$$\begin{aligned}
u &= (k - p')^2 = (p - k')^2 \\
&\approx -2k \cdot p' \approx -2p \cdot k'
\end{aligned} \tag{10.26}$$

Using these relations, the scattering probability may be expressed as

$$|T_{fi}|^2 = \frac{2e^4}{t^2} (s^2 + u^2) \tag{10.27}$$

We employ the formula for the differential cross section for elastic scattering,

$$\frac{d\sigma}{d\Omega} = \frac{1}{64\pi^2} \frac{|T_{fi}|^2}{s} \tag{10.28}$$

so for the t -channel scattering of two spin-half particles with electron charge (e.g. electrons and muons),

$$\boxed{\frac{d\sigma}{d\Omega} = \frac{e^4}{32\pi^2 s} \frac{s^2 + u^2}{t^2}} \tag{10.29}$$

Chapter 11

$e^- e^+$ annihilation

The annihilation process $e^- e^+ \rightarrow \mu^- \mu^+$ is related to the scattering process $e^- \mu^- \rightarrow e^- \mu^-$ as can be seen by comparing their diagrams. The diagram for the annihilation process is which is the same as for

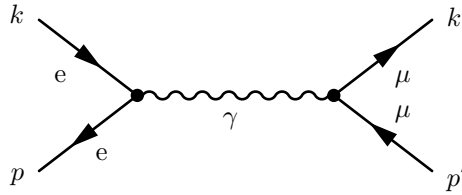


Figure 11.1: Diagram for the s-channel electron annihilation process to positrons.

t-channel elastic scattering, only rotated by 90° . The rotation is equivalent to exchanging k' with $-p$. The consequence of this transformation is simply that the roles of s and t are swapped in the probability $|T_{fi}|^2$, so the differential cross section for the annihilation process is

$$\boxed{\frac{d\sigma}{d\Omega} = \frac{e^4}{32\pi^2 s} \frac{t^2 + u^2}{s^2}} \quad (11.1)$$

11.1 Total cross section

We wish to integrate the differential cross section in the limit where the masses of the particles involved become zero.

Write the kinematic Mandelstam variables in term of energies:

$$\begin{aligned} s &= (k + p)^2 \approx 2k \cdot p \\ &= 2 \begin{pmatrix} E_{e-} \\ E_{e-} \end{pmatrix} \cdot \begin{pmatrix} E_{e+} \\ -E_{e+} \end{pmatrix} \\ &= 4E_{e-} E_{e+} \end{aligned} \quad (11.2)$$

$$\begin{aligned}
t &= (k - k')^2 \approx -2k \cdot k' \\
&= -2 \begin{pmatrix} E_{\text{e}^-} \\ E_{\text{e}^-} \end{pmatrix} \cdot \begin{pmatrix} E_{\mu^-} \\ E_{\mu^-} \cdot \cos \theta \end{pmatrix} \\
&= -2E_{\text{e}^-} E_{\mu^-} (1 - \cos \theta)
\end{aligned} \tag{11.3}$$

$$\begin{aligned}
u &= (k - p')^2 \approx -2k \cdot p' \\
&= -2 \begin{pmatrix} E_{\text{e}^-} \\ E_{\text{e}^-} \end{pmatrix} \cdot \begin{pmatrix} E_{\mu^+} \\ -E_{\mu^+} \cdot \cos \theta \end{pmatrix} \\
&= -2E_{\text{e}^-} E_{\mu^+} (1 + \cos \theta)
\end{aligned} \tag{11.4}$$

Then the differential cross section becomes

$$\begin{aligned}
\frac{d\sigma}{d\Omega} &= \frac{e^4}{32\pi^2 s} \frac{4E_{\mu^-}^2 (1 - \cos \theta)^2 + 4E_{\mu^+}^2 (1 + \cos \theta)^2}{16E_{\text{e}^-}^2} \\
&= \frac{e^4}{128\pi^2 s} \frac{E_{\mu^-}^2 (1 - \cos \theta)^2 + E_{\mu^+}^2 (1 + \cos \theta)^2}{E_{\text{e}^-}^2}
\end{aligned} \tag{11.5}$$

Now we choose the centre of momentum frame where $E_{\text{e}^-} = E_{\mu^-} = E_{\text{e}^+} = E_{\mu^+}$ for massless particles. Then the differential cross section becomes

$$\frac{d\sigma}{d\Omega} = \frac{e^4}{64\pi^2 s} (1 + \cos^2 \theta) \tag{11.6}$$

which can be easily integrated:

$$\begin{aligned}
\sigma &= \frac{e^4}{64\pi^2 s} \int (1 + \cos^2 \theta) d\Omega \\
&= \frac{e^4}{64\pi^2 s} \left(4\pi + 2\pi \int_{-1}^1 \cos^2 \theta d(\cos \theta) \right) \\
&= \frac{e^4}{64\pi^2 s} \left(4\pi + \frac{4\pi}{3} \right) \\
&= \frac{e^4}{12\pi s}.
\end{aligned} \tag{11.7}$$

Finally we use that the fine structure constant $\alpha = \frac{e^2}{4\pi}$ (see (1.14)) to get

$$\boxed{\sigma = \frac{4\pi\alpha^2}{3s}}. \tag{11.8}$$

11.2 R at $\text{e}^- \text{e}^+$ colliders

The process $\text{e}^- \text{e}^+ \rightarrow \mu^- \mu^+$ may be generalised to include other allowed particles in the final state, shown in Figure 11.2. The process is exclusively s -channel except in the case for final-state electrons, where t - and

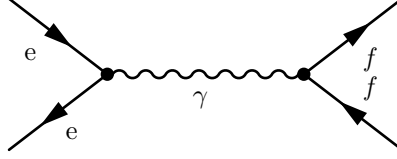


Figure 11.2: The diagram for general s -channel $e^- e^+$ annihilation with final state fermions in QED.

u - channels contribute, and in fact dominate at low energies. Also, muons are simpler to detect. For these reasons, we use the process with final-state muons as a ‘standard candle’ and define the ratio R ,

$$R = \frac{\sigma(e^- e^+ \rightarrow q \bar{q})}{\sigma(e^- e^+ \rightarrow \mu^- \mu^+)} \quad (11.9)$$

At low energies, only u and d quarks are accessible in the final state. They instantly hadronise into pions or ρ mesons, for example. The cross section is proportional to the square of the quark charge and we simply add the cross sections for distinguishable final states,

$$R_{ud} = \left[\left(\frac{2}{3} \right)^2 + \left(\frac{-1}{3} \right)^2 \right] \times 3 = \frac{5}{3} \quad (11.10)$$

where the factor of 3 is due to colour multiplicity of the quark states. In this simple treatment, R increases in steps to $\frac{6}{3}$, $\frac{10}{3}$, $\frac{11}{3}$ up to the CM energy $\sqrt{s} = 2m_b \simeq 9.3 \text{ GeV}$. When the final state quarks combine to form resonances (e.g. ρ : 770 MeV, J/ψ : 3.1 GeV, $\Upsilon(4S)$: 10.6 GeV) R increases above these predictions due to the enhanced cross section.

The BarBar $e^- e^+$ collider operated at the $\Upsilon(4S)$ resonance, allowing measurement of R at about 3.84 (expected 3.67). The higher measured value can be accounted for by QCD higher order $O(\alpha_S)$ QCD corrections due to gluon radiation.

Similarly, the LEP collider operated at the Z resonance $\sqrt{s} = 91 \text{ GeV}$. An analogous quantity R_Z is defined

$$R = \frac{\sigma(Z \rightarrow q \bar{q})}{\sigma(Z \rightarrow \mu^- \mu^+)} \quad (11.11)$$

To lowest order, $P_Z = 20.09$ and it is measured to be 20.79 ± 0.04 . The 3.5% discrepancy is fully explained by higher order QCD corrections involving gluons.

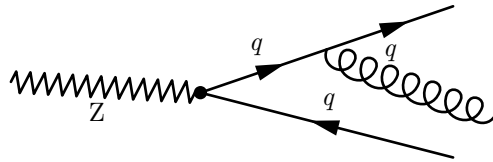


Figure 11.3: Z decay into quark final states with gluon radiation. This diagram contributes to the $O(\alpha_S)$ QCD correction to R_Z .

11.3 Helicity conservation at high energies

Recall the chiral projection operators from Section 9.7,

$$P_R = \frac{1}{2} (1 + \gamma^5), \quad P_L = \frac{1}{2} (1 - \gamma^5).$$

As discussed above, in the limit where $m \rightarrow 0$, helicity and chirality have the same eigenstates. The left-handed chiral state is given, for example, by $U_L = P_L U$.

Using the fact that γ^5 – and hence P_L and P_R – is Hermitian and $\gamma^\mu \gamma^5 = -\gamma^5 \gamma^\mu$, we see that $P_L \gamma^\mu = \gamma^\mu P_R$ and therefore

$$\bar{U}_L = (P_L U)^\dagger \gamma^0 = U^\dagger P_L \gamma^0 = U^\dagger \gamma^0 P_R = \bar{U} P_R. \quad (11.12)$$

Similarly, $\bar{U}_R = \bar{U} P_L$.

Now consider the QED current

$$\bar{U} \gamma^\mu U = (\bar{U}_L + \bar{U}_R) \gamma^\mu (U_L + U_R) \quad (11.13)$$

and look at a cross-term specifically,

$$\begin{aligned} \bar{U}_L \gamma^\mu U_R &= \bar{U} P_R \gamma^\mu P_R U \\ &= \bar{U} \gamma^\mu P_L P_R U \\ &= 0 \end{aligned} \quad (11.14)$$

because $P_L P_R = 0$. This means there are no chirality-changing currents in QED and hence QED conserved chirality, or equivalently helicity in the high energy limit.

Chapter 12

Massless Spin-1 Particles

We approach the quantum description of photons via classical electromagnetism, since we know via the correspondence principle that Maxwell's equations describe their dynamics.

12.1 Maxwell's equation and the classical potential

For fields \mathbf{E} and \mathbf{B} in a vacuum (i.e. not in material), Maxwell's equations are:

1. $\nabla \cdot \mathbf{E} = \rho$, the charge density (Poisson's equation);
2. $\nabla \cdot \mathbf{B} = 0$, no magnetic monopoles;
3. $\nabla \times \mathbf{E} = -\frac{\partial \mathbf{B}}{\partial t}$, Faraday's law;
4. $\nabla \times \mathbf{B} = \mathbf{j} + \frac{\partial \mathbf{E}}{\partial t}$ where \mathbf{j} is the charge current density (Ampère's law).

We define the vector potential such that

$$\boxed{\mathbf{B} = \nabla \times \mathbf{A}} \quad (12.1)$$

so Maxwell II is automatically satisfied. Substituting into Maxwell III,

$$\begin{aligned} \nabla \times \mathbf{E} &= -\frac{\partial}{\partial t} (\nabla \times \mathbf{A}) \\ &= -\nabla \times \frac{\partial \mathbf{A}}{\partial t} \end{aligned} \quad (12.2)$$

$$\Rightarrow \nabla \times \left(\mathbf{E} + \frac{\partial \mathbf{A}}{\partial t} \right) = 0. \quad (12.3)$$

The solution to this equation defines the scalar potential,

$$\mathbf{E} + \frac{\partial \mathbf{A}}{\partial t} = -\nabla \phi. \quad (12.4)$$

Substituting into Maxwell I,

$$\rho = -\nabla^2 \phi - \frac{\partial}{\partial t} \nabla \cdot \mathbf{A} \quad (12.5)$$

Now consider Maxwell IV. The left-hand side is

$$\nabla \times \mathbf{B} = \nabla \times (\nabla \times \mathbf{A}) \quad (12.6)$$

$$= \nabla(\nabla \cdot \mathbf{A}) - \nabla^2 \mathbf{A} \quad (12.7)$$

and the right-hand side is

$$\begin{aligned} \mathbf{j} + \frac{\partial \mathbf{E}}{\partial t} &= \mathbf{j} - \frac{\partial}{\partial t} \left(\nabla \phi + \frac{\partial \mathbf{A}}{\partial t} \right) \\ &= \mathbf{j} - \nabla \frac{\partial \phi}{\partial t} - \frac{\partial^2 \mathbf{A}}{\partial t^2}. \end{aligned} \quad (12.8)$$

Equating (12.7) and (12.8) gives an expression for the 3-current,

$$\mathbf{j} = \frac{\partial^2 \mathbf{A}}{\partial t^2} - \nabla^2 \mathbf{A} + \nabla \left(\frac{\partial \phi}{\partial t} + \nabla \cdot \mathbf{A} \right). \quad (12.9)$$

Also, (12.5) can be written

$$\rho = \frac{\partial^2 \phi}{\partial t^2} - \nabla^2 \phi - \frac{\partial}{\partial t} \left(\frac{\partial \phi}{\partial t} + \nabla \cdot \mathbf{A} \right) \quad (12.10)$$

so we can write Maxwell's equations in covariant form:

$$\boxed{j^\mu = \partial^2 A^\mu - \partial^\mu \partial_\nu A^\nu} \quad (12.11)$$

where the 4-current is $j^\mu = \begin{pmatrix} \rho \\ \mathbf{j} \end{pmatrix}$ and the 4-potential is $A^\mu = \begin{pmatrix} \phi \\ \mathbf{A} \end{pmatrix}$.

12.2 Gauge transformations and the Lorenz condition

Equation (12.11) is invariant under gauge transformations that have the form

$$A^\mu \rightarrow A^\mu + \partial^\mu f \quad (12.12)$$

for some scalar f ; this is easily verified by direct substitution. For a global gauge transformation f is constant but for local gauge transformations f can be a function of the coordinates.

This degree of freedom may be frozen out by the choice of a particular 'gauge'. The Lorenz¹ gauge is the most natural choice with the condition

$$\partial_\mu A^\mu = 0 \quad (12.13)$$

such that all electrodynamics (Maxwell's equations) are simply described by

$$\boxed{\partial^2 A^\mu = j^\mu}. \quad (12.14)$$

12.2.1 Polarisation states of a free photon

Since the 4-potential A^μ describes the photon, there are 4 possible orthogonal polarisations available to it. However, the Lorenz gauge removes one degree of freedom.

¹The Lorenz gauge is named after Ludwig Lorenz and is Lorentz invariant, named after the work of Hendrik Lorentz.

For a free photon, we have that the charge current $j^\mu = 0$. Therefore,

$$\partial^2 A^\mu = 0 \quad (12.15)$$

with polarised plane wave solutions $A^\mu = \epsilon_i^\mu e^{-ipx}$ where ϵ_i^μ are the polarisation 4-vectors. Therefore, the Lorenz condition becomes

$$p_\mu \epsilon_i^\mu = 0. \quad (12.16)$$

This has removed one degree of freedom from the available polarisation states.

Now consider the gauge transformation

$$A^\mu \rightarrow A^\mu + \partial^\mu \left(i\alpha e^{-ipx} \right). \quad (12.17)$$

Then

$$\partial_\mu \partial^\mu \left(\alpha e^{-ipx} \right) = -i\alpha p^2 e^{-ipx} = 0 \quad (12.18)$$

since $p^2 = 0$ for a free photon (it's massless). Therefore the photon is unchanged by such a gauge transformation, which can be written

$$\epsilon_i^\mu \rightarrow \epsilon_i^\mu + \alpha p^\mu. \quad (12.19)$$

We are therefore free to make the gauge choice $\epsilon_i^0 = \epsilon_i^3 = 0$ (with the spatial axes chosen such that $p^0 = p^3 = E$) which corresponds to $\alpha = -\epsilon_{\mu}^i p^\mu / \epsilon_{\nu}^i \epsilon_i^\nu$.

For a free photon with 4-momentum $p = (E, 0, 0, E)^T$, the surviving polarisation states are

$$\epsilon_1^\mu = \begin{pmatrix} 0 \\ 1 \\ 0 \\ 0 \end{pmatrix} \quad \text{and} \quad \epsilon_2^\mu = \begin{pmatrix} 0 \\ 0 \\ 1 \\ 0 \end{pmatrix}$$

which can be combined to give circular polarisations

$$\epsilon_R^\mu = \frac{1}{\sqrt{2}}(\epsilon_1^\mu + i\epsilon_2^\mu) \quad \text{and} \quad \epsilon_L^\mu = \frac{1}{\sqrt{2}}(\epsilon_1^\mu - i\epsilon_2^\mu)$$

which correspond to the ± 1 helicity photon.

In summary, a free spin-1 particle loses one degree of freedom under gauge fixing in electrodynamics. A second gauge fixing removes another degree of freedom, but this relies on the fact that the particle is both massless and free. Therefore, the free photon has only two possible transverse polarisations. In contrast, a virtual photon may also have timelike or longitudinal polarisation.

12.3 Virtual photons and the photon propagator

We saw when discussing the electrodynamics of scalars that the potential (8.14), $A^\mu = -g^{\mu\nu} j_\nu / q^2$, is a solution of Maxwell's equations in the Lorenz gauge, $\partial^2 A^\mu = j^\mu$. There, this was verified by substitution but now it will be derived via the propagator approach.

As a functional of the spatial propagator, $G(x'; x)$, the potential is given by

$$A^\mu(x') = \int G(x'; x) j^\mu(x) d^4x. \quad (12.20)$$

Applying the d'Alembertian differential operator, the left-hand side of the Lorenz condition may be expressed

$$\partial^2 A^\mu(x') = \int \left[\partial^2 G(x'; x) \right] j^\mu(x) d^4x \quad (12.21)$$

where we have used that $\partial_\mu j^\mu = 0$ since the 4-current should be conserved (not explicitly shown for spin-1). The right hand side is

$$j^\mu = \int \delta^{(4)}(x' - x) j^\mu(x) d^4x. \quad (12.22)$$

Therefore, we have that

$$\partial^2 G(x'; x) = \delta^{(4)}(x' - x). \quad (12.23)$$

Now Fourier transform into momentum-space using $q^\mu = -i\partial^\mu$,

$$\frac{1}{(2\pi)^4} \int (iq)^2 \mathcal{G}(q) e^{-iq(x'-x)} d^4q = \frac{1}{(2\pi)^4} \int e^{-iq(x'-x)} d^4q \quad (12.24)$$

from which we see that the momentum-space propagator is $\mathcal{G}(q) = -1/q^2$. Then the potential is

$$A^\mu(x) = \frac{-j^\mu(x)}{q^2} = \frac{-g^{\mu\nu} j_\nu(x)}{q^2} \quad (12.25)$$

By convention, we actually define $\boxed{\mathcal{G}(q) = -ig^{\mu\nu}/q^2}$.

12.3.1 Momentum-space propagators

Generalising the above, the momentum-space propagator may be obtained by inverting the equation of motion for a free particle and multiplying by $-i$.

The Klein-Gordon equation gives $(\partial^2 + m^2)\psi = 0$ for free scalars. Therefore, the propagator is

$$\frac{-i}{(iq)^2 + m^2} = \frac{i}{q^2 - m^2}. \quad (12.26)$$

Now consider the Dirac equation for free spin- $\frac{1}{2}$ particles. From (9.17), the equation of motion is

$$(i\gamma^\mu \partial_\mu - m)\psi = 0.$$

Then, using that $i\partial_\mu = p_\mu$ (note the lower-index form), the propagator is

$$\begin{aligned} \frac{-i}{\gamma^\mu q_\mu - m} &= \frac{i}{\gamma^\mu q_\mu - m} \\ &= \frac{i(\not{q} + m)}{(\not{q} - m)(\not{q} - m)} \\ &= \frac{i(\not{q} + m)}{q^2 - m^2} \\ &= i \frac{\sum u_S \bar{u}_{S'}}{q^2 - m^2} \end{aligned} \quad (12.27)$$

where on the third line we have used that, from the properties of the γ -matrices, $\not{q}^2 = \gamma^\mu q_\mu \gamma^\nu q_\nu = q^2$ and the spinor completeness relation has been used to obtain the last line. The sum is over all possible spins, S and S' .

12.4 Longitudinal and timelike virtual photons

Since we cannot imply the Lorenz gauge condition, virtual photons have four available polarisation states: two transverse, longitudinal, and timelike.

12.4.1 Coulomb's law

The amplitude for photon exchange between two currents is given by

$$\begin{aligned} A &= j_\mu^A \left(\frac{-ig^{\mu\nu}}{q^2} \right) j_B^\nu \\ &= j_\mu^A \left(\frac{-i}{q^2} \right) j_B^\mu. \end{aligned} \quad (12.28)$$

Now the momentum exchange is q^μ . But we know that the four-current is conserved by QED and therefore $q_\mu j^\mu = 0$.

We are free to choose that the photon travels along the z - or t -axes, so $q_1 j^1 = q_2 j^2 = 0$. Then the continuity equation becomes

$$q_\mu j^\mu = q_0 j^0 - q_3 j^3 = 0. \quad (12.29)$$

Substituting back into the amplitude,

$$\begin{aligned} A &= \frac{-i}{q^2} \left[j_0^A j_B^0 - j_3^A j_B^3 \right] \\ &= \frac{-i}{q^2} \left[j_0^A j_B^0 - \frac{q_0^2}{q_3^2} (j_0^A j_B^0) \right] \\ &= \frac{-i}{q_0^2 - q_3^2} \left[\frac{q_3^2 - q_0^2}{q_3^2} j_0^A j_B^0 \right] \\ &= i \frac{j_0^A j_B^0}{q_3^2}. \end{aligned} \quad (12.30)$$

This is Coulomb's law for electromagnetism in 3-momentum space.

12.4.2 Completeness relation

For free photons, the two allowed transverse polarisations give the completeness relation

$$\sum_{P,Q} \epsilon_\mu^P \epsilon_Q^\nu = (0, 1, 0, 0) \begin{pmatrix} 0 \\ 1 \\ 0 \\ 0 \end{pmatrix} + (0, 0, 1, 0) \begin{pmatrix} 0 \\ 0 \\ 1 \\ 0 \end{pmatrix} = \begin{pmatrix} 1 & 0 \\ 0 & 1 \end{pmatrix} = I_2. \quad (12.31)$$

In the case of virtual photons with four allowed polarisations, this becomes

$$\sum_{P,Q} \epsilon_\mu^P \epsilon_Q^\nu = \begin{pmatrix} -1 & 0 & 0 & 0 \\ 0 & 1 & 0 & 0 \\ 0 & 0 & 1 & 0 \\ 0 & 0 & 0 & 1 \end{pmatrix} = -g^{\mu\nu} \quad (12.32)$$

which embeds the completeness relation for real photons.

Chapter 13

Compton Scattering

There are two leading order diagrams for the process $\gamma e \rightarrow \gamma e$, shown in Figure 13.1. Note the similarity to electron-positron annihilation (rotate by 90°).

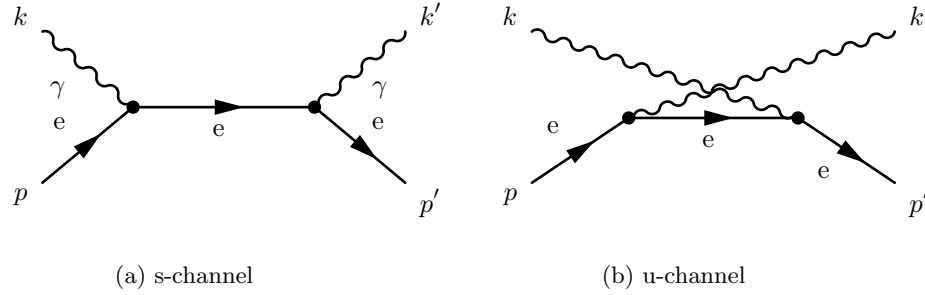


Figure 13.1: Diagrams for the Compton scattering process $\gamma e \rightarrow \gamma e$.

The total scattering probability is given by $|\mathcal{M}|^2$ where $\mathcal{M} = \mathcal{M}_s + \mathcal{M}_u$, such that $|\mathcal{M}|^2 = |\mathcal{M}_s|^2 + |\mathcal{M}_u|^2 + 2\text{Re}(\mathcal{M}_s^* \mathcal{M}_u)$.

13.1 s-channel

Consider the s-channel diagram 13.1a as a double scattering process. The scattering amplitude is given by

$$i\mathcal{M}_s = \int \int \phi^*(x_2) V(x_2) G_0(x_2; x_1) V(x_1) \phi(x_1) d^4 x_1 d^4 x_2 \quad (13.1)$$

$$= \bar{u}(p') (-ie\gamma^\mu) \epsilon_\mu^*(k') \left(\frac{i(\not{p} + \not{k} + m)}{(p+k)^2 - m^2} \right) (-ie\gamma^\nu) \epsilon_\nu(k) u(p) \quad (13.2)$$

where the second line can be obtained using Feynman rules.

Now in the massless limit where $m \rightarrow 0$,

$$\mathcal{M}_s = \frac{-e^2}{s} \bar{u}(p') \gamma^\mu \epsilon_\mu^*(k') (\not{p} + \not{k}) \gamma^\nu \epsilon_\nu(k) u(p) \quad (13.3)$$

hence

$$\begin{aligned}
|\mathcal{M}_s|^2 &= \frac{e^4}{s^2} \left[(\bar{u}(p') \gamma^\mu \epsilon_\mu^*(k') (\not{p} + \not{k}) \gamma^\nu \epsilon_\nu(k) u(p)) (\bar{u}(p) \gamma^\rho \epsilon_\rho(k') (\not{p} + \not{k}) \gamma^\sigma \epsilon_\sigma^*(k) u(p')) \right] \\
&= \frac{e^4}{s^2} \left[\epsilon_\rho(k') \epsilon_\mu^*(k') \epsilon_\nu(k) \epsilon_\sigma^*(k) \bar{u}(p') \gamma^\mu (\not{p} + \not{k}) \gamma^\nu u(p) \bar{u}(p) \gamma^\rho (\not{p} + \not{k}) \gamma^\sigma u(p') \right]
\end{aligned} \tag{13.4}$$

where in the last line all the (Dirac scalar) polarisation vectors have been collected together. We now employ the completeness relation,

$$\sum \epsilon_\mu(p) \epsilon_\nu^*(p) = -g_{\mu\nu} \tag{13.5}$$

where the sum is over all polarisations of the photon. Performing the sum over spins using the electron completeness relation (9.76) ($\sum u \bar{u} = \not{p} + m$) and averaging over all initial spin states (divide by 4),

$$|\mathcal{M}_s|^2 = \frac{e^4}{4s^2} \text{Tr} [g_{\rho\mu} g_{\nu\sigma} (\not{p}' + m) \gamma^\mu (\not{p} + \not{k}) \gamma^\nu (\not{p} + m) \gamma^\rho (\not{p} + \not{k}) \gamma^\sigma] \tag{13.6}$$

$$= \frac{e^4}{4s^2} \text{Tr} [(\not{p}' + m) \gamma^\mu (\not{p} + \not{k}) \gamma^\nu (\not{p} + m) \gamma_\mu (\not{p} + \not{k}) \gamma_\nu] \tag{13.7}$$

$$= \frac{e^2}{s^2} \text{Tr} [\not{p}' (\not{p} + \not{k}) \not{p} (\not{p} + \not{k})] \tag{13.8}$$

where to get the final line the electron mass terms have been neglected and the relation $\gamma^\mu \not{p} \gamma_\mu = -2\not{p}$ used. Now use the fact that $p \cdot p = m^2$ is small to neglect the terms containing \not{p}^2 or higher and use trace theorems to expand,

$$|\mathcal{M}_s|^2 = \frac{e^2}{s^2} \text{Tr} [\not{p}' \not{k} \not{p} \not{k}] \tag{13.9}$$

$$= \frac{4e^4}{s^2} [(p' \cdot k)(p \cdot k) - (p' \cdot p)(k \cdot k) - (p' \cdot k)(k \cdot p)] \tag{13.10}$$

$$= \frac{4e^2}{s^2} [2(p' \cdot k)(p \cdot k)] \tag{13.11}$$

where the last equation comes from the fact that $k \cdot k = 0$ for the massless photon.

Now recall the Mandelstam variables,

$$s = (k + p)^2 = (k' + p')^2, \quad t = (k - k')^2 = (p - p')^2, \quad u = (k - p')^2 = (p - k')^2.$$

In the massless limit, we can approximate,

$$s = (k + p)^2 \approx 2k \cdot p, \quad u = (k - p')^2 \approx -2p' \cdot k. \tag{13.12}$$

Substituting into the result from above,

$$|\mathcal{M}_s|^2 = 2e^4 \frac{-u}{s}. \tag{13.13}$$

13.2 u-channel

For the u-channel, the same steps yield the swapping of the s and u variables,

$$|\mathcal{M}_u|^2 = 2e^4 \frac{-s}{u}. \tag{13.14}$$

13.3 Interference term

Now the remaining term is $2 \text{Re}(\mathcal{M}_s^* \mathcal{M}_u)$. Taking the Hermitian conjugate of (13.3),

$$\mathcal{M}_s^* = -\frac{e^2}{s} \bar{u}(p) \gamma^\mu \epsilon_\mu(k') (\not{p} + \not{k}) \gamma^\nu \epsilon_\nu^*(k) u(p'). \quad (13.15)$$

For the u-channel matrix element, we simply swap $k \leftrightarrow -k'$ so that $s \leftrightarrow u$,

$$\mathcal{M}_u = -\frac{e^2}{u} \bar{u}(p') \gamma^\rho \epsilon_\rho^*(-k) (\not{p} - \not{k}') \gamma^\sigma \epsilon_\sigma(-k') u(p). \quad (13.16)$$

Multiplying these together,

$$\begin{aligned} \mathcal{M}_s^* \mathcal{M}_u &= \frac{e^4}{su} [\bar{u}(p) \gamma^\mu \epsilon_\mu(k') (\not{p} + \not{k}) \gamma^\nu \epsilon_\nu^*(k) u(p') \bar{u}(p') \gamma^\rho \epsilon_\rho^*(-k) (\not{p} - \not{k}') \gamma^\sigma \epsilon_\sigma(-k') u(p)] \\ &= \frac{e^4}{su} \frac{1}{4} \text{Tr}[g_{\mu\rho} g_{\nu\sigma} (\not{p} + m) \gamma^\mu (\not{p} + \not{k}) \gamma^\nu (\not{p}' + m) \gamma^\rho (\not{p} - \not{k}') \gamma^\sigma] \quad (\text{sum-average and completeness relations}) \\ &= \frac{e^4}{su} \frac{1}{4} \text{Tr}[(\not{p} + m) \gamma^\mu (\not{p} + \not{k}) \gamma^\nu (\not{p}' + m) \gamma_\mu (\not{p} - \not{k}') \gamma_\nu] \quad (\text{index gymnastics}) \\ &\approx \frac{e^4}{su} \frac{1}{4} \text{Tr}[\not{p} \gamma^\mu (\not{p} + \not{k}) \gamma^\nu \not{p}' \gamma_\mu (\not{p} - \not{k}') \gamma_\nu] \quad (\text{ignore } m) \\ &= \frac{e^4}{su} \frac{1}{4} \text{Tr}[-2(\not{p} + \not{k}) \gamma^\mu \not{p} \not{p}' \gamma_\mu (\not{p} - \not{k}')] \quad (\gamma_\nu \not{a} \not{b} \gamma^\nu = -2 \not{a} \not{b} \Rightarrow \gamma_\nu \not{a} \gamma^\mu \not{b} \gamma^\nu = -2 \not{b} \gamma^\mu \not{a}) \\ &= \frac{-2e^4}{su} \text{Tr}[(\not{p} + \not{k})(\not{p} \cdot \not{p}')(\not{p} - \not{k}')] \quad (\gamma^\mu \not{p} \not{p}' \gamma_\mu = 4 \not{p} \cdot \not{p}') \\ &= \frac{-2e^4}{su} (p \cdot p') 4 [(p + k) \cdot (p - k')] \quad (\text{Tr}[\not{a} \not{b}] = 4 a \cdot b) \\ &= \frac{-8e^4}{su} (p \cdot p') (p \cdot p + k \cdot p - p \cdot k' - k \cdot k') \end{aligned} \quad (13.17)$$

Now use that

$$t \approx -2p \cdot p' \approx -2k \cdot k', \quad s \approx 2p \cdot k, \quad u \approx -2p \cdot k' \quad (13.18)$$

and neglect the $p \cdot p = m^2$ term,

$$\begin{aligned} \mathcal{M}_s^* \mathcal{M}_u &= \frac{-8e^4}{su} \frac{-t}{2} \left(\frac{s}{2} + \frac{u}{2} + \frac{t}{2} \right) \\ &= 2e^4 \frac{t}{su} (s + u + t) \end{aligned} \quad (13.19)$$

Hence the interference contribution to the cross-section is

$$2 \text{Re}(\mathcal{M}_s^* \mathcal{M}_u) = 2e^4 \frac{2t}{su} (s + u + t). \quad (13.20)$$

13.4 Cross-section

From (5.29) we know that $s + u + t = m^2 \approx 0$ for real (i.e. not virtual) photons. This means that, for a real photon scattering from an approximately massless electron, the s- and u-channel diagrams have no interference.

Hence the differential cross-section is given by

$$\frac{d\sigma}{d\Omega} = \frac{1}{64\pi^2 s} 2e^4 \left(\frac{-u}{s} + \frac{-s}{u} \right) \quad (13.21)$$

Conversely, for a virtual photon $s + u + t = Q^2$ giving a differential cross-section

$$\frac{d\sigma}{d\Omega} = \frac{1}{64\pi^2 s} 2e^4 \left(\frac{-u}{2} + \frac{-s}{u} + \frac{2t}{su} Q^2 \right) \quad (13.22)$$

13.4.1 $e^-e^+ \rightarrow \gamma\gamma$ cross-section

Note that rotating the diagrams in Figure 13.1 by 90° yields all allowed diagrams for $e^-e^+ \rightarrow \gamma\gamma$. Under this transformation we simply swap s and t in the scattering amplitude calculation, so the cross-section in the case real photons is

$$\frac{d\sigma(e^-e^+ \rightarrow \gamma\gamma)}{d\Omega} = \frac{1}{64\pi^2 s} 2e^4 \left(\frac{-u}{t} + \frac{-t}{u} \right). \quad (13.23)$$

13.4.2 Total cross-section when $m \rightarrow 0$, $s \rightarrow \infty$

Taking large s , (13.21) becomes

$$\left. \frac{d\sigma}{d\Omega} \right|_{s \rightarrow \infty} = \frac{1}{64\pi^2} \frac{-2e^4}{u}. \quad (13.24)$$

Substituting $u \approx -2p \cdot k'$,

$$\left. \frac{d\sigma}{d\Omega} \right|_{s \rightarrow \infty} = \frac{1}{64\pi^2} \frac{e^4}{p \cdot k'} \quad (13.25)$$

Now we choose to evaluate the cross-section in the centre-of-mass frame, where

$$p = \begin{pmatrix} E_e \\ \mathbf{p} \end{pmatrix}, \quad k' = \begin{pmatrix} E_\gamma \\ \mathbf{k}' \end{pmatrix}.$$

Then

$$\begin{aligned} p \cdot k' &= E_e E_\gamma - \mathbf{p} \cdot \mathbf{k}' \\ &= E_e E_\gamma + |\mathbf{p}| E_\gamma \cos \theta \end{aligned} \quad (13.26)$$

where we have used that $\mathbf{p} \cdot \mathbf{k}' = -\mathbf{p} \cdot \mathbf{p}' = -|\mathbf{p}| |\mathbf{p}'| \cos \theta = -|\mathbf{p}| E_\gamma \cos \theta$. Now in the small mass case, expand E_e

$$E_e = \left(|\mathbf{p}|^2 + m^2 \right)^{\frac{1}{2}} \approx |\mathbf{p}| \left(1 + \frac{m^2}{2|\mathbf{p}|^2} \right), \quad (13.27)$$

giving

$$\begin{aligned} p \cdot k' &= |\mathbf{p}| \left(1 + \frac{m^2}{2|\mathbf{p}|^2} \right) E_\gamma + |\mathbf{p}| E_\gamma \cos \theta \\ &= |\mathbf{p}| E_\gamma \left(1 + \cos \theta + \frac{m^2}{2|\mathbf{p}|^2} \right) \end{aligned} \quad (13.28)$$

Now in the massless electron case, we have that $|\mathbf{p}| = \sqrt{s}/2 = E_\gamma$. Therefore,

$$p \cdot k' = \frac{s}{4} \left(1 + \cos \theta + \frac{2m^2}{s} \right) \quad (13.29)$$

up to first order in m^2 . Substituting this result into (13.25)

$$\left. \frac{d\sigma}{d\Omega} \right|_{s \rightarrow \infty} = \frac{e^4}{64\pi^2} \frac{4}{s \left(1 + \cos \theta + \frac{2m^2}{s} \right)} \quad (13.30)$$

$$= \frac{\alpha^2}{s \left(1 + \cos \theta + \frac{2m^2}{s} \right)} \quad (13.31)$$

using $\alpha = e^2/4\pi$. This is easily integrable,

$$\begin{aligned} \sigma &= \frac{\alpha^2}{s} \int \frac{d\Omega}{1 + \cos \theta + \frac{2m^2}{s}} \\ &= \frac{2\pi\alpha^2}{s} \int_{-1}^1 \frac{d \cos \theta}{1 + \cos \theta + \frac{2m^2}{s}} \\ &= \frac{2\pi\alpha^2}{s} \ln \left[1 + \cos \theta + \frac{2m^2}{s} \right]_{-1}^1 \\ &= \frac{2\pi\alpha^2}{s} \ln \left[\frac{2 + \frac{2m^2}{s}}{\frac{2m^2}{s}} \right] \\ &= \frac{2\pi\alpha^2}{s} \ln \left[\frac{s}{m^2} + 1 \right] \\ &\approx \frac{2\pi\alpha^2}{s} \ln \left(\frac{s}{m^2} \right). \end{aligned} \quad (13.32)$$

Chapter 14

Massive Spin-1 Particles

14.1 Polarisations

In chapter 12, we saw that for massless spin-1 particles, the equations of motion (Maxwell's equations) can be expressed in covariant form by (12.11):

$$j^\mu = \partial^2 A^\mu - \partial^\mu \partial_\nu A^\nu.$$

The term $\partial^2 A^\mu$ may be expanded as $(\frac{\partial^2}{\partial t^2} - \nabla^2)A^\mu = (-E^2 + p^2)A^\mu$. Now we note that for on-shell massless particles, the combination $-E^2 + p^2 = 0$. Therefore, we replace this combination with the analogous term for massive particles, $(-E^2 + p^2 + m^2)A^\mu = \partial^2 A^\mu + m^2 A^\mu$,

$$\partial^2 A^\mu + m^2 A^\mu - \partial^\mu \partial_\nu A^\nu = j^\mu \quad (14.1)$$

where j^μ is zero for a free massive spin-1 particle and non-zero when it is a virtual propagator. This is the Proca equation.

Differentiating with ∂_μ ,

$$\partial_\mu \partial^\nu \partial_\nu A^\mu + m^2 \partial_\mu A^\mu - \partial_\mu \partial^\mu \partial_\nu A^\nu = \partial_\mu j^\mu = 0 \quad (14.2)$$

where the final equality $\partial_\mu j^\mu = 0$ follows from continuity of the 4-current. Now the first and third terms are equal, as can be seen from index contraction (or swap $\mu \leftrightarrow \nu$ and commute ∂_μ and ∂_ν in one term), so we identify

$$m^2 \partial_\mu A^\mu = 0 \quad (14.3)$$

which is nothing but the Lorenz gauge condition (12.13) for $m^2 \neq 0$. Therefore, massless spin-1 fields automatically satisfy the Lorenz gauge and we cannot 'gauge away' any degrees of freedom as we did in the massless case.

The field may be expressed in its polarisation states as

$$A^\mu = \epsilon_i^\mu e^{-ipx} \quad (14.4)$$

with possible spatial polarisations

$$\epsilon_1 = \begin{pmatrix} 0 \\ 1 \\ 0 \\ 0 \end{pmatrix}, \quad \epsilon_2 = \begin{pmatrix} 0 \\ 0 \\ 1 \\ 0 \end{pmatrix}, \quad \epsilon_3 = \begin{pmatrix} 0 \\ 0 \\ 0 \\ 1 \end{pmatrix}.$$

Given the field now has some mass, we are free to consider its rest frame where $p^\mu = (m, 0, 0, 0)^T$. Therefore the condition $p_\mu \epsilon_i^\mu = 0$ in the rest frame.

14.1.1 Transformation of the polarisation vector

Now consider a particle with momentum p along the z -axis, without loss of generality, or equivalently a boost of $-p$ from the rest frame. The 4-momentum is $p^\mu = (E, 0, 0, p)^T$. It is clear that polarisations ϵ_1 and ϵ_2 will remain the same since the field is perpendicular to the boost. To determine how ϵ_3 transforms we use the Lorenz gauge condition,

$$\begin{aligned} 0 &= \partial_\mu A^\mu = \partial_\mu (\epsilon_3^\mu e^{-ipx}) \\ &= \epsilon_3^\mu (-ip_\mu) e^{-ipx} = 0 \\ \Rightarrow \quad p_\mu \epsilon_3^\mu & \end{aligned} \tag{14.5}$$

Now the covariant (index-down) form of the 4-momentum is $p_\mu = (E, 0, 0, -p)$, so the above equation is satisfied by

$$\epsilon_3^\mu(p) = \frac{1}{m} \begin{pmatrix} p \\ 0 \\ 0 \\ E \end{pmatrix} = \frac{1}{m} \begin{pmatrix} p \\ 0 \\ 0 \\ \sqrt{p^2 + m^2} \end{pmatrix} \tag{14.6}$$

where the $1/m$ factor normalises the polarisation vector for free (on-shell) vector bosons.

14.2 Completeness relation

For free massive vector bosons the completeness relation is given by the sum of outer products,

$$\sum_i \epsilon_i \epsilon_i^\dagger = \begin{pmatrix} 0 \\ 1 \\ 0 \\ 0 \end{pmatrix} (0, 1, 0, 0) + \begin{pmatrix} 0 \\ 0 \\ 1 \\ 0 \end{pmatrix} (0, 0, 1, 0) + \frac{1}{m^2} \begin{pmatrix} p \\ 0 \\ 0 \\ E \end{pmatrix} (p, 0, 0, E) \tag{14.7}$$

$$= \begin{pmatrix} \frac{p^2}{m^2} & 0 & 0 & 0 \\ 0 & 1 & 0 & 0 \\ 0 & 0 & 1 & 0 \\ 0 & 0 & 0 & \frac{E^2}{m^2} \end{pmatrix} \tag{14.8}$$

$$= -g^{\mu\nu} + \frac{p^\mu p^\nu}{m^2}. \tag{14.9}$$

Verifying the last equality,

$$-g^{00} + \frac{p^0 p^0}{m^2} = -1 + \frac{E^2}{m^2} = \frac{-m^2 + E^2}{m^2} = \frac{p^2}{m^2} \tag{14.10}$$

and

$$-g^{33} + \frac{p^3 p^3}{m^2} = 1 + \frac{p^2}{m^2} = \frac{m^2 + p^2}{m^2} = \frac{E^2}{m^2}. \tag{14.11}$$

14.3 Virtual vector bosons

14.3.1 Polarisations

For virtual massive vector bosons there is no longer the constraint that $E^2 - p^2 = m^2$, so a timelike polarisation is ostensibly allowed. However, imposing the Lorenz gauge condition removes this degree of freedom, just as in the massless case. Now the virtual 4-momentum is $q^\mu = (\nu, \mathbf{q})^T$. Therefore,

$$-Q^2 = q_\mu q^\mu = \nu^2 - \mathbf{q} \cdot \mathbf{q}, \quad (14.12)$$

where $Q^2 - m^2$ is the *virtuality* of the particle. So when travelling along the z -axis, $q_z = \sqrt{\nu^2 + Q^2}$, giving

$$q^\mu(\nu) = \begin{pmatrix} \nu \\ 0 \\ 0 \\ \sqrt{\nu^2 + Q^2} \end{pmatrix}. \quad (14.13)$$

Therefore, following the procedure above, the polarisation states of a virtual vector boson are

$$\epsilon_1 = \begin{pmatrix} 0 \\ 1 \\ 0 \\ 0 \end{pmatrix}, \quad \epsilon_2 = \begin{pmatrix} 0 \\ 0 \\ 1 \\ 0 \end{pmatrix}, \quad \epsilon_3 = \frac{1}{Q^2} \begin{pmatrix} \sqrt{\nu^2 + Q^2} \\ 0 \\ 0 \\ \nu \end{pmatrix}. \quad (14.14)$$

14.3.2 Propagator

For a massive spin-1 field, we had the Proca equation (14.1),

$$\partial^2 A^\mu + m^2 A^\mu - \partial^\mu \partial_\nu A^\nu = j^\mu$$

and from differentiating,

$$m^2 \partial_\mu A^\mu = \partial_\mu j^\mu. \quad (14.15)$$

Substituting into the Proca equation,

$$\begin{aligned} & (\partial^2 + m^2) A^\mu - \frac{1}{m^2} \partial^\mu \partial_\nu j^\nu = j^\mu \\ \Rightarrow & (\partial^2 + m^2) A^\mu = \frac{1}{m^2} \partial^\mu \partial_\nu j^\nu + j^\mu \\ & = \frac{1}{m^2} \partial^\mu \partial^\nu j_\nu + g^{\mu\nu} j_\nu \\ & = \left(g^{\mu\nu} + \frac{1}{m^2} \partial^\mu \partial^\nu \right) j_\nu. \end{aligned} \quad (14.16)$$

Now using that $q^\mu = i\partial^\mu$, $\partial^\mu \partial^\nu = -q^\mu q^\nu$,

$$(\partial^2 + m^2) A^\mu = \left(g^{\mu\nu} - \frac{q^\mu q^\nu}{m^2} \right) j_\nu \quad (14.17)$$

from which we identify the virtual vector boson propagator

$$\boxed{\mathcal{G}(q^\mu) = \frac{i}{-q^2 + m^2} \left(g^{\mu\nu} - \frac{q^\mu q^\nu}{m^2} \right)}. \quad (14.18)$$

Decay

In an s-channel process, the propagating particle is seen to decay with a characteristic lifetime

$$\Gamma = \frac{4\pi}{m^2} \frac{1}{32\pi^2} |T_{fi}^2| p_f. \quad (14.19)$$

We therefore modify the wavefunction such that $\psi^\dagger \psi \sim e^{-\Gamma t}$,

$$\psi \sim e^{-imt - \frac{\Gamma}{2}t}. \quad (14.20)$$

By analogy, we replace $im \rightarrow im + \frac{\Gamma}{2}$ (equivalently $m \rightarrow m - \frac{i\Gamma}{2}$) such that $m^2 \rightarrow (m - \frac{i\Gamma}{2})^2 \approx m^2 - i\Gamma m$ where the approximation holds for $\Gamma \ll m$ (true for real-world examples),

$$\mathcal{G}_{\text{decay}}(q^\mu) = \frac{i}{-q^2 + m^2 - i\Gamma m} \left(g^{\mu\nu} - \frac{q^\mu q^\nu}{m^2 - i\Gamma m} \right). \quad (14.21)$$

Appendix A

Experiments of the Last 60 Years

Experiments of the last 60 years

September 30, 2012

Contents

1.1	The early years	2
1.2	Neutrino experiments	3
1.2.1	The Gargamelle experiment	3
1.2.2	Underground experiments	4
1.2.3	Solar neutrinos	4
1.3	High-energy colliding-beam experiments (and some fixed-target results)	5
1.3.1	Lepton-nucleon experiments	5
1.3.2	Lepton-lepton colliders	9
1.3.3	Hadron-hadron colliders	12
1.4	Combining results from different colliders	13

1.1 The early years

Until the 1950s, particle physics was studied by observing cosmic rays in cloud chambers and nuclear emulsion. Around this time, nucleon-nucleon scattering experiments were carried out at cyclotrons and energies became high enough for pions to be produced. Then pion-nucleon scattering was studied. In 1952 Fermi et al. observed

$$\pi^+ + P \xrightarrow{\Delta^{++}} \pi^+ + P \quad (1)$$

which was a big discovery. Also from electron beams, photons could be made and the reaction

$$\gamma + P \xrightarrow{\Delta^+} \gamma + P \quad (2)$$

studied although the rate was much lower because of the electromagnetic coupling.

Other processes were also observed :

$$\pi^+ \rightarrow \mu^+ + \nu_\mu \quad (3)$$

$$\mu^+ \rightarrow e^+ + \bar{\nu}_\mu + \nu_e \quad (4)$$

where the latter is purely leptonic and so provoked large theoretical interest.

In 1956, parity violation in the weak interaction was discovered (predicted by Lee and Yang [1] who received the Nobel Prize). The Wu experiment [2] was the β decay of cobalt-60 nuclei polarised by an external magnetic field, see Fig. 1. The cobalt nuclei are aligned in the magnetic field and are in a state $J = 5$. By conservation of angular momentum, as the $^{60}\text{Ni}^*$ is fixed, the electron and neutrino spins have to be parallel. And as the electron and neutrino are emitted in opposite directions, they have opposite chirality. It was observed that electrons were emitted preferentially opposite to the direction of the magnetic field and not isotropically.

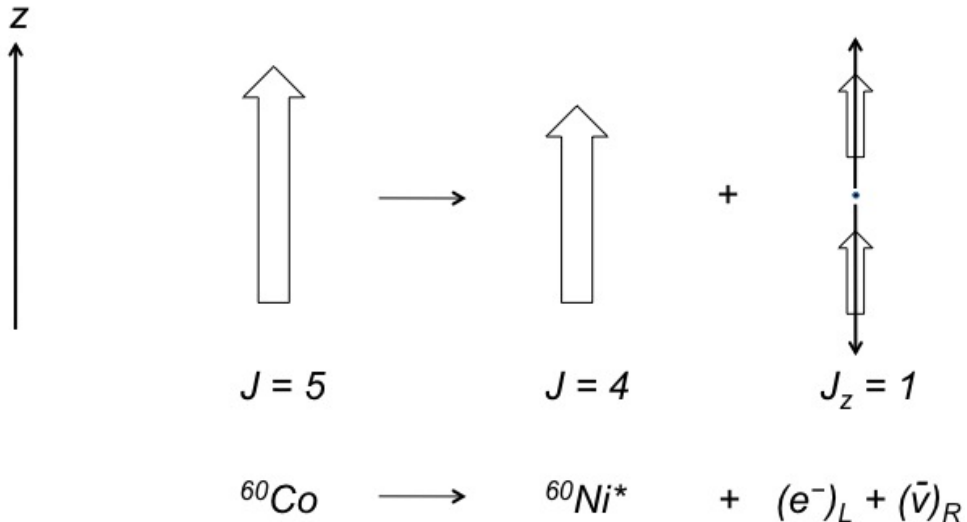


Figure 1: The ^{60}Co experiment where the electron is emitted preferentially opposite the direction of the spin of the ^{60}Co nucleus.

During the 1950s and 1960s, large numbers of mesons and baryons were discovered and these were classified into e.g. octets and decuplets depending on their quantum numbers such as

strangeness and isospin. This led to the use of the $SU(3)$ group to describe these particles [See Symmetries and Conservation Laws course] which accidentally worked as the underlying group, as we now know, is $SU(3)$, but this arises from the colours and not the as-know-then three quarks, u , d and s . These meson classifications can be found in “Particle Physics” by Martin & Shaw.

1.2 Neutrino experiments

[Also see course on Neutrino Physics]

1.2.1 The Gargamelle experiment

Using the CERN proton synchrotron, protons were extracted from the accelerator and impinged on a thin Beryllium target within a neutrino horn. In the target, pions and kaons were created and the horn partially selected either positive or negative charges. The partially focused π^+ decayed to $\mu^+ + \nu_\mu$. An iron shield filtered out the remaining hadrons and muons. Measurements of the muons enabled the neutrino spectrum to be determined. Then the neutrinos passed into the large heavy-liquid bubble chamber, Gargamelle. An initial observation of a single electron track coming from it being scattered by a neutrino was the first weak neutral current event. This was unequivocally confirmed by the deep inelastic scattering experiment in which the charge current reaction,

$$\nu_\mu + P \rightarrow \mu^+ + X, \quad (5)$$

as shown schematically in Fig. 2 (left), was expected. This reaction was observed, but the process,

$$\nu_\mu + P \rightarrow \nu_\mu + X, \quad (6)$$

as shown in schematically in Fig. 2 (right), was also seen. This constituted the discovery of neutral currents in 1974 [3].

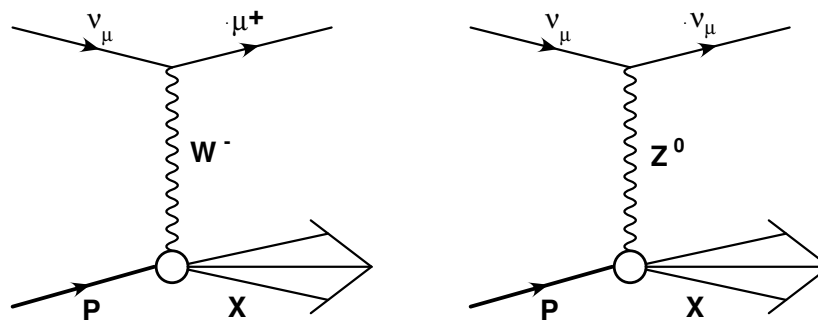


Figure 2: Feynman cartoons of the (left) charge current and (right) neutral current processes for neutrino-proton collisions.

The results, along with electroweak theory, allowed the mass of the W Boson to be predicted to be $M_W \sim 70 \text{ GeV}$ which led to the development of the $S\bar{p}p$ S collider at CERN to search for the mediators of the weak force.

1.2.2 Underground experiments

Large underground experiments were built to measure the rate of neutrinos to try and understand such puzzles as the solar neutrino problem as well as looking for proton decay.

- Solar neutrinos are produced primarily by

$$P + P \rightarrow d + e^+ + \nu_e. \quad (7)$$

- Atmospheric neutrinos are produced primarily by proton bombardment of the upper atmosphere

$$P + N \rightarrow \pi^+(K^+) + H \quad (8)$$

$$\text{with } \pi^+(K^+) \rightarrow \mu^+ + \nu_\mu \quad (9)$$

$$\text{with } \mu^+ \rightarrow e^+ + \bar{\nu}_\mu + \nu_e \quad (10)$$

For the production of atmospheric neutrinos, we would crudely expect $N(\nu_e)/N(\nu_\mu) \sim 1/2$. This ratio was measured by SuperKamiokande to be closer to 1, demonstrating that muon neutrinos were missing. They also measured an azimuthal variation, i.e. $N(\nu_\mu)$ versus $N(\nu_e)$ for neutrinos from the above atmosphere and from the other side of the earth. About half from the other side of the earth were lost suggesting the neutrinos oscillated into ν_τ [4]. With oscillations, this implies that neutrinos have a mass as they must when they have $v < c$.

A large detector of water was used to look for :

$$\nu_\mu + N \rightarrow \mu^- + H \quad (11)$$

$$\nu_e + N \rightarrow e^- + H \quad (12)$$

Both μ^- and e^- were detected by ~ 5000 phototubes by considering their characteristic signals for Cherenkov light. The muon signal rings are sharp whereas those for electrons are more diffuse.

1.2.3 Solar neutrinos

In the experiment by Ray Davies [5] mainly “high” energy (14 MeV) neutrinos were used from the process :

$$p + {}^7\text{Be} \rightarrow {}^8\text{B} + \gamma \quad (13)$$

$${}^8\text{B} \rightarrow {}^8\text{Be} + e^+ + \nu_e \quad (14)$$

They looked for the reaction

$$\nu_e + {}^{37}\text{Cl} \rightarrow e^- + {}^{37}\text{Ar} \quad (15)$$

for neutrinos impinging on a tank of C_2Cl_4 . There were not as many such reactions as was expected in the Standard Model. To detect low-energy neutrinos, tanks of Galium were used

$$\nu_e + \text{Ga} \rightarrow \text{Ge} + e^- . \quad (16)$$

These were also produced at a low rate.

In the Sudbury Neutrino Observatory (SNO), a tank of heavy water (D_2O) was used to detect the following reaction

$$\nu_e + n \rightarrow e^- + p . \quad (17)$$

Again a deficit of electron neutrinos was seen, 1/3 of that expected [6]. Combined with the Kamiokande results, this explained the solar neutrino problem where we see 1/3 of neutrinos are of electron type and 2/3 oscillate into muon and tau neutrinos. This was further confirmed at SNO when they added salt to the water [7] increasing the sensitivity to ν_μ and ν_τ :

$$\nu_{e/\mu/\tau} + n \rightarrow \nu_{e/\mu/\tau} + n_{\text{scat}} \quad (18)$$

$$\text{then } n + {}^{35}\text{Cl} \rightarrow {}^{36}\text{Cl} + \gamma . \quad (19)$$

This was then consistent with the expected total solar neutrino flux.

The discovery of neutrino oscillations and hence that neutrinos have mass was in contradiction to expectations from the Standard Model. This is the only example of the Standard Model being proven wrong, hence the increased interest in neutrino experiments over the last 10 years or so. Further neutrino oscillation experiments are ongoing at reactors (source of copious low-energy neutrinos from β decay) and at accelerators, such as MINOS and T2K. These have recently measured θ_{13} to be non-zero and quite large (see results from Daya Bay and RENO in particular).

1.3 High-energy colliding-beam experiments (and some fixed-target results)

There are various different types of colliding beams which have different properties and can probe different phenomena. Some experiments/colliders are dedicated (e.g. Belle/Babar or lepton-flavour violation, $\mu \rightarrow e$, etc.) or multi-purpose (e.g. LHC, LEP, etc.). Can classify colliders into three types :

1. e^+e^- : this is purely leptonic, is therefore clean and has a controlled centre-of-mass energy. It has a large discovery potential as well as precision physics. Limited by synchrotron radiation, so need to consider linear colliders.
2. $NN(PP)$: highest energy and large discovery potential. Messy.
3. lN : Mixture of the two. One probe and one structured object.

1.3.1 Lepton-nucleon experiments

In the period 1950–70, deep inelastic scattering experiments using e^- , ν and μ beams were used to probe the structure of the proton and neutron. In particular, pioneering experiments at SLAC (Hofstadter et al. [8]) measured the size of the proton ($\sim 10^{-13}\text{m}$) with indications of a substructure which was measured in subsequent experiments. The results suggested that scattering occurred off point-like objects in the nucleon and $\sim 50\%$ of the nucleon interacted in this way. The remaining 50% was carried by the gluons. This was the beginning of QCD.

At HERA, this has been advanced further in eP collisions. Electrons (or positrons) at 27.5 GeV collided with protons of 920 GeV, yielding a centre-of-mass energy of about 320 GeV. There were two multi-purpose detectors which measured a wide range of phenomena : proton and photon structure; other aspects of QCD; electroweak physics; and searches for beyond the Standard Model (e.g. leptoquarks).

We will here discuss two closely related measurements. Firstly the structure of the proton which has been measured over a vast kinematic range compared to the first measurements in the 1960s. The basic process is shown in Fig. 3 (left), where a neutral current (a neutral propagator) process results in the electron scattering in the detector and a photon with squared four-momentum, Q^2 , exchanged. This is essentially related to the wavelength of the probe, i.e. high Q^2 implies a high resolving power. The other relevant variable is the proton's momentum fraction, x , carried by the struck quark. This can be visualised in Fig. 4, where the struck quark has a momentum, xp .

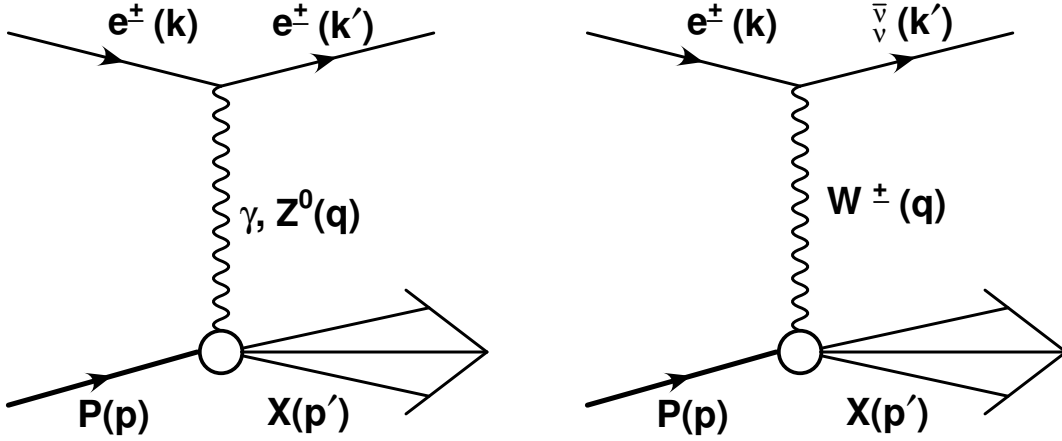


Figure 3: Feynman cartoons of (left) neutral current and (right) charge current eP scattering.

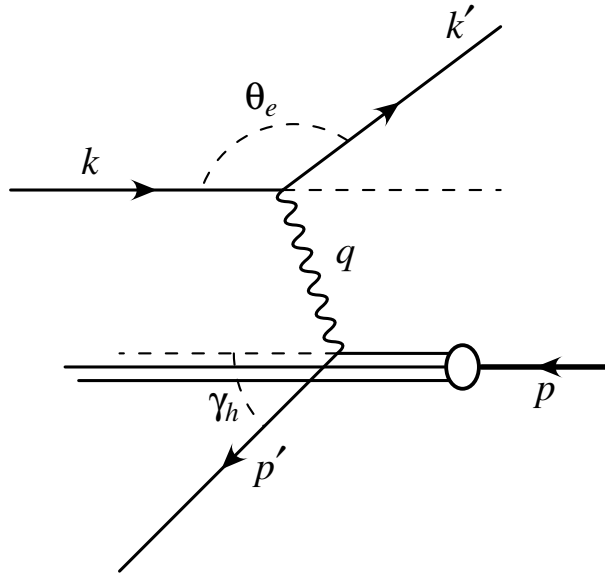


Figure 4: More detailed Feynman cartoon of eP deep inelastic scattering and its kinematics.

Figure 5 shows the cross section for deep inelastic scattering versus Q^2 for different fixed values of x for the HERA data as well as the earlier fixed-target data. The region of high x probes

the quark densities in the the proton and low x probes the gluon density. Overall, this gives us precise knowledge of the structure of matter, one of the fundamental goals of physics. Also, practically, such knowledge is needed by current colliders which use protons (e.g. LHC) so that you know what you are colliding.

H1 and ZEUS

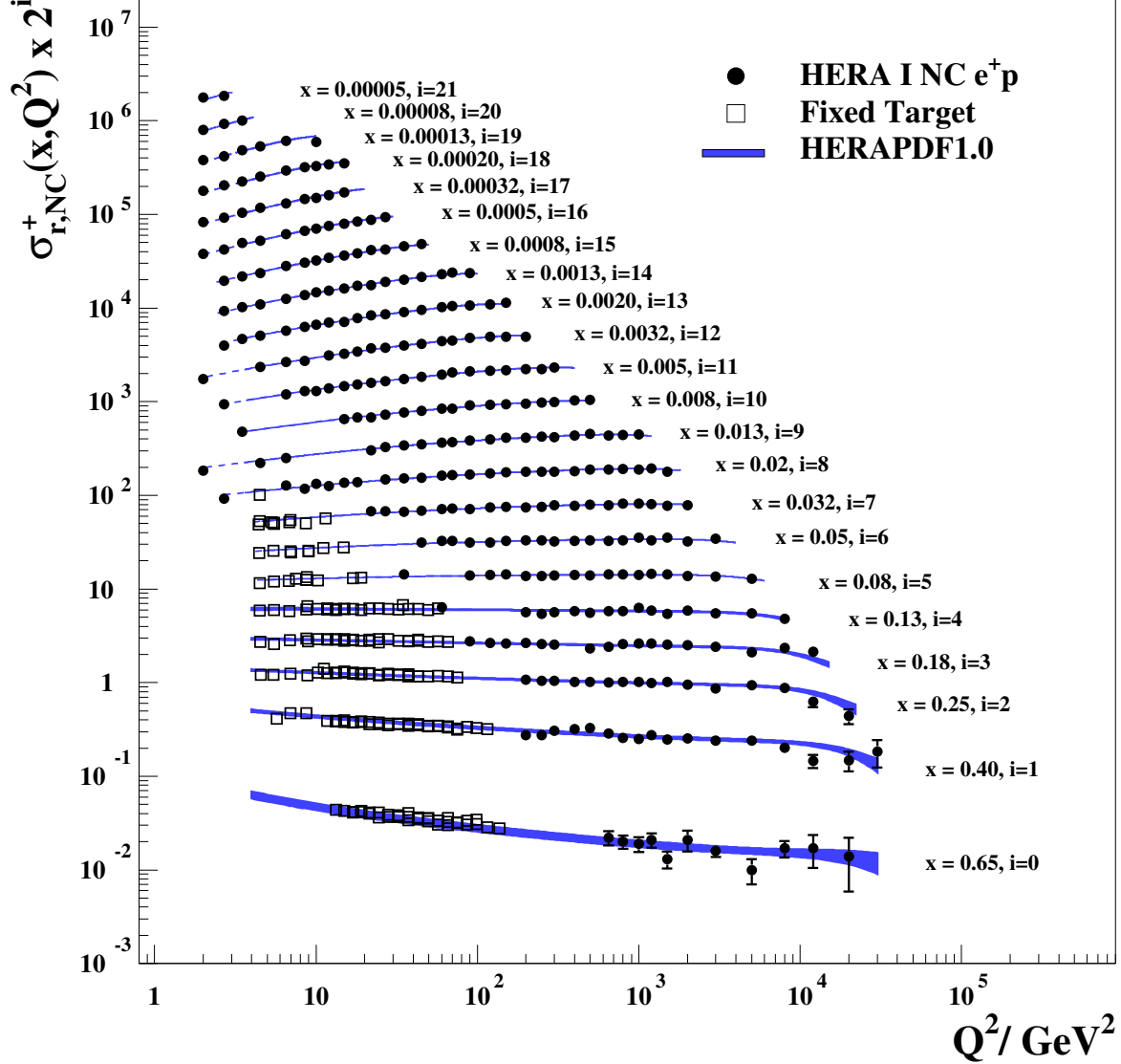


Figure 5: Cross section for neutral current deep inelastic scattering versus the virtuality, Q^2 , at different values of x . From [9].

Another classic measurement made at HERA [10] is shown in Fig. 6 in which the neutral current cross section was measured at high Q^2 and also the charge current (see Fig. 3 (right)) cross section. At low Q^2 , the neutral current cross section is dominated by photon exchange which is very much higher than the charge current cross section. The cross sections for the two process are, however, observed to unify at $Q^2 \sim M_{W,Z}^2 \sim 10^4 \text{ GeV}^2$.

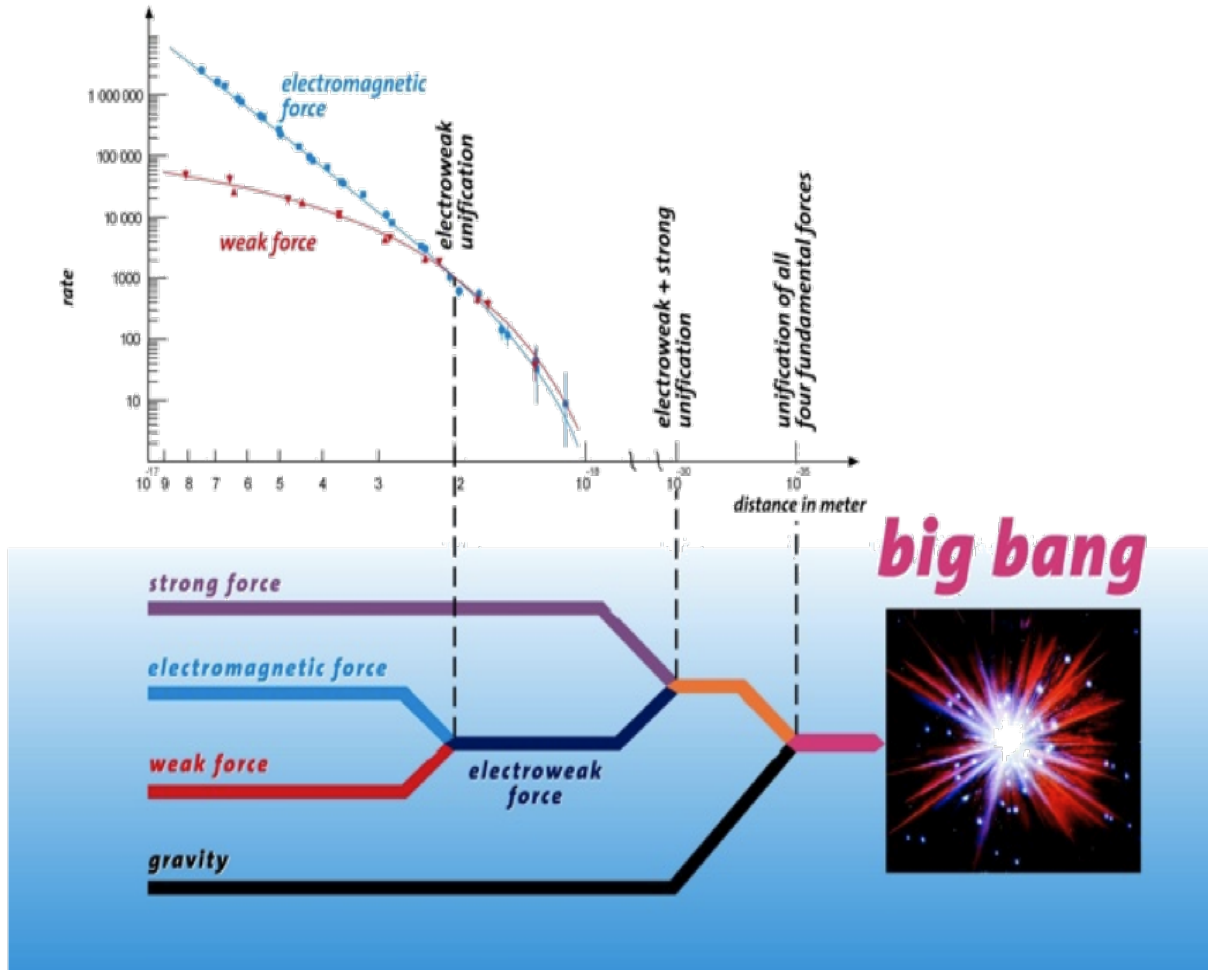


Figure 6: Measurements of neutral current (electromagnetic force) and charge current (weak force) cross sections at HERA demonstrating the scale at which the forces unify. Note the scale for unification with the strong force and gravity. Although a schematic, (publicity plot) the data are the real HERA measurements, here shown as a function of distance but usually plotted versus the scale, Q^2 , with the point of unification at about $Q^2 \sim M_{W,Z}^2 \sim 10^4 \text{ GeV}^2$.

1.3.2 Lepton-lepton colliders

There have been a multitude of e^+e^- experiments with a centre-of-mass energy of a few to over 200 GeV. There is planning for a linear e^+e^- collider of \mathcal{O} (TeV). Some highlights.

The charm quark was discovered in 1974 at SLAC [11] and $P+Be$ at BNL [12] via the detection of the decay of the bound state, the J/ψ meson, to a pair of muons, $M_{J/\psi} \sim 3.1$ GeV. A scan of the e^+e^- total cross section, Fig. 7, shows how discoveries were made and why collider beam energies can be chosen.

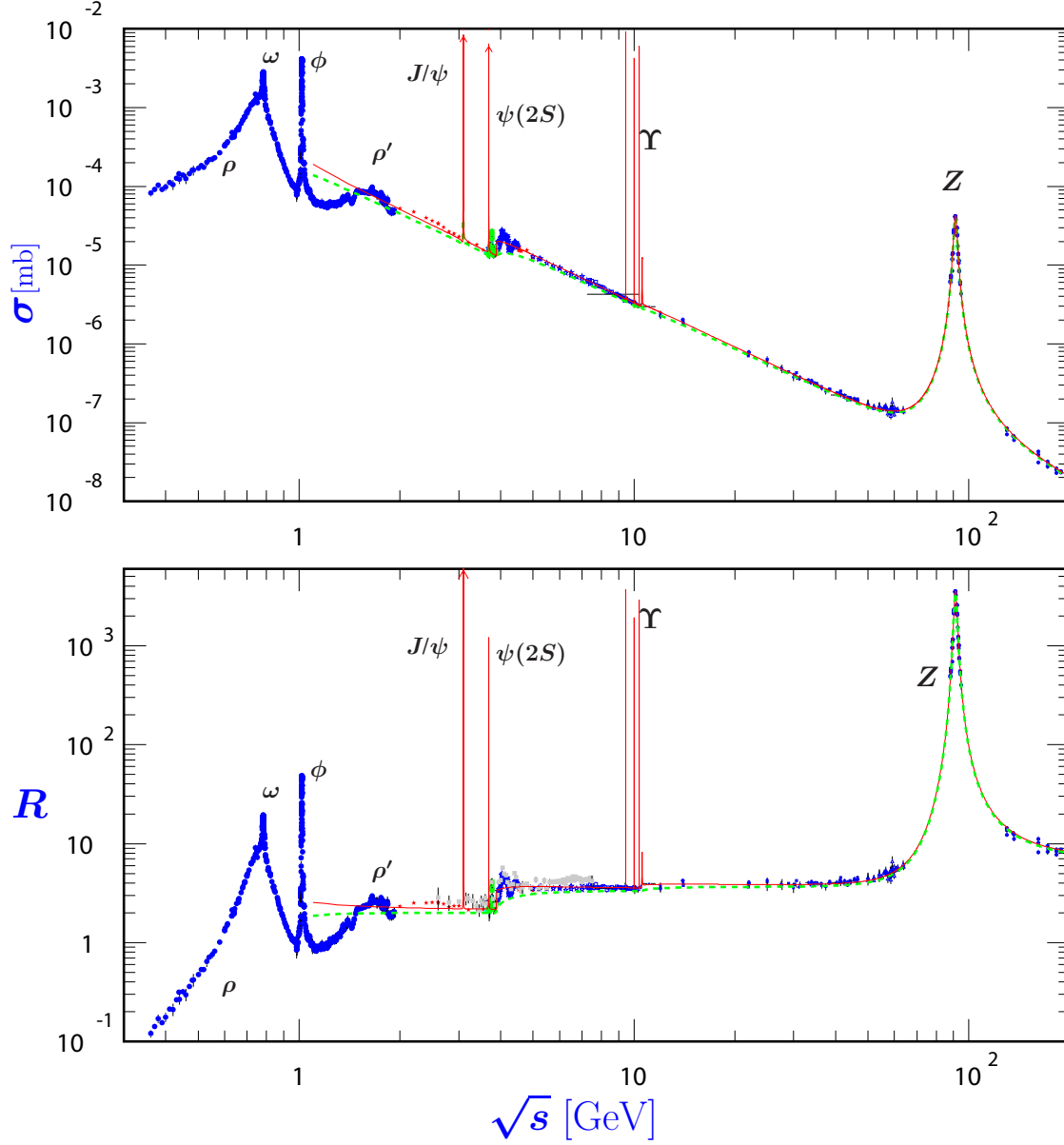


Figure 7: Measurement of the total cross section, $e^+e^- \rightarrow \text{hadrons}$, and ratio, $e^+e^- \rightarrow \text{hadrons}/e^+e^- \rightarrow \mu^+\mu^-$, as a function of the centre-of-mass energy, \sqrt{s} . The curves are a guide using simple theoretical models. From [14].

In 1979, the gluon was discovered [13] by the experiments at the PETRA collider in DESY with $\sqrt{s} = 35$ GeV. Although electron-positron collisions are a clean leptonic environment, they can be powerful probes of QCD. The gluon was discovered through the observation of three-jet

events. Most simply, one would expect two jets to be produced of equal energy and back-to-back as shown schematically in Fig. 8 (left). However, in the detector, three jets (see schematic in Fig. 8 (right)) were observed where one of the quarks had radiated a gluon.

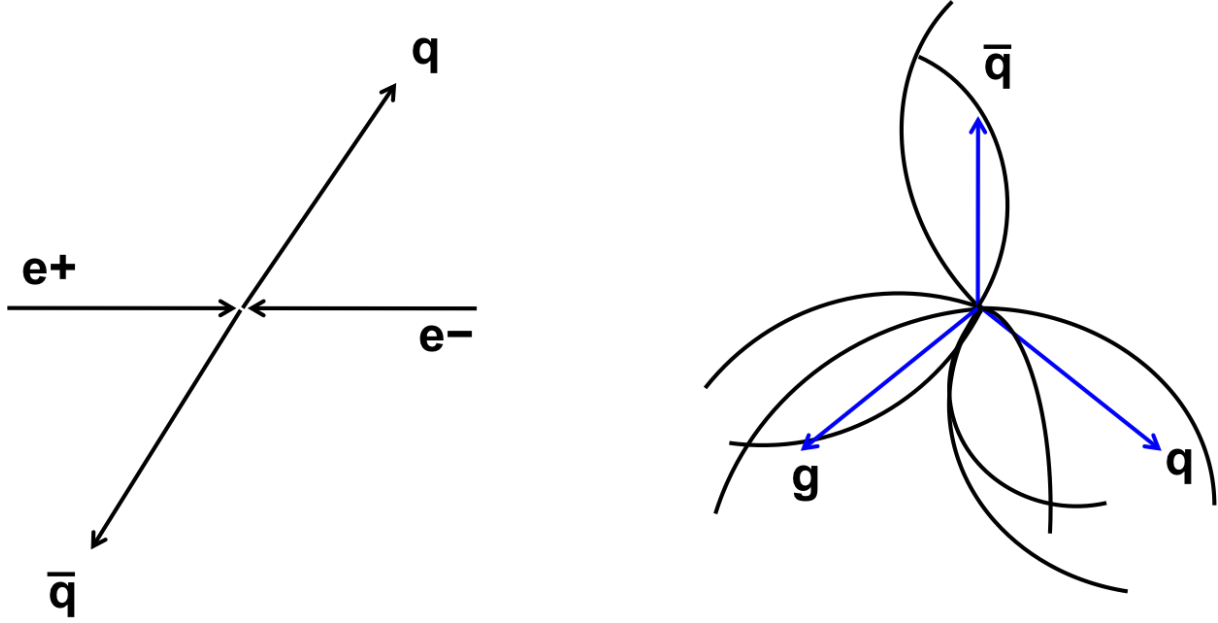


Figure 8: (Left) schematic of an e^+e^- collision in which a quark and anti-quark are produced back-to-back. (Right) Additional events observed in which a star-like, three-jet, configuration was seen, consistent with the additional production of a gluon.

In 1989, the Large Electron-Positron (LEP) collider turned on embarking (along with SLD, a linear collider running at $\sqrt{s} \sim M_Z$) on a new era of precision physics. Initial LEP running was at the Z peak, ~ 91 GeV, then moved through $2M_W \sim 160$ GeV and finally up to just over 200 GeV, looking for the Higgs Boson. There were four multi-purpose experiments which were most famous for precision measurements of electroweak parameters such as M_Z and M_W . The measurement of the cross section as a function of \sqrt{s} was fundamental in measuring M_Z and constraining the number of neutrinos, see Fig. 9.

The values for M_Z and M_W are [14] :

$$M_Z = 91.1876 \pm 0.0021 \text{ GeV} \quad (20)$$

$$M_W = 80.385 \pm 0.015 \text{ GeV} \quad (21)$$

where the latter is still being improved by the Tevatron. In the absence of direct measurements, precise determinations of known parameters constrain new physics phenomena, e.g. the mass of the Higgs Boson. In its final throws, LEP also searched for the Higgs, via Higgsstrahlung (see Fig. 10), where a virtual Z results in a real Z and a Higgs Boson. The centre-of-mass energy was constantly cranked up as $\sqrt{s} > M_H + M_Z$ is required.

Limits of circular e^+e^- machines are being reached due to the rate of energy loss due to synchrotron radiation. The next planned major collider is the International Linear Collider (ILC). This would complement the LHC because of the precisely controlled initial state and cleaner final states. It could also act as a “factory” for e.g. $t\bar{t}$ production, Higgsstrahlung or pair production of exotic particles.

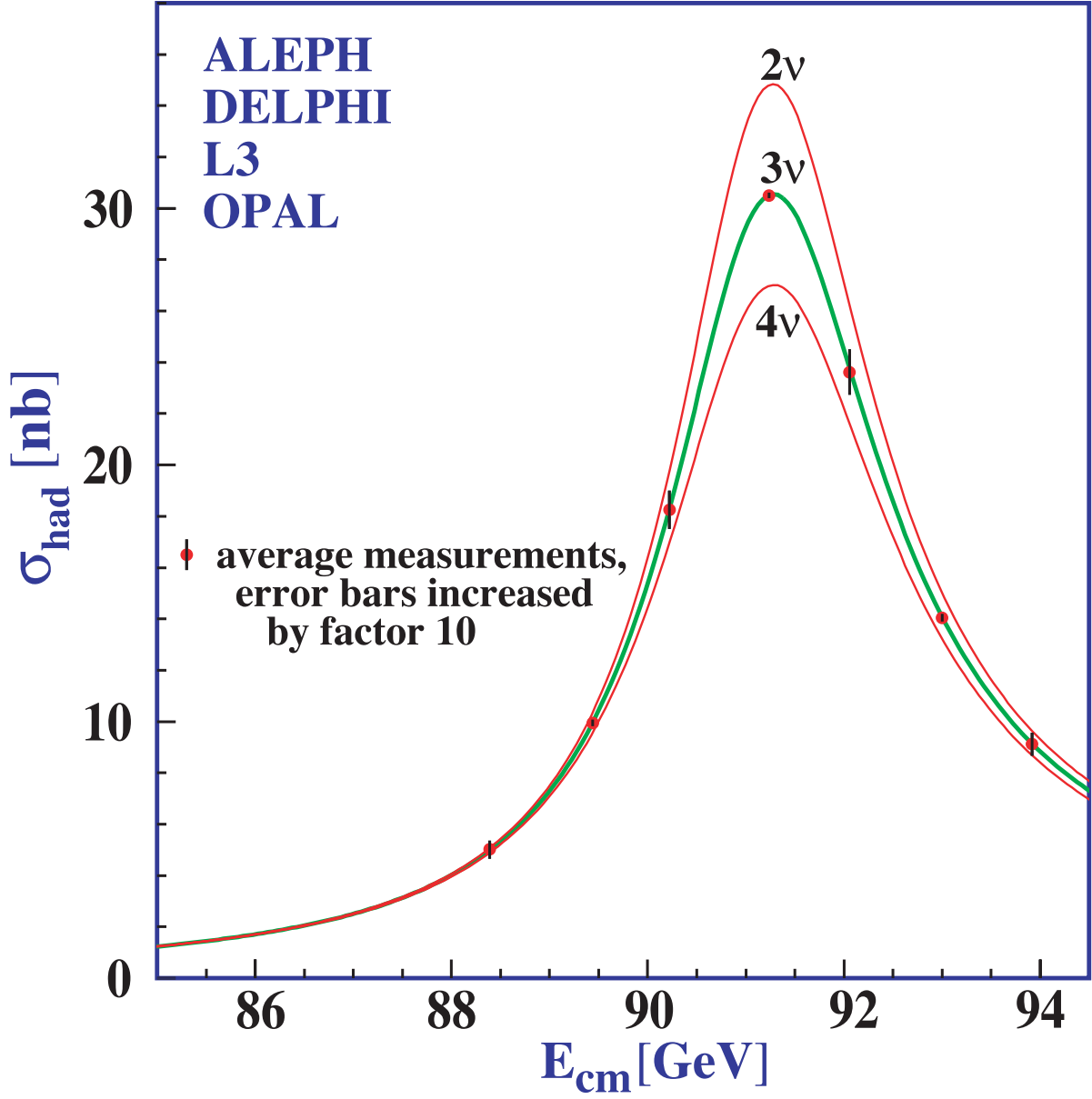


Figure 9: Combined LEP data on the cross section, $e^+e^- \rightarrow \text{hadrons}$, as a function of centre-of-mass energy near M_Z . The curves show the predictions of the Standard Model with two, three, and four species of light neutrinos. The asymmetry of the curve is produced by initial-state radiation. Note that the error bars have been increased by a factor ten for display purposes. From [14, 15].



Due to hadronic structure and multitude of final states, these are more complex than e^+e^- colliders. But they are usually at the energy frontier and thereby produce discoveries and measurements of known phenomena over a large kinematic range. Some of the major results are as follows.

Figure 1 displays the total cross sections for various particle-particle and particle-photon interactions as a function of the center-of-mass energy \sqrt{s} (GeV). The y-axis represents the total cross section in millibarns (mb) on a logarithmic scale from 10^{-4} to 10^2 . The x-axis represents \sqrt{s} in GeV on a logarithmic scale from 1 to 10^4 .

The plot is divided into three panels:

- Top Panel:** Shows hadronic cross sections for $\bar{p}(p)p$ (blue), Σ^-p (purple), $K^\mp p$ (red), and $\pi^\mp p$ (green). The $\bar{p}(p)p$ cross section is the highest, followed by Σ^-p , $K^\mp p$, and $\pi^\mp p$.
- Middle Panel:** Shows the photonic cross section γp (black). The cross section is relatively flat around 10 mb at low energies and increases slightly at higher energies.
- Bottom Panel:** Shows the photoproduction cross section $\gamma\gamma$ (green). The cross section is the lowest, starting around 10^{-3} mb and increasing with energy.

Arrows indicate the energy range where the cross sections are measured. Theoretical predictions are shown as solid lines, and experimental data points with error bars are shown as open circles.

The bottom quark was discovered [16] in 1977 by production of Υ mesons decaying into a pair

of muons in p Be collisions at Fermilab. As is often the case for discoveries, this was seen in the spectrum of the invariant mass of the muon pair, see Fig. 12, with a clear resonance structure observed.

The W and Z bosons were discovered in the early 1980s [17] at the $S\bar{p}p$ S collider at CERN, $\sqrt{s} = 540$ GeV. The leptonic decays of the W and Z were measured as these have relatively low backgrounds compared to hadronic channels. Similarly, the top quark was discovered by CDF and D0 [18] at $\sqrt{s} = 1800$ GeV in 1995.

Not a discovery, but a measurement which can lead to such and has a lot of physics, examples of which are shown in Figs. 13 and 14, is the inclusive jet cross section. This distribution which falls over many orders of magnitudes probes the highest scales and could reveal new physics, e.g. quark substructure, and provides a powerful test of QCD.

1.4 Combining results from different colliders

Combining results from different colliders can simply benefit a measurement by increasing the precision (cf. M_W) or providing an independent cross-check (cf. discovery of the J/ψ). Before these can be done, one has to check that the physics at the different colliders is the same, a far from trivial question. An example is the universality of fragmentation which states that the final state process of fragmentation (or hadronisation) is independent of the initial particle, e.g. if the available energy at collision is the same, then the momentum spectrum of the produced particles does not depend on the flavour of collision. Figure 15 shows [14, 20] the scaled momentum and that the trends seen in e^+e^- and ep collisions are the same. This relies on the concept of factorisation in which parts of the process, e.g. the hard scatter and fragmentation, can be split into two parts and e.g. the factorisation is universal.

The result of combining different data measuring the strong coupling, α_s , is shown in Fig. 16. The different sets of data provide extra precision, some have a wider kinematic range and so test the “running” more rigorously. The data are not only from different colliders but measure completely different processes, e.g. jet cross sections, τ decays, electroweak fits, etc.. This has led to a precision of 0.6%.

One of the primary reasons for measuring α_s to increased precision is to predict the point of when the weak, strong and electromagnetic forces unify. Given their current precision and their expected evolution with energy, the three forces will not unify at any scale, see Fig. 17 (left). Inclusion of a model of Supersymmetry which modifies the evolution of couplings “solves” this problem, see Fig. 17 (right).

Finally, the “holy grail” of particle physics is the search for the Higgs Boson. As discussed before, LEP ruled this out for masses below about 114 GeV. Recently, the ATLAS [22] and CMS experiments [23] have both discovered a new particle which looks like a Higgs Boson with a mass of about 125 GeV [indications have also been seen by the Tevatron experiments]. Both LHC experiments have published signals of about 6σ , combining various channels, see Fig. 18.

References

- [1] T.D. Lee and C.N. Yang, Phys. Rev. **104** (1956) 254.
- [2] C.S. Wu et al., Phys. Rev. **105** (1957) 1413.
- [3] F.J. Hasert et al., Phys. Lett. **46** (1973) 121;
F.J. Hasert et al., Phys. Lett. **46** (1973) 138.
- [4] SuperKamiokande Collaboration, Phys. Rev. Lett. **86** (2001) 5651;
SuperKamiokande Collaboration, Phys. Lett. **B 539** (2002) 179.

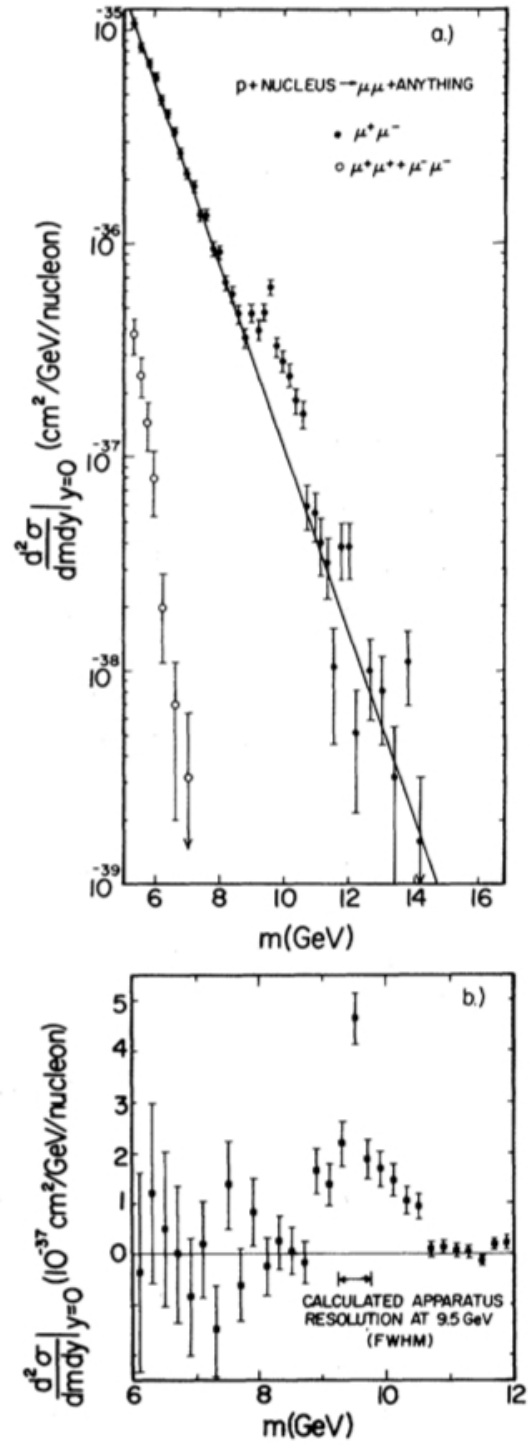


Figure 12: Distribution of Invariant mass of pairs of muons, showing clear enhancement above the continuum at about 9.5 GeV. From [16].

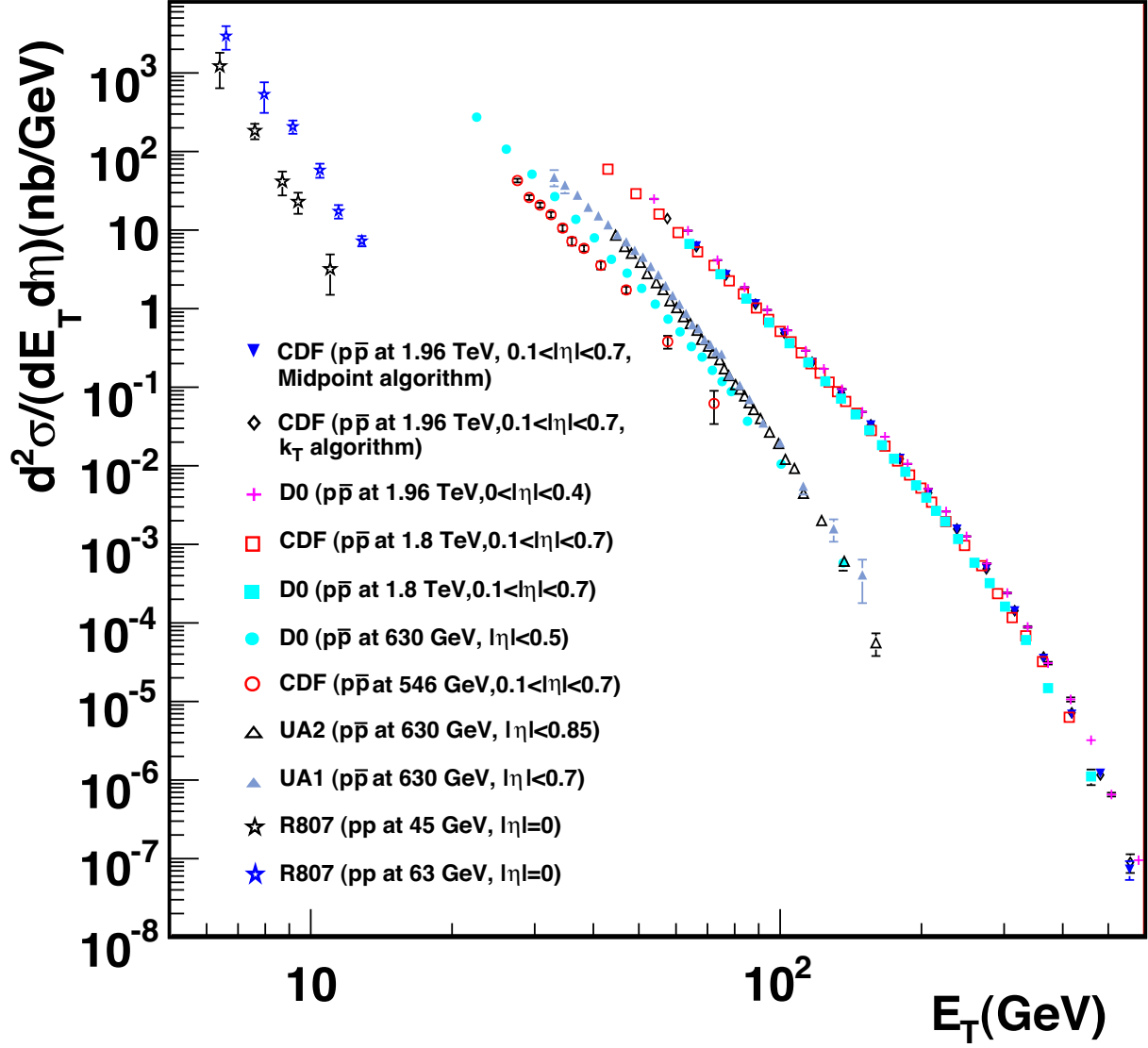


Figure 13: Inclusive jet cross section (pre-LHC) as a function of jet p_T . From [14].

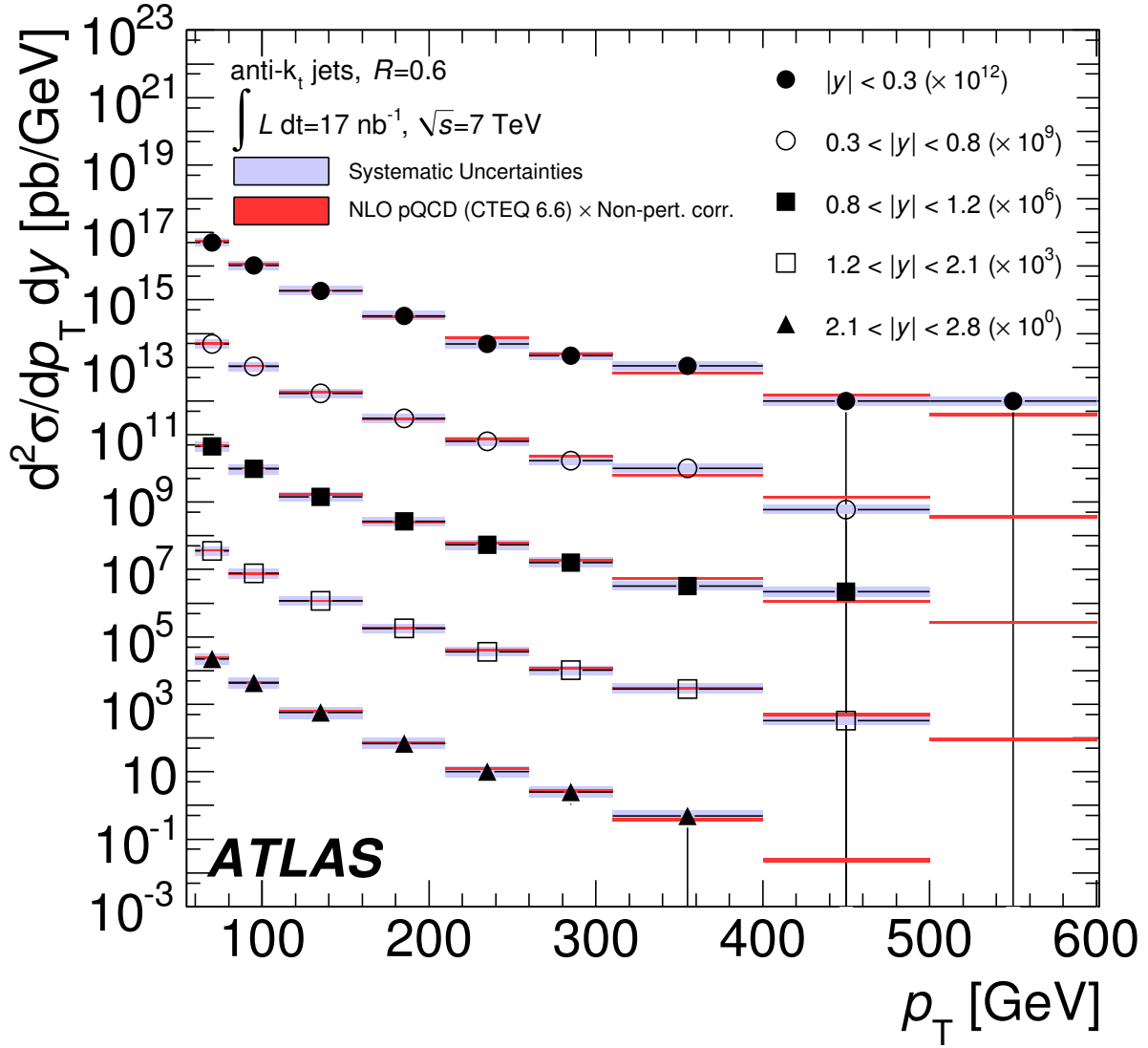


Figure 14: Inclusive jet double-differential cross section as a function of jet p_T in different regions of rapidity. From [19].

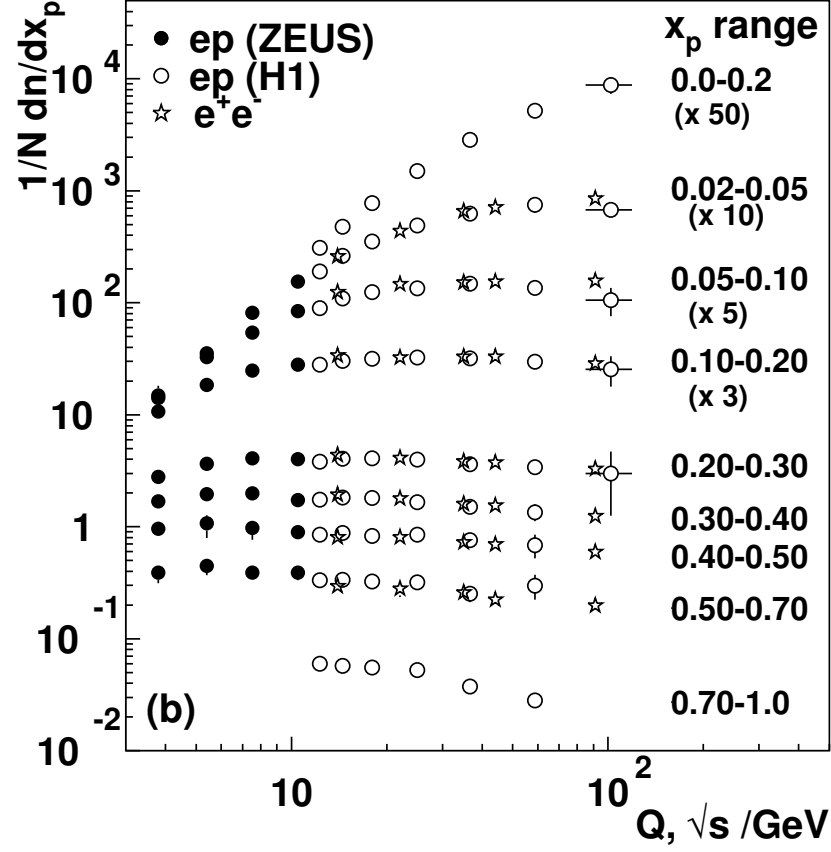


Figure 15: Scaling violations of the fragmentation function for all charged particles in deep inelastic scattering and e^+e^- interactions. From [14].

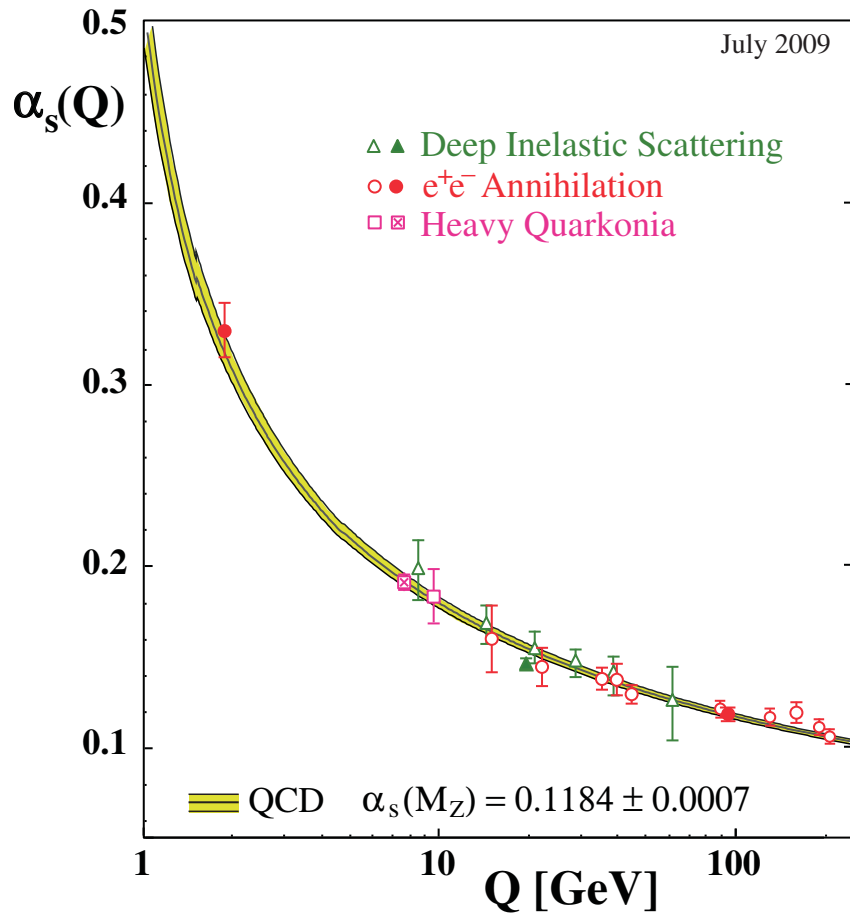


Figure 16: Compilation of measurements of the strong coupling, α_s , versus the scale of the interaction. From [21].

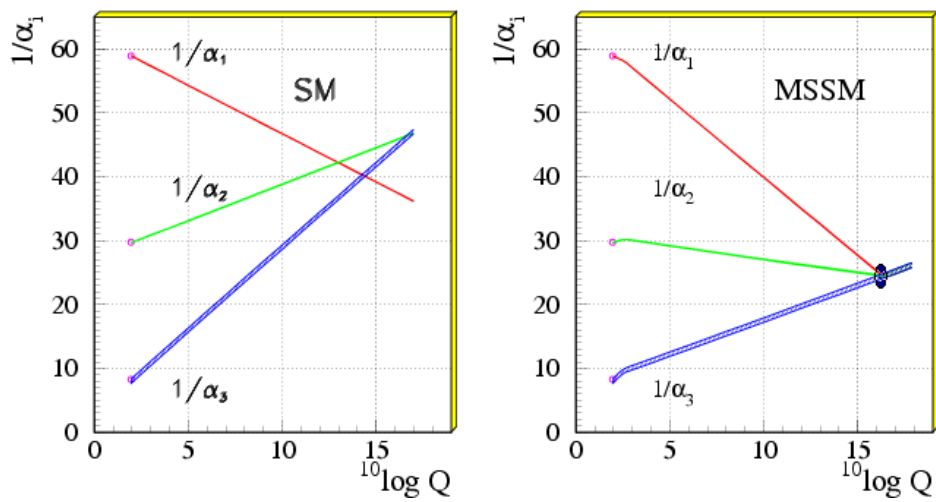


Figure 17: Gauge coupling unification in non-SUSY GUTs on the left versus SUSY GUTs on the right using the LEP data as of 1991. From [24].

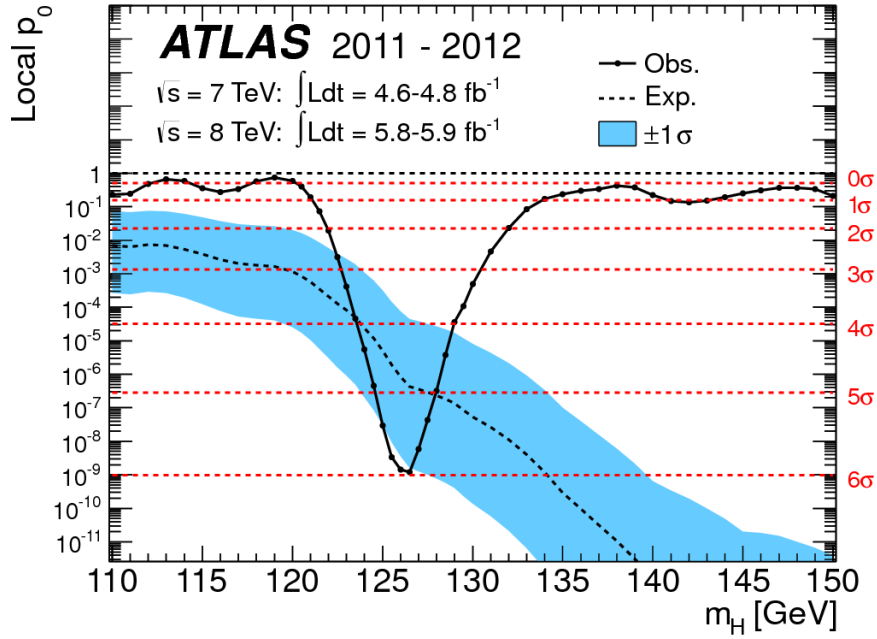


Figure 18: Limit on Higgs Boson from ATLAS as of August 2011. From [22].

- [5] R. Davis, D.S. Harmer and K.C. Hoffman, Phys. Rev. Lett. **20** (1968) 1205.
- [6] SNO Collaboration, Phys. Rev. Lett. **87** (2001) 071301; SNO Collaboration, Phys. Rev. Lett. **89** (2002) 011301;
- [7] SNO Collaboration, Phys. Rev. Lett. **92** (2004) 181301.
- [8] R. Hofstadter, H.R. Fechter and J.A. McIntyre, Phys. Rev. **92** (1953) 978.
- [9] H1 and ZEUS Collaborations, JHEP **1** (2010) 1.
- [10] Several papers go into this plot. As examples of such measurements, see
ZEUS Collaboration, Euro. Phys. J. **C 70** (2010) 945;
H1 Collaboration, Euro. Phys. J. **C 19** (2001) 269.
- [11] J.-E. Augustin et al., Phys. Rev. Lett. **33** (1974) 1406.
- [12] J.J. Aubert et al., Phys. Rev. Lett. **33** (1974) 1404.
- [13] JADE Collaboration, Phys. Lett. **B 91** (1980) 142;
JADE Collaboration, Phys. Lett. **B 101** (1981) 129;
MARK J Collaboration, Phys. Rev. Lett. **43** (1979) 830;
MARK J Collaboration, Phys. Rev. Lett. **50** (1983) 2051;
PLUTO Collaboration, Phys. Lett. **B 86** (1979) 418;
PLUTO Collaboration, Z. Phys. **C 28** (1985) 365;
TASSO Collaboration, Phys. Lett. **B 86** (1979) 243;
TASSO Collaboration, Phys. Lett. **B 97** (1980) 453.
- [14] K. Nakamura et al. (Particle Data Group), J. Phys. **G 37** (2010) 075021; and 2011 partial update for the 2012 edition. <http://pdgl.b1.gov>
- [15] ALEPH Collaboration, Euro. Phys. J. **C 14** (2000) 1;
DELPHI Collaboration, Euro. Phys. J. **C 16** (2000) 371;
L3 Collaboration, Euro. Phys. J. **C 16** (2000) 1;
OPAL Collaboration, Euro. Phys. J. **C 19** (2001) 587;
The ALEPH, DELPHI, L3, OPAL, SLD Collaborations, Phys. Rept. **427** (2006) 257.
- [16] S.W. Herb et al., Phys. Rev. Lett. **39** (1977) 252.
- [17] UA1 Collaboration, Phys. Lett. **B 107** (1981) 320;
UA1 Collaboration, Phys. Lett. **B 122** (1983) 103;

- UA1 Collaboration, Phys. Lett. **B 126** (1983) 398;
 UA2 Collaboration, Phys. Lett. **B 122** (1983) 476;
 UA2 collaboration, Phys. Lett. **B 129** (1983) 130.
- [18] CDF Collaboration, Phys. Rev. Lett. **74** (1995) 2626; D0 Collaboration, Phys. Rev. Lett. **74** (1995) 2632;
- [19] ATLAS Collaboration, Euro. Phys. J. **C 71** (2011) 1512.
- [20] TASSO Collaboration, Z. Phys. **C 47** (1990) 187;
 ZEUS Collaboration, Phys. Lett. **B 414** (1997) 428;
 H1 Collaboration, Phys. Lett. **B 654** (2007) 148;
 DELPHI Collaboration, Phys. Lett. **B 311** (1993) 408;
 ZEUS Collaboration, JHEP **6** (2010) 009; Erratum, *ibid.* JHEP **10** (2010) 030
- [21] S. Bethke, Euro. Phys. J. **C 64** (2009) 689.
- [22] ATLAS Collaboration, Phys. Lett. **B 716** (2012) 1.
- [23] CMS Collaboration, Phys. Lett. **B 716** (2012) 30.
- [24] D.I. Kazakov, [hep-ph/0012288](#).

Appendix B

Special Relativity

$c = 1$ throughout. $N = 4$. Metric signature: $(-, +, +, +)$.

Chapter 1

Tensors

Tensors serve to isolate intrinsic geometric and physical properties from those that merely depend on the coordinates. Therefore tensor analysis finds an application in relativity, since the subject is about coordinate transformations.

1.1 Index notation

Index notation is powerful since it encodes complex information about a mathematical object in a compact form.

For instance, a vector is expressed as

$$\mathbf{A} = \begin{pmatrix} A^0 \\ A^1 \\ A^2 \\ A^3 \end{pmatrix} \quad (1.1)$$

but we can refer to a contravariant component of the vector in abstract index notation as A^μ .

A tensor, $A_{j\dots n}^{i\dots k}$, with s upper (contravariant) and t lower (covariant) indices has valence (s, t) . If two tensors of the same valence have equal components in any one reference frame, then they are equal. This demonstrates that tensor equations express physical facts that transcend the coordinate system.

Some simple rules allow slick calculations with tensor algebra, avoiding having to write things out in a clunky way.

- Conserve valence differentially ($s - t$) on either side of equations.

- Sum over repeated indices. To conserve valence, there must be one lower and one upper repeated dummy index.
- Contraction. The sum over an index reduces the rank of the equation. e.g. $A_{j\mu}^i B_k^\mu = C_{jk}^i$.
- Substitution. The action of a delta is to contract one index and substitute another: $\delta_i^\mu A_{\mu jk} = A_{ijk}$.

1.2 Mathematical treatment of tensors

Consider a vector space, \mathcal{V}_N , spanned the set of (real) variables $\{x^i\}$. Any non-singular linear transformation of $\{x^i\}$ may be regarded as a change of basis in \mathcal{V}_N .

A tensor is an object in \mathcal{V}_N which that may be described by its components, which form an ordered set of (real) numbers $\{x^0, x^1, \dots, x^N\}$.

1.2.1 Rank

A tensor of rank r has $M = N^r$ components.

Rank	Components
0 (Scalar)	1
1 (Vector)	4
2	16
Antisymmetric 2	6

What sort of object should be used to describe physical fields? The electromagnetic field may be described in terms of two 3-vector fields, \mathbf{E} and \mathbf{B} . We therefore wish to encode six components, so require at least a second-rank tensor (for $N = 4$). With sixteen components to play with, introducing the right degeneracy gives the right object for the job: an antisymmetric second-rank tensor.

$$T^{ab} = -T^{ba} \quad (1.2)$$

1.2.2 Coordinate transformations

The coordinate transformations of interest are non-singular (i.e. reversible) and differentiable.

For simplicity, define the partial derivatives:

$$\frac{\partial x^{i'}}{\partial x^i} \equiv p_{i'}^i, \quad \frac{\partial x^i}{\partial x^{i'}} \equiv p_{i'}^i, \quad \frac{\partial^2 x^{i'}}{\partial x^i \partial x^j} \equiv p_{ij}^{i'}, \quad \text{etc.} \quad (1.3)$$

By the chain rule,

$$p_{i'}^i p_{i''}^{i'} = p_{i''}^i \quad (1.4)$$

and

$$p_{i'}^i p_j^{i'} = \delta_j^i \quad (1.5)$$

The index notation is a powerful tool that helps navigate coordinate transformations. Contravariant components are described by upper indices and covariant components by lower indices. Using the rules of index notation, the transformation of quantities may be deduced.

For a general mixed tensor,

$$\boxed{A_{j' \dots n'}^{i' \dots k'} = A_{j \dots n}^{i \dots k} p_{i'}^i \dots p_k^{k'} p_{j'}^j \dots p_{n'}^n} \quad (1.6)$$

(1.6) is the qualification rule for tensors in certain applications where a coordinate transformation is defined, such as in relativity. Therefore tensors which transform in the way described by (1.6) are qualified (or ‘Lorentz’) tensors.

Explicit transformations for tensors of rank 0 to 2 are calculated from (1.6). It is useful to write out the Jacobian matrix,

$$J = \begin{pmatrix} \gamma & -\beta\gamma & 0 & 0 \\ -\beta\gamma & \gamma & 0 & 0 \\ 0 & 0 & 1 & 0 \\ 0 & 0 & 0 & 1 \end{pmatrix} \equiv \mathcal{L} \quad (1.7)$$

for the Lorentz transformation, where the components are labelled as $\mathcal{L}^{i'}_i$.

Rank 0 - Scalars

Since a rank 0 tensor has no indices, its transformation is that of a *Lorentz invariant* quantity,

$$A \rightarrow A \quad (1.8)$$

Rank 1 - Covariant vectors

$$A^\mu \rightarrow A^{\mu'} = \mathcal{L}^{\mu'}_\mu A^\mu \quad (1.9)$$

or in expanded notation,

$$\mathbf{A} \rightarrow \mathbf{A}' = \mathcal{L} \mathbf{A} = \begin{pmatrix} \gamma & -\beta\gamma & 0 & 0 \\ -\beta\gamma & \gamma & 0 & 0 \\ 0 & 0 & 1 & 0 \\ 0 & 0 & 0 & 1 \end{pmatrix} \begin{pmatrix} t \\ x \\ y \\ z \end{pmatrix} \quad (1.10)$$

Rank 2

As with any other tensor, the components transform according to (1.6):

$$A^{\mu\nu} \rightarrow A'^{\mu'\nu'} = \mathcal{L}^{\mu'}_{\mu} \mathcal{L}^{\nu'}_{\nu} A^{\mu\nu} \quad (1.11a)$$

$$= \mathcal{L}^{\mu'}_{\mu} A^{\mu\nu} \mathcal{L}^{\nu'}_{\nu} \quad (1.11b)$$

$$= \mathcal{L}^{\mu'}_{\mu} A^{\mu\nu} (\mathcal{L}^T)_{\nu}^{\nu'} \quad (1.11c)$$

or in expanded notation,

$$\mathbb{A} \rightarrow \mathbb{A}' = \mathcal{L} \mathbb{A} \mathcal{L}^T \quad (1.12)$$

1.2.3 Differentiation

A partial derivative is written

$$\frac{\partial}{\partial x^{\mu}} \equiv \partial_{\mu}. \quad (1.13)$$

Comma notation may be used to reduce clutter and indicate the result that this derivative raises the valence of a tensor by one covariant index,

$$\partial_a \phi \equiv \phi_{,a} \quad (1.14)$$

This is often used in contraction, for example in field equations,

$$\partial_{\mu} J^{\mu} = 0. \quad (1.15)$$

1.3 Index gymnastics

It is often useful to convert between contravariant and covariant components of a tensor. This is possible in a (pseudo-)Riemannian metric space, where the metric is given by the quadratic differential form

$$\mathbf{ds}^2 = g_{\mu\nu} dx^{\mu} dx^{\nu}. \quad (1.16)$$

$g_{\mu\nu}$ is the metric tensor and in flat spacetime, the Minkowski metric tensor is

$$g_{\mu\nu} = \begin{pmatrix} -1 & 0 & 0 & 0 \\ 0 & 1 & 0 & 0 \\ 0 & 0 & 1 & 0 \\ 0 & 0 & 0 & 1 \end{pmatrix} \quad (1.17)$$

where the chosen signature is $(-, +, +, +)$.

Define g^{ij} as the inverse of g_{ij} , such that:

$$g^{ij} g_{jk} = \delta_k^i \quad (1.18)$$

Now we may define contravariant components of a tensor to be those given by

$$A_i^{j\dots} = g_{i\mu} A^{\mu j\dots} \quad (1.19)$$

So the action of the metric tensor is to raise or lower indices.

Chapter 2

Coordinate transformations

2.1 Non-relativistic boost

In classical physics, the coordinate substitution for a boost along the x -axis is given by the Galilean transformation,

$$\begin{pmatrix} t' \\ x' \\ y' \\ z' \end{pmatrix} = \begin{pmatrix} 1 & 0 & 0 & 0 \\ -v & 1 & 0 & 0 \\ 0 & 0 & 1 & 0 \\ 0 & 0 & 0 & 1 \end{pmatrix} \begin{pmatrix} t \\ x \\ y \\ z \end{pmatrix} \quad (2.1)$$

2.2 Postulates of special relativity

Principle of relativity - The laws of physics are the same in all inertial reference frames.

Invariance of c - There is a finite maximum speed for signal propagation, which is the same in all reference frames.

2.3 The Lorentz transformation

The relativistic transformation places space and time on an equal footing:

$$\begin{pmatrix} t' \\ x' \\ y' \\ z' \end{pmatrix} = \begin{pmatrix} \gamma & -\beta\gamma & 0 & 0 \\ -\beta\gamma & \gamma & 0 & 0 \\ 0 & 0 & 1 & 0 \\ 0 & 0 & 0 & 1 \end{pmatrix} \begin{pmatrix} t \\ x \\ y \\ z \end{pmatrix} \quad (2.2)$$

Chapter 3

Transformation of velocity

Consider the 4-velocity, $U^\mu = (\gamma_u c, \gamma_u \mathbf{u})$ in some frame S. Then viewed in some other frame S', moving at velocity \mathbf{v} in the x-direction, U^μ transforms as a four-vector:

$$\begin{pmatrix} \gamma'_u \\ \gamma'_u u'_\parallel \\ \gamma'_u u'_\perp \\ 0 \end{pmatrix} = \begin{pmatrix} \gamma & -\beta\gamma & 0 & 0 \\ -\beta\gamma & \gamma & 0 & 0 \\ 0 & 0 & 1 & 0 \\ 0 & 0 & 0 & 1 \end{pmatrix} \begin{pmatrix} \gamma_u \\ \gamma_u u_\parallel \\ \gamma_u u_\perp \\ 0 \end{pmatrix} \quad (3.1)$$

Which gives

$$\frac{\gamma_{u'}}{\gamma_u \gamma_v} = \frac{1}{1 - \mathbf{u} \cdot \mathbf{v}} \quad (3.2)$$

Therefore, the final answers are

$$\boxed{u'_\parallel = \frac{u_\parallel - v}{1 - \mathbf{u} \cdot \mathbf{v}}} \quad (3.3)$$

and

$$\boxed{u'_\perp = \frac{u_\perp}{\gamma_v (1 - \mathbf{u} \cdot \mathbf{v})}} \quad (3.4)$$

Chapter 4

Pure forces

For a pure force

$$\boxed{\frac{dm}{dt} = 0} \quad (4.1)$$

$$U_\mu F^\mu = \frac{dP^\mu}{dt} U_\mu \quad (4.2a)$$

$$= mA^\mu U_\mu - \frac{dm}{dt} \quad (4.2b)$$

$$= -\frac{dm}{dt} \quad \text{since } A^\mu \text{ and } U^\mu \text{ are orthogonal,} \quad (4.2c)$$

$$= 0 \quad \text{for a pure force.} \quad (4.2d)$$

Also,

$$U_\mu F^\mu = \gamma^2 \left(-\frac{dE}{dt} + \mathbf{u} \cdot \mathbf{f} \right) \quad (4.3)$$

Therefore

$$\boxed{\frac{dE}{dt} = \mathbf{u} \cdot \mathbf{f}} \quad (4.4)$$

for a pure force.

4.1 Expression for 3-force

3-force is defined by

$$\mathbf{f} = \frac{d\mathbf{p}}{dt} \quad (4.5a)$$

$$= \frac{d}{dt} (m\gamma\mathbf{u}) \quad (4.5b)$$

$$= \underbrace{\frac{dm}{dt}}_0 \gamma\mathbf{u} + m \frac{d\gamma}{dt} \mathbf{u} + m\gamma \frac{d\mathbf{u}}{dt} \quad (4.5c)$$

$$= m \frac{d\gamma}{dt} \mathbf{u} + m\gamma \mathbf{a} \quad (4.5d)$$

Now use the equation $E = \gamma m$. Therefore,

$$\mathbf{f} \cdot \mathbf{u} = \frac{dE}{dt} = m \frac{d\gamma}{dt} \quad \text{for pure force.} \quad (4.6)$$

So

$$\boxed{\mathbf{f} = \gamma m \mathbf{a} + (\mathbf{f} \cdot \mathbf{u}) \mathbf{u}} \quad (4.7)$$

Chapter 5

Transformation of force

Consider the 4-force,

$$F^\mu = \gamma \begin{pmatrix} \frac{dE}{dt} \\ \mathbf{f} \end{pmatrix} \quad (5.1)$$

Transforming gives

$$f'_\parallel = \frac{\gamma_u \gamma_v}{\gamma_{u'}} \left(f_\parallel - v \frac{dE}{dt} \right) \quad (5.2a)$$

$$f'_\perp = \frac{\gamma_u}{\gamma_{u'}} f_\perp \quad (5.2b)$$

A quick method to find $\frac{\gamma_u \gamma_v}{\gamma_{u'}}$

Take $U^\mu = \gamma_u(1, \mathbf{u})$ and $V^\mu = \gamma_v(1, \mathbf{v})$ in a general frame. Then

$$U_\mu V^\mu = -\gamma_u \gamma_v (1 - \mathbf{u} \cdot \mathbf{v}) \quad (5.3)$$

But in the frame of a particle moving with V^μ , $V^{\mu'} = (1, 0)$ and $U^{\mu'} = \gamma_{u'}(1, \mathbf{u}')$. Therefore

$$U_{\mu'} V^{\mu'} = -\gamma_{u'} \quad (5.4)$$

is invariant. Equating the expressions for the scalar product of the velocities,

$$\boxed{\frac{\gamma_u \gamma_v}{\gamma_{u'}} = \frac{1}{1 - \mathbf{u} \cdot \mathbf{v}}} \quad (5.5)$$

So we get

$$f'_{\parallel} = \frac{f_{\parallel} - v \frac{dE}{dt}}{1 - \mathbf{u} \cdot \mathbf{v}} \quad (5.6a)$$

$$\Rightarrow f'_{\parallel} = \frac{f_{\parallel} - v(\mathbf{f} \cdot \mathbf{u})}{1 - \mathbf{u} \cdot \mathbf{v}} \quad \text{for a pure force.} \quad (5.6b)$$

and

$$f'_{\perp} = \frac{f_{\perp}}{\gamma_v (1 - \mathbf{u} \cdot \mathbf{v})} \quad (5.7)$$

Chapter 6

The Doppler effect

Consider the invariant $K_\mu U^\mu$. In the rest frame of the source, $K^a = (\omega_0, 0, 0, 0)^T$ and $U^a = (1, 0, 0, 0)^T$, so

$$K_\mu U^\mu = -\omega_0. \quad (6.1)$$

In the observer frame, $K^a = (\omega, \mathbf{k})^T$ and $U^a = (\gamma, \gamma \mathbf{v})$, so

$$K_\mu U^\mu = \gamma(-\omega + \mathbf{k} \cdot \mathbf{v}) \quad (6.2a)$$

$$= \gamma\omega(-1 + \frac{kv}{\omega} \cos \theta) \quad (6.2b)$$

$$= -\gamma\omega(1 - \frac{v}{v_p} \cos \theta) \quad (6.2c)$$

Equating (6.1) and (6.2c),

$$\boxed{\frac{\omega}{\omega_0} = \frac{1}{\gamma(1 - (v/v_p) \cos \theta)}} \quad (6.3)$$

Appendix C

Fermi *beta*-Decay

Chapter 1

Fermi theory of β -decay

Fermi's Golden Rule gives the rate in general form,

$$\Gamma = 2\pi |A_{fi}|^2 \frac{dN}{dE_f} \quad (1.1)$$

1.1 The matrix element

$$A_{fi} = \langle \Psi_f | A | \Psi_i \rangle \quad (1.2)$$

where $\langle x | \Psi_i \rangle = \psi_i$ and $\langle x | \Psi_f \rangle = \psi_f \phi_e \phi_\nu$. From the diagram for β -decay $\langle x | A | x \rangle = G_F \equiv g_w^2 / M_W^2$. Therefore the matrix element is given by

$$A_{fi} = G_F \int_{\text{nucleus}} d^3\mathbf{x} \phi_e^* \phi_\nu^* \psi_f^* \psi_i \quad (1.3)$$

Next we make the assumptions that the electron and neutrino may be treated as plane waves. That is,

$$\phi_e(\mathbf{x}) = \frac{1}{\sqrt{V}} \exp(-i \mathbf{p}_e \cdot \mathbf{x}) \quad (1.4a)$$

$$\phi_\nu(\mathbf{x}) = \frac{1}{\sqrt{V}} \exp(-i \mathbf{p}_\nu \cdot \mathbf{x}) \quad (1.4b)$$

Then

$$\phi_e^* \phi_\nu^* = \frac{1}{V} e^{i \mathbf{p} \cdot \mathbf{x}} \quad (1.5a)$$

$$= 1 + i \mathbf{p} \cdot \mathbf{x} - (\mathbf{p} \cdot \mathbf{x})^2 + \dots \quad (1.5b)$$

$$\approx 1 \quad (1.5c)$$

Therefore

$$A_{fi} \approx \frac{G_F}{V} \underbrace{\int d^3 \mathbf{x} \phi_f^* \phi_i}_{M_{fi}} \quad (1.6a)$$

$$= \frac{G_F}{V} M_{fi} \quad (1.6b)$$

So the expression for the rate becomes

$$\Gamma = 2\pi \frac{G_F^2}{V^2} |M_{fi}|^2 \frac{dN}{dE_f} \quad (1.7)$$

1.2 Density of states

Assume the daughter nucleus is so heavy it doesn't recoil, so we don't need to include a density of states for it.

$$dN = \left(4\pi \frac{V}{(2\pi)^3} p_e^2 dp_e \right) \left(4\pi \frac{V}{(2\pi)^3} p_\nu^2 dp_\nu \right) \quad (1.8a)$$

$$= \frac{(4\pi)^2}{(2\pi)^6} V^2 p_e^2 p_\nu^2 dp_e dp_\nu \quad (1.8b)$$

Now we take $E_f = E_e + E_\nu$, therefore $dE_f = dE_\nu = dp_\nu$ for a fixed E_e (assuming $E_\nu \approx p_\nu$).

$$\frac{dN}{dE_f} = \frac{(4\pi)^2}{(2\pi)^6} V^2 p_e^2 (E_f - E_e)^2 dp_e \quad (1.9)$$

so

$$\boxed{d\Gamma = 2\pi G_F^2 |M_{fi}|^2 \frac{1}{4\pi^4} (E_f - E_e)^2 p_e^2 dp_e} \quad (1.10)$$

Integrating through possible electron momenta from 0 to p_f (and using $p_e \approx E_e$), we obtain the result

$$\boxed{\Gamma \propto E_f^5} \quad (1.11)$$

1.3 Assumptions

- $|Q| \ll M_W$, so the propagator factor is purely the mass of the exchange boson;
- The wavefunctions for the electron and neutrino may be approximated as plane waves;
- $(\mathbf{p}_e + \mathbf{p}_\nu) \cdot \mathbf{x} \ll 1$, which simplifies the matrix element to some scalar multiple of the nuclear form factor;
- The daughter nucleus is heavy and there is no recoil, so there is no density of states;
- The electron and neutrino are ultrarelativistic, so $E \approx p$.

Appendix D

2-Flavor Neutrino Model

1 2-flavour neutrino model

1.1 Mixing

$$\begin{pmatrix} \nu_e \\ \nu_\mu \end{pmatrix} = \begin{pmatrix} \cos \theta & \sin \theta \\ -\sin \theta & \cos \theta \end{pmatrix} \begin{pmatrix} \nu_1 \\ \nu_2 \end{pmatrix} \quad (1)$$

Start with ν_e :

$$\begin{aligned} |\psi(0)\rangle &= |\nu_e\rangle \\ &= \cos \theta |\nu_1\rangle + \sin \theta |\nu_2\rangle \end{aligned} \quad (2)$$

In contrast to neutral meson mixing, we work in the lab frame and approximate the neutrinos as plane waves. The mass eigenstates evolve with a time-dependent complex phase.

$$|\psi(t)\rangle = \cos \theta e^{-i\phi_1} |\nu_1\rangle + \sin \theta e^{-i\phi_2} |\nu_2\rangle \quad (3)$$

So the ν_e survival amplitude is given by

$$\langle \nu_e | \psi(t) \rangle = \cos^2 \theta e^{-i\phi_1} + \sin^2 \theta e^{-i\phi_2} \quad (4)$$

therefore the survival probability is

$$P(\nu_e \rightarrow \nu_e) = \cos^4 \theta + \sin^4 \theta + 2 \sin^2 \theta \cos^2 \theta \cos(\Delta\phi) \quad (5)$$

This can be rearranged into a more convenient form. First, complete the square:

$$\cos^4 \theta + \sin^4 \theta = \underbrace{(\cos^2 \theta + \sin^2 \theta)^2}_{1} - 2 \sin^2 \theta \cos^2 \theta \quad (6)$$

to give

$$P(\nu_e \rightarrow \nu_e) = 1 - 2 \sin^2 \theta \cos^2 \theta (1 - \cos(\Delta\phi)) \quad (7)$$

Now use the double-angle formula:

$$\sin \theta \cos \theta = \frac{1}{2} \sin(2\theta) \quad (8)$$

so

$$P(\nu_e \rightarrow \nu_e) = 1 - \frac{1}{2} \sin^2(2\theta) [1 - \cos(\Delta\phi)] \quad (9)$$

and the half-angle formula

$$\cos(\Delta\phi) = 1 - 2 \sin^2 \left(\frac{\Delta\phi}{2} \right) \quad (10)$$

giving the final result

$$P(\nu_e \rightarrow \nu_e) = 1 - \sin^2(2\theta) \sin^2 \left(\frac{\Delta\phi}{2} \right) \quad (11)$$

1.2 Plane wave approximation

Under the approximation to plane waves, the phase is given by

$$\phi_i = p_i L + Et \quad (12)$$

where we assume all neutrinos have the same energy E .

So the phase difference is $\Delta\phi = (p_1 - p_2)L$.

Expand the momentum in terms of the mass for each mass eigenstate:

$$p_i = (E + m_i^2)^{\frac{1}{2}} \quad (13)$$

$$\simeq E + \frac{m_i^2}{2E} \quad (14)$$

using $m_i \ll E$.

Hence,

$$\Delta\phi = (m_1^2 - m_2^2) \frac{L}{2E} \equiv \frac{\Delta m_{12}^2 L}{2E} \quad (15)$$

Inserting this into (11), we get the final answer

$$P(\nu_e \rightarrow \nu_e) = 1 - \sin^2(2\theta) \sin^2\left(\frac{\Delta m_{12}^2 L}{4E}\right) \quad (16)$$

Appendix E

Electroweak Unification

1 Electroweak Unification

1.1 The electroweak interaction

Summary of fields and interactions:

Field	Current	Coupling	Charge
$W^{+, \mu}$	$j_\mu^+ = \bar{u}\gamma_\mu \frac{1}{2}(1 - \gamma^5)u$	$g/\sqrt{2}$	$2I_3$
$W^{-, \mu}$	$j_\mu^- = \bar{u}\gamma_\mu \frac{1}{2}(1 - \gamma^5)u$	$g/\sqrt{2}$	$2I_3$
$W^{0, \mu}$	$j_\mu^0 = \bar{u}\gamma_\mu \frac{1}{2}(1 - \gamma^5)u$	g	I_3
B^μ	$j_\mu^Y = \bar{u}\gamma_\mu u$	$g'/2$	Y
A^μ	$j_\mu^{EM} = \bar{u}\gamma_\mu u$	e	Q
Z^μ	$\{j_\mu^{NC}\}$	$\{g_z\}$	$\{\}$

Quantities in $\{\text{curly braces}\}$ are to be found by the theory.

$$Q = I_3 + \frac{1}{2}Y \quad (1)$$

The full current is given by $J_\mu = \text{charge} \times j_\mu$ and the field is then

$$F^\mu = \frac{1}{q^2 - M^2} \tilde{g} J^\mu \quad (2)$$

where \tilde{g} is the appropriate coupling constant.

In the GSW basis, the full electroweak interaction is

$$\frac{g}{\sqrt{2}} J_\mu^+ W^{+, \mu} + \frac{g}{\sqrt{2}} J_\mu^- W^{-, \mu} + g J_\mu^0 W^{0, \mu} + \frac{g'}{2} J_\mu^Y B^\mu \quad (3)$$

with neutral current

$$g J_\mu^0 W^{0, \mu} + \frac{g'}{2} J_\mu^Y B^\mu \quad (4)$$

1.2 Change of basis

The observed and GSW fields are related through the Weinberg angle, θ_W ,

$$\begin{pmatrix} A^\mu \\ Z^\mu \end{pmatrix} = \begin{pmatrix} \cos \theta_W & \sin \theta_W \\ -\sin \theta_W & \cos \theta_W \end{pmatrix} \begin{pmatrix} B^\mu \\ W^{0, \mu} \end{pmatrix} \quad (5)$$

In this basis, the electroweak neutral current becomes

$$g J_\mu^0 (\sin \theta_W A^\mu + \cos \theta_W Z^\mu) + \frac{g'}{2} J_\mu^Y (\cos \theta_W A^\mu - \sin \theta_W Z^\mu) \quad (6)$$

$$= \left(g \sin \theta_W J_\mu^0 + \frac{g'}{2} \cos \theta_W J_\mu^Y \right) A^\mu + \left(g \cos \theta_W J_\mu^0 - \frac{g'}{2} \sin \theta_W J_\mu^Y \right) Z^\mu \quad (7)$$

1.3 The electromagnetic interaction

The electromagnetic part of the electroweak interaction is associated with the photon (A^μ) field:

$$eJ_\mu^{EM} \equiv g \sin \theta_W J_\mu^0 + \frac{g'}{2} \cos \theta_W J_\mu^Y \quad (8)$$

Using $J_\mu^{EM} = J_\mu^0 + \frac{1}{2} J_\mu^Y$ from (1),

$$eJ_\mu^0 + \frac{e}{2} J_\mu^Y \equiv g \sin \theta_W J_\mu^0 + \frac{g'}{2} \cos \theta_W J_\mu^Y \quad (9)$$

Giving the unification condition:

$$e = g \sin \theta_W = g' \cos \theta_W \quad (10)$$

1.4 The weak neutral current

Now consider the part of the electroweak interaction associated with the Z^μ field:

$$g_Z J_\mu^Z = g \cos \theta_W J_\mu^0 - \frac{g'}{2} \sin \theta_W J_\mu^Y \quad (11)$$

Use $g' = g \frac{\sin \theta_W}{\cos \theta_W}$ from the unification condition,

$$g_Z J_\mu^Z = \frac{g}{\cos \theta_W} \left[\cos^2 \theta_W J_\mu^0 - \sin^2 \theta_W \frac{J_\mu^Y}{2} \right] \quad (12)$$

Then $J_\mu^Y = 2(J_\mu^{EM} - J_\mu^0)$ from (1),

$$g_Z J_\mu^Z = \frac{g}{\cos \theta_W} \left[\cos^2 \theta_W J_\mu^0 - \sin^2 \theta_W (J_\mu^{EM} - J_\mu^0) \right] \quad (13)$$

$$= \frac{g}{\cos \theta_W} \left[J_\mu^0 - \sin^2 \theta_W J_\mu^{EM} \right] \quad (14)$$

Now expand out the currents as

$$J_\mu^0 = \bar{u} \gamma_\mu \frac{1}{2} (1 - \gamma^5) I_3 u \quad (15)$$

$$J_\mu^{EM} = \bar{u} \gamma_\mu Q u \quad (16)$$

$$g_Z J_\mu^Z = \frac{g}{\cos \theta_W} \bar{u} \gamma_\mu \left[\frac{1}{2} (1 - \gamma^5) I_3 - \sin^2 \theta_W Q \right] u \quad (17)$$

$$= \frac{g}{\cos \theta_W} \bar{u} \gamma_\mu \left[\frac{1}{2} (1 - \gamma^5) I_3 - \sin^2 \theta_W \left\{ \frac{1}{2} (1 + \gamma^5) + \frac{1}{2} (1 - \gamma^5) \right\} Q \right] u \quad (18)$$

$$= \frac{g}{\cos \theta_W} \bar{u} \gamma_\mu \left[\frac{1}{2} (1 - \gamma^5) (I_3 - Q \sin^2 \theta_W) - \frac{1}{2} (1 + \gamma^5) Q \sin^2 \theta_W \right] u \quad (19)$$

From this, the right- and left-handed couplings can be deduced:

$$g_L = I_3 - Q \sin^2 \theta_W \quad (20)$$

$$g_R = -Q \sin^2 \theta_W \quad (21)$$

1.5 Z boson mass

The degeneracy on the mass of the Z boson is lifted by electroweak symmetry breaking. From the form of the weak neutral current (19), the vertex factor is $g/\cos \theta_W$.

Considering the return to Fermi theory in the low-energy limit, for the process $\nu_e e \rightarrow \nu_e e$, we get $G_F/\sqrt{2} = g^2/(8M_Z^2 \cos^2 \theta_W)$.

For a charged-current weak interaction, we get $G_F/\sqrt{2} = g^2/(8M_W^2)$.

Therefore, comparing these,

$$M_W = M_Z \cos \theta_W \quad (22)$$

1.6 Vector and axial couplings

Above, the couplings of the weak neutral field Z_μ to right- and left-handed fermions was deduced. Alternatively, we can find its coupling to the vector (γ_μ) and axial ($\gamma_u \gamma^5$) parts:

$$g_z J_\mu^Z = \frac{g}{\cos \theta_W} \bar{u} \gamma_\mu \left[\frac{1}{2} (1 - \gamma^5) I_3 - \sin^2 \theta_W Q \right] u \quad (23)$$

$$= \frac{g}{\cos \theta_W} \bar{u} \gamma_\mu \left[\left(\frac{1}{2} I_3 - Q \sin^2 \theta_W \right) - \frac{1}{2} I_3 \gamma^5 \right] u \quad (24)$$

$$\equiv \frac{g}{\cos \theta_W} \bar{u} \gamma_\mu \left[\frac{c_V}{2} - \frac{c_A}{2} \gamma^5 \right] u \quad (25)$$

Therefore, we can identify the vector and axial coupling constants:

$$c_V = I_3 - 2Q \sin^2 \theta_W \quad (26)$$

$$c_A = I_3 \quad (27)$$

Appendix F

Lorentz Invariant Phase Space

1 Lorentz-invariant phase space

From Fermi's Golden Rule

$$\Gamma = 2\pi |\mathcal{M}|^2 R_n(E) \quad (1)$$

where R_n is the Lorentz-invariant phase space, similar to the density of states, or the number of possible states per energy interval per unit volume, dN/dE .

1.1 General case

The coordinate of a motion in phase space is given by a six-dimensional vector.

In a universe with periodic boundary conditions, the elementary volume is $(2\pi)^3$.

Hence, the number of states available to one particle, using a Lorentz-invariant measure, is

$$\begin{aligned} N_1 &= \frac{\text{Total volume}}{\text{Elementary volume}} \\ &= \frac{1}{(2\pi)^3} \int d^3\mathbf{x} \frac{d^3\mathbf{p}}{2E} \\ &= \frac{V}{(2\pi)^3} \int \frac{d^3\mathbf{p}}{2E} \end{aligned} \quad (2)$$

For n particles,

$$N_n = \frac{V^n}{(2\pi)^{3n}} \int \prod_{i=1}^{n-1} \frac{d^3\mathbf{p}_i}{2E_i} \quad (3)$$

where the n th momentum is not integrated over due to conservation.

This constraint also be imposed with a Dirac delta function. Use the fact that

$$\int d\mathbf{p}_n \delta^{(3)}\left(\sum_{j=1}^n \mathbf{p}_j - \mathbf{p}\right) = \int d\mathbf{p}_n \delta^{(3)}(0) = 1 \quad (4)$$

to write

$$N_n = \frac{V^n}{(2\pi)^{3n}} \int \prod_{i=1}^n \frac{d^3\mathbf{p}_i}{2E_i} \delta^{(3)}\left(\sum_{j=1}^n \mathbf{p}_j - \mathbf{p}\right) \quad (5)$$

Now the density of states is defined

$$R_n(E) = \left. \frac{dN_n}{dE} \right|_{V=1} \quad (6)$$

so we have

$$R_n(E) = \frac{1}{(2\pi)^{3n}} \frac{d}{dE} \int \prod_{i=1}^n \frac{d^3\mathbf{p}_i}{2E_i} \delta^{(3)}\left(\sum_{j=1}^n \mathbf{p}_j - \mathbf{p}\right) \quad (7)$$

Energy is conserved through the statement

$$\int dE \delta(\sum_{k=1}^n E_k - E) = 1 \quad (8)$$

inserting this into the density of states

$$R_n(E) = \frac{1}{(2\pi)^{3n}} \int \prod_{i=1}^n \frac{d^3 \mathbf{p}_i}{2E_i} \delta^{(3)}\left(\sum_{j=1}^n \mathbf{p}_j - \mathbf{p}\right) \delta\left(\sum_{k=1}^n E_k - E\right) \quad (9)$$

1.2 Two bodies

The expression $R_n(E)$ simplifies for $n = 2$. For the centre-of-mass frame ($\mathbf{p} = 0$), we have

$$\begin{aligned} R_2(E) &= \frac{1}{(2\pi)^6} \int \frac{d^3 \mathbf{p}_1}{2E_1} \int \frac{d^3 \mathbf{p}_2}{2E_2} \delta^{(3)}(\mathbf{p}_1 + \mathbf{p}_2) \delta(E_1 + E_2 - E) \\ &= \frac{1}{(2\pi)^6} \int \frac{d^3 \mathbf{p}_1}{4E_1 E_2} \delta(E_1 + E_2 - E) \\ &= \frac{4\pi}{(2\pi)^6} \int dp \frac{p^2}{4E_1 E_2} \delta(E_1 + E_2 - E) \end{aligned} \quad (10)$$

where the last step assumes no angular dependance on the momentum.

Now use $E_1 dE_1 = p dp$ so

$$R_2(E) = \frac{\pi}{(2\pi)^6} \int dE_1 \frac{p}{E_2} \delta(E_1 + E_2 - E) \quad (11)$$

We can write E_2 in terms of E_1 :

$$E_2 = \sqrt{E_1^2 - m_1^2 + m_2^2} \quad (12)$$

Therefore

$$R_2(E) = \frac{\pi}{(2\pi)^6} \int dE_1 \frac{p}{E_2} \delta[f(E_1)] \quad (13)$$

where $f(E_1) = E_1 + \sqrt{E_1^2 - m_1^2 + m_2^2} - E$.

Now use the fact that

$$\delta(f(x)) \left| \frac{df}{dx} \right|_{x=0} = \delta(x) \quad (14)$$

and $f' = E/E_2$ to get the final result

$$R_2(E) = \frac{\pi}{(2\pi)^6} \int dE_1 \frac{p}{E} \delta(E_1) \quad (15)$$